

Comparative analysis of *Drosophila athabasca* cuticular hydrocarbons for
generation of synthetic material to study evolutionary implications

By

Brittany Lynn Gay

Submitted in partial fulfillment of the requirements for

Bachelor of Science (ACS) and for

Honors in the Department of Chemistry

UNION COLLEGE

June 2017

Acknowledgements

This thesis would have never been completed if it were not for some exceptional people both in the Chemistry Department and beyond.

I am extraordinarily grateful for all of the support (both in the lab and outside of it) that Prof. Kehlbeck has provided me over the last two and a half years. I aspire to be even a fraction of how dedicated she is to her profession and to the people in her life who matter most. I've never learned more from another person as I have from her.

I owe much gratitude to Prof. Yukilevich, as he has been the provider of all of the flies that have given their lives to further the understanding of cuticular hydrocarbons. Prof. McGarrah's guidance and teachings have made me a better chemist and taught me great respect for instrumentation and the tremendous efforts required to maintain them.

I also want to thank Kim Bolduc, John Shuler, Nar Lin, and Dan Jackson, for always making S340 an entertaining place to be – even when we weren't doing chemistry. I am incredibly indebted to all of the professors in the Chemistry Department: Anderson (and Charlie), Carroll, Huisman, Fox, Hagerman, LAMS, Paulick, and Dr. A, who have taught me, watched me struggle, and made me into a better person, academic, and researcher. I would not be going to graduate school had I not learned and grown from all of you.

There are many, many other faculty, staff members, and friends outside of the Chemistry Department that deserve just as much thanks. Without them, I would not have experienced so much personal growth. I am forever grateful to them.

Table of Contents

Table of Figures.....	5
Table of Appendix Tables and Figures	7
Abstract.....	11
Introduction	12
1. Cuticular Hydrocarbons	12
1.1 Properties of CHCs.....	12
1.2 Potential Roles of CHCs	12
2. Drosophila Athabasca	16
3. Characterization and Identification	17
3.1. Gas Chromatography – Mass Spectrometry	18
3.2. Chemical Derivatization of Unsaturated CHCs.....	19
3.3. Chemical Derivatization of Saturated CHCs	21
3.4. Retention Indices for Literature Comparison.....	22
4. Synthesis of Identified CHCs.....	22
4.1 Monoene Synthesis.....	23
4.2. Dienes.....	24
4.3. Branched CHCs.....	25
5. Quantification	26
Materials and Methods	27
Materials.	27
Synthesis.	27
Identification.	28
DMSD Derivatization.....	28
Bromination.....	28
Bromination with Molecular Bromine.	29
Synthesis of Identified CHCs.....	29
Synthesis of 2-methylhexacosane.	29
Quantification of CHCs using External Standard Curves.....	30
Results.....	31
Analysis of Linear Alkane Standards.....	31
Identification of Branched Alkanes.....	33
Derivatization of Branched Alkanes Using Molecular Bromine.....	35
Identification of Monoenes.	43
Identification of Dienes.....	51
Identification of <i>cis</i>-Vaccenyl Acetate	54
Identification of Saturated and Unsaturated Carboxylic Acids	56
Identification of Methyl Esters.....	59
Quantification of CHCs Using External Standard Curves	61
Intra-racial Variability	63
Inter-racial Variability	64
Discussion	72
Identification of Linear Alkanes.....	72
Identification of Branched Alkanes.....	72
Identification of Monoenes	73
Identification of Dienes.....	74

Identification of <i>cis</i> -Vaccenyl Acetate	75
Identification of Carboxylic Acids and Methyl Esters	76
Quantification of CHCs Using External Standard Curves	76
Intra-racial Variability	77
Inter-racial Variability	80
Conclusions and Future Work.....	82
References	83
Appendix A. Table of All Identified Compounds.	87
Appendix B – Linear Alkane Standard Mass Spectra.....	89
Appendix C – 2-Methyl Branched Alkane Mass Spectra.....	122
Appendix D – Pre- and Post-Bromination Mass Spectra of 2-Methyl Branched Alkanes.....	129
Appendix E – Mass Spectra of Natural, Underivatized Monoenes and Dienes	132
Appendix F – Carboxylic Acids and Methyl Esters	142
Appendix G – External Standard Curves of Synthetic CHCs	150

Table of Figures

- Figure 1.** Geographical distribution of *D. Athabasca* races. WN is located in the blue region, EA in red, and EB in orange. ²⁶ _____ 16
- Figure 2.** Alternate methods of locating positions of unsaturation in CHCs: (a) epoxidation of the double bond and (b) OsO₄ oxidation, followed by silylation. Dashed lines indicated possible fragmentation patterns when analyzed by EI-MS. However, these methods both lead to convoluted results when compounds contain multiple positions of unsaturation. ³⁴ _____ 19
- Figure 3.** DMDS derivatization of mono-unsaturated CHCs results in a single adduct with a reliable fragmentation pattern, indicated by the dashed line.³⁴ _____ 20
- Figure 4.** Adducts produced when dienes separated by three or fewer methylene groups are derivatized by DMDS. (a) Illustrates adducts formed when 1eq. of DMDS is used and only one pi bond reacts, while (b) shows the cyclic thioether adduct formed with both double bonds react with 2 eq. of DMDS. _____ 21
- Figure 5.** Bromination, elimination, and subsequent DMDS derivatization analysis of branched alkanes for determination of branching location and size. _____ 22
- Figure 6.** Cis-directed Wittig reaction initially utilized to produce monoene CHCs.³⁶ However, difficult geometric isomer separation resulted in exploration of other synthetic routes for these compounds. _ 23
- Figure 7.** Production of cis-alkene CHCs with a single position of unsaturation is accomplished through nucleophilic substitution with a deprotonated acetylene and a primary alkyl halide, followed by hydrogenation to the cis isomer.^{38,39} _____ 24
- Figure 8.** General synthetic route for the production of cis-diene CHCs. ^{40,41} _____ 24
- Figure 9.** Synthetic scheme for the preparation of 2-methyl branched alkane CHCs via a nucleophilic substitution using a deprotonated terminal acetylene, followed by hydrogenation to the saturated alkane. _____ 25
- Figure 10.** Alternative route for the production of 2-methyl branched CHCs using a Grignard reaction, followed by alcohol dehydration and hydrogenation. _____ 25
- Figure 11.** Mass spectrum of CHC located at 22.90 m. Compared to mass spectra of n-alkanes, this CHC was determined to be n-tricosane. _____ 32
- Figure 12.** Fragmentation pattern of 2-methyl branched alkanes. A loss of 43 m/z is indicative of the loss of a propyl group, while [M-15]⁺ corresponds to loss of a single methyl group. _____ 33
- Figure 13.** Mass spectrum of CHC observed at 30.12 m in all three races of *D. athabasca*. Peaks at 337, 365, and 380, are indicative of a methyl branch at the second carbon of a C26-chain, or 2-methylhexacosane, based on the fragmentation pattern in Figure 12. _____ 34
- Figure 14.** An extract of 25 EB flies (blue) was subjected to brominating conditions. Post-bromination, the sample was analyzed by identical GC-MS methods to afford the spectrum in red. _____ 36

- Figure 15.** 2-methylhexacosane mass spectrum pre-bromination (top, red) and post-bromination (bottom, blue). A loss of two m/z in the post-bromination mass spectrum is indicative of an elimination reaction, and not bromination. _____ 38
- Figure 16.** Mass spectral comparison of fly 2-MeC26 (red) and synthetic 2-Me-C26 (blue). Identical mass spectra confirm the identity of 2-methylhexacosane as a branched alkane located at ~30.12 m. _ 40
- Figure 17.** Fragmentation pattern of 3-methyl branched CHCs. A loss of 15 m/z corresponds to a loss of a methyl group, loss of 29 m/z corresponds to loss of an ethyl, and loss of 57 m/z corresponds to a loss of a sec-butyl group. _____ 41
- Figure 18.** Mass spectrum of CHC at 24.42 m in EB flies. Fragments at $[M-15]^+$, $[M-29]^+$ and $[M-57]^+$ are indicative of a methyl branch at the 3rd carbon of a C23-chain, or 3-methyltricosane. _____ 42
- Figure 19.** DMDS-derivatized (green) versus unreacted survey (blue) of a 25-fly CHC extract from EB flies. Peaks that disappear upon reaction with DMDS are classified as unsaturated and further investigated. New peaks in the DMDS chromatogram are also investigated. _____ 44
- Figure 20.** DMDS-derivatized mass spectrum containing two sets of fragments corresponding to 11- and 12-pentacosene. Insets are fragmentation patterns of the identified pentacosene DMDS adducts. _ 46
- Figure 21.** Mass spectrum of DMDS derivatized CHCs. A total mass of 416 m/z , along with three sets of fragments indicates three different tricosene (C23:1) isomers with unsaturations at the 9th, 10th, and 11th carbons. _____ 48
- Figure 22.** Mass spectrum of DMDS-derivatized 12-tetracosene. The symmetry of 12-tetracosene results in the observation of only a single peak. _____ 50
- Figure 23.** Mass spectrum of DMDS-derivatized 10,14-pentacosadiene with one equivalent of DMDS. Inset is the fragmentation patterns of the thioether adducts of this derivatization. Signals at 395 and 347 m/z correspond to cleavage of one SCH_3 group and two SCH_3 groups, respectively. Signals at 427 m/z and 379 m/z correspond to small amounts of cyclic adduct shown in Figure 24. _____ 52
- Figure 24.** Mass spectrum of DMDS-derivatized 10,14-pentacosadiene, cyclic adduct. Inset is the fragmentation patterns of the thioether adducts of this derivatization. (2 molar equivalents of DMDS reagent). The signal at 207 m/z is due to column bleed. _____ 53
- Figure 25.** Mass spectrum of the CHC at 20.5 m, identified as cVA, exclusively found in males from all races of *D. athabasca*. As reported, no molecular ion was observed in this spectrum.⁴⁶ Inset is the chemical structure of cVA. _____ 55
- Figure 26.** Fragmentation pattern of unsaturated carboxylic acids analyzed by EI-MS. _____ 56
- Figure 27.** Mass spectrum of a CHC at 19.32 m in all races. The fragmentation pattern of this CHC was compared to literature spectra and determined to be oleic acid. Synthetic oleic acid was subsequently analyzed via GC-MS to confirm this identification (see overlay in Figure G7 in Appendix G). _____ 57
- Figure 28.** Mass spectrum of a CHC at 15.19 m. Using the NIST 14 Mass Spectral Library, this compound was identified as hexadecanoic acid. _____ 58
- Figure 29.** Mass spectral fragmentation pattern of methyl esters. _____ 59

Figure 30. Mass spectrum of a CHC at 14.36 m. The fragmentation pattern illustrated in Figure 29 was used to identify this compound as methyl hexadecanoate.	60
Figure 31. External calibration curve generated from standards of known concentrations of synthetic (Z)11-tricosene. Linear regression analysis using this curve allowed for quantification of CHCs in single fly samples.	62
Figure 32. Overlaid CHC profiles for four individual flies of EA race. LK1 and LK23 are two isofemale lines of EA, labeled according to original field collection. CHC profiles have been standardized by peak area to reveal both qualitative and quantitative differences between lines.	65
Figure 33. Area standardized CHC profiles of an EA female (blue) and male (red).	66
Figure 34. Overlaid CHC profiles for eight individuals of different isofemale lines from the EB race. CHC profiles have been standardized by area to reveal both qualitative and quantitative differences between lines.	67
Figure 35. Area standardized CHC profiles of an EB female (blue) and male (red).	68
Figure 36. Overlaid CHC profiles for ten individuals of different isofemale lines from the WN race. CHC profiles have been standardized by area to reveal both qualitative and quantitative differences between lines.	69
Figure 37. Area standardized CHC profiles of a WN female (blue) and male (red).	70
Figure 38. Overlaid chromatograms from 100-fly CHC extracts of EA (blue), WN (red), and EB (green), standardized by peak area. 100-fly extracts were used to eliminate random variability that may occur in single fly samples.	71

Table of Appendix Tables and Figures

Table A1. Retention times, KRI values, and identities of all identified CHCs.

Figure B1. Mass spectrum of C7, or n-heptane, a purchased standard. The structure, chemical formula and expected M⁺ are inset.

Figure B2. Mass spectrum of C8, n-octane, a purchased standard. The structure, chemical formula and expected M⁺ are inset.

Figure B3. Mass spectrum of C9, or n-nonane, a purchased standard. The structure, chemical formula and expected M⁺ are inset.

Figure B4. Mass spectrum of C10, or n-decane, a purchased standard. The structure, chemical formula and expected M⁺ are inset.

Figure B5. Mass spectrum of C11, or n-undecane, a purchased standard. The structure, chemical formula and expected M⁺ are inset.

Figure B6. Mass spectrum of C12, or n-dodecane, a purchased standard. The structure, chemical formula and expected M^+ are inset.

Figure B7. Mass spectrum of C13, or n-tridecane, a purchased standard. The structure, chemical formula and expected M^+ are inset.

Figure B8. Mass spectrum of C14, or n-tetraecane, a purchased standard. The structure, chemical formula and expected M^+ are inset.

Figure B9. Mass spectrum of C15, or n-pentadecane, a purchased standard. The structure, chemical formula and expected M^+ are inset.

Figure B10. Mass spectrum of C16, or n-hexadecane, a purchased standard. The structure, chemical formula and expected M^+ are inset.

Figure B11. Mass spectrum of C17, or n-heptadecane, a purchased standard. The structure, chemical formula and expected M^+ are inset.

Figure B12. Mass spectrum of C18, n-octadecane, a purchased standard. The structure, chemical formula and expected M^+ are inset.

Figure B13. Mass spectrum of C19, or n-nonadecane, a purchased standard. The structure, chemical formula and expected M^+ are inset.

Figure B14. Mass spectrum of C20, or n-eicosane, a purchased standard. The structure, chemical formula and expected M^+ are inset.

Figure B15. Mass spectrum of C21, or n-heneicosane, a purchased standard. The structure, chemical formula and expected M^+ are inset.

Figure B16. Mass spectrum of C22, or n-docosane, a purchased standard. The structure, chemical formula and expected M^+ are inset.

Figure B17. Mass spectrum of C23, or n-tricosane, a purchased standard. The structure, chemical formula and expected M^+ are inset.

Figure B18. Mass spectrum of C24, or n-tetracosane, a purchased standard. The structure, chemical formula and expected M^+ are inset.

Figure B19. Mass spectrum of C25, or n-pentacosene, a purchased standard. The structure, chemical formula and expected M^+ are inset.

Figure B20. Mass spectrum of C26, or n-hexacosane, a purchased standard. The structure, chemical formula and expected M^+ are inset.

Figure B21. Mass spectrum of C27, or n-heptacosene, a purchased standard. The structure, chemical formula and expected M^+ are inset.

Figure B22. Mass spectrum of C28, or n-octacosane, a purchased standard. The structure, chemical formula and expected M^+ are inset.

Figure B23. Mass spectrum of C29, or n-nonacosane, a purchased standard. The structure, chemical formula and expected M^+ are inset.

Figure B24. Mass spectrum of C30, or n-triacontane, a purchased standard. The structure, chemical formula and expected M^+ are inset.

Figure B25. Mass spectrum of C31, or n-untriacontane, a purchased standard. The structure, chemical formula and expected M^+ are inset.

Figure B26. Mass spectrum of C32, or n-dotriacontane, a purchased standard. The structure, chemical formula and expected M^+ are inset.

Figure B27. Mass spectrum of C33, or n-tritriacontane, a purchased standard. The structure, chemical formula and expected M^+ are inset.

Figure B28. Mass spectrum of C34, or n-tetracontane, a purchased standard. The structure, chemical formula and expected M^+ are inset.

Figure B29. Mass spectrum of C35, or n-pentatriacontane, a purchased standard. The structure, chemical formula and expected M^+ are inset.

Figure B30. Mass spectrum of C36, or n-hexatriacontane, a purchased standard. The structure, chemical formula and expected M^+ are inset.

Figure B31. Mass spectrum of C37, or n-heptatriacontane, a purchased standard. The structure, chemical formula and expected M^+ are inset.

Figure B32. Mass spectrum of C38, or n-octatriacontane, a purchased standard. The structure, chemical formula and expected M^+ are inset.

Figure C1. Mass spectrum of 2-methyltricosane, a purchased standard. Peaks at $[M-15]^+$ and $[M-43]^+$ indicate a branch at the second carbon. The chemical structure of this CHC is inset.

Figure C2. Mass spectrum of a CHC identified as 2-methyltetracosane. Peaks at $[M-15]^+$ and $[M-43]^+$ indicate a branch at the second carbon. The chemical structure of this CHC is inset.

Figure C3. Mass spectrum of a CHC identified as 2-methylpentacosane. Peaks at $[M-15]^+$ and $[M-43]^+$ indicate a branch at the second carbon. The chemical structure of this CHC is inset.

Figure C4. Mass spectrum of a CHC identified as 2-methylheptacosane. Peaks at $[M-15]^+$ and $[M-43]^+$ indicate a branch at the second carbon. The chemical structure of this CHC is inset.

Figure C5. Mass spectrum of a CHC identified as 2-methyloctacosane. Peaks at $[M-15]^+$ and $[M-43]^+$ indicate a branch at the second carbon. The chemical structure of this CHC is inset.

Figure C6. Mass spectrum of a CHC identified as 2-methyltriacontane. Peaks at $[M-15]^+$ and $[M-43]^+$ indicate a branch at the second carbon. The chemical structure of this CHC is inset.

Figure D1. Pre-bromination and post-bromination mass spectra of 2-methyldocosane. The loss of two m/z indicates an elimination reaction occurred.

Figure D1. Pre-bromination and post-bromination mass spectra of 2-methyloctacosane. The loss of two m/z indicates an elimination reaction occurred.

Figure E1. Mass spectrum of a proposed monoene, C22:1, or docosene. DMDS-derivatization must be performed to determine the location of the unsaturation.

Figure E2. Mass spectrum of a underivatized (*Z*)11-tricosene.

Figure E3. Mass spectrum of 7-tricosene, another CHC identified in *D. Athabasca*.

Figure E4. Mass spectrum of a tetracosadiene, C₂₄:2 with unknown positions of unsaturation. DMDS derivatization must be performed to accurately determine the location of the unsaturations.

Figure E5. Mass spectrum of underivatized 12-tetracosene.

Figure E6. Mass spectrum of underivatized 10,14-pentacosadiene.

Figure E7. Mass spectrum of the underivatized (Z)11-pentacosene/ (Z)12-pentacosene mixture.

Figure E8. Mass spectrum of a proposed heptacosadiene (C₂₇:2). DMDS derivatization must be performed to locate the positions of the double bonds in this CHC.

Figure E9. Mass spectrum of a proposed heptacosene (C₂₇:1). DMDS derivatization must be performed to locate the positions of the unsaturation in this CHC.

Figure F1. Mass spectrum of methyl tetradecanoate.

Figure F2. Mass spectrum of a tetradecenoic acid.

Figure F3. Mass spectrum of tetradecanoic acid.

Figure F4. Mass spectrum of a proposed hexadecenoic acid. DMDS derivatization must be performed to locate the position of unsaturation.

Figure F5. Mass spectrum of an octadecadienoic acid. The location of the two unsaturations in this CHC must be further investigated using DMDS derivatization.

Figure F6. Mass spectrum of synthetic oleic acid used to identify the CHC at 19.32 m in all races of *D. athabasca*.

Figure F7. Mass spectrum of octadecanoic acid.

Figure G1. External standard curves for (Z)7-tricosene.

Figure G2. External standard curve for (Z)7-pentacosene.

Figure G3. External standard curve for (Z,Z)7,11-pentacosadiene.

Figure G4. External standard curve for (Z)9-tricosene.

Figure G5. External standard curve for (Z,Z)7,11-heptacosadiene.

Abstract

GAY, BRITTANY, L. Comparative analysis of *Drosophila athabasca* cuticular hydrocarbons for generation of synthetic materials to study evolutionary implications. Union College, Department of Chemistry, June 2017.

ADVISOR: JOANNE D. KEHLBECK

Cuticular hydrocarbons (CHCs) have been studied extensively and their roles explored for various species of insects. However, only a single reported study has focused on the role of CHCs in *Drosophila athabasca*, a species of fruit fly native to North America. The work herein describes advances in identification, synthesis and quantification of biologically relevant CHCs present in this species. Identifying CHC profile differences among *D. athabasca* sub-races (Eastern A, Eastern B and WestNorthern) was performed using multiple analytical techniques. Synthesis of proposed structures confirmed their identity. External standard curves were used to quantify CHCs. GC-MS analysis of CHCs from several isofemale lines of *D. athabasca* reveals multiple monoenes, dienes, and branched alkanes. Positions of unsaturation within CHCs were determined using dimethyl disulfide (DMDS) derivatization and branching locations were determined via bromination and subsequent elimination. Synthesis of mono- and di- unsaturated CHCs was accomplished through alkyl substitution, followed by *cis*-selective reduction. Branched alkanes were generated in a similar fashion or through coupled Grignard-elimination-reduction schemes. External standard curves, generated from synthesized compounds, can be used to produce synthetic profiles for continued exploration of CHC role within the *D. athabasca* system.

Introduction

1. Cuticular Hydrocarbons

1.1 Properties of CHCs

The cuticle is a flexible, waxy barrier that protects the insect from its environment.¹ The surface is coated with a thin epicuticular layer composed of various long-chain hydrocarbons, alcohols and other organic compounds, derived from fatty acids.² Typical CHCs range in chain length from 19 to 30 carbons, although some species of ants possess compounds with upwards of 47 carbons.³ Additionally, CHCs possess a wide range of structural features, including branching and unsaturation in the form of monoenes, dienes, and trienes. Researchers continue to propose biological roles for CHCs based upon these features.

1.2 Potential Roles of CHCs

Studies of insect CHCs have found various multifaceted biological functions ranging from signaling to environmental protection. Numerous compounds have been observed to participate in discrimination among individuals, recognition of species⁴, and other social interactions, such as mate selection.^{5,6} Additionally, the hydrophobic nature of CHCs provides significant capabilities for resisting water loss.

1.2.1 *Desiccation Resistance*

It has been proposed that the primary function of the cuticle is to regulate water loss in insects, a mechanism of desiccation prevention.⁷ The outermost epicuticular layer is mainly comprised of straight chain alkanes, closely packed as a result of geometric constraints. This forms a rigid, hydrophobic structure,

preventing water loss, trans-cuticularly.² Previous research has observed insects that inhabit warmer climates possess a higher ratio of *n*-alkanes, suggesting a possible role in water regulation. Relative to alkenes and branched CHCs, the low vapor pressure of *n*-alkanes may maintain water regulation in warmer climates. Comparatively, insects living in colder climates have higher abundances of unsaturated and branched CHCs.⁸ As reported by Rouault et al., *D. melanogaster* individuals possessing “tropical”, long-chain, *n*-alkanes were better equipped for preventing water loss compared to flies expressing shorter chain alkanes.⁹

Similarly, experimental comparisons between *D. serrata* and *D. birchii* observed decreased resistance to desiccation in *D. birchii*. Relative to *D. serrata*, *D. birchii* expressed fewer quantities of methyl-branched alkanes, which have higher melting temperatures than alkenes.¹⁰ Chung and Carroll correlated altered mating success with climate-based evolutionary changes in CHCs describing a possible mechanism for speciation.¹⁰

1.2.2 Communication

While CHCs may indeed provide a mechanism for anti-desiccation, potential development into signaling molecules is plausible, and has been suggested.^{2,10} As signaling molecules, individuals would be able to communicate with members of their species or given subgroup. This communication, among groups or between individuals, is vital for continuation of a species, especially in insects. Multiple modes of communication exist in insects, including: visual, auditory, tactile, olfactory and gustatory signaling.¹ However, the use of chemical signals is suggested to be the primary, most primitive form of communication among insects.^{4,11} Though

suggested, the interaction between certain chemical signals and their resulting social behaviors are not well understood.¹² Multiple investigations into potential chemicals that may function as signaling molecules have been aimed at CHCs.^{1,3,10,11,13-22} The large sampling of structural motifs would provide the specificity necessary for unique chemical signaling required to elicit a variety behavioral responses.¹²

The higher vapor pressures and variety in chemical space of alkenes and branched CHCs, suggest that they may act as short-range signaling molecules, with greater complexity leading to increased specificity within biological systems. For example, as the number of double bonds increases, or the position of the branch changes, the specificity and selectivity of the CHC changes, as well.⁸ Such increased specificity leads to potential increases in selectivity, and may ultimately drive biological processes such as speciation.

1.2.2.1) Recognition Signals

Social insects require a mechanism of recognition to communicate among kin and between species. Numerous studies have implicated chemical components in communication across a wide variety of social insects. Research in understanding nestmate recognition in social insects has primarily focused on identification of CHCs to determine biological function.

Predator exploitation of chemical recognition signals allows access into otherwise impermeable nest barriers created by prey. For example, the staphylinid beetle (*Trichopsenius frosti*) biosynthesizes and expresses the same CHC profile as its host termite, *Reticulitermes flavipes*.²³ By mimicking the CHC profile, the beetle is

able to infiltrate the termite nest without being detected as a threat. Several aphid parasites express CHC profiles that mimic that of the aphid. When attempting to forage the aphid colonies, the parasites with mimicking CHCs are ignored and those with non-mimicking CHCs profile are attacked by the tending ants.²⁴

1.2.2.2) Sex Pheromones

A number of CHCs have been identified in *Drosophila* that influence the sexual selection process. Two major diene compounds, (Z,Z)7,11-heptacosadiene and (Z,Z)7,11-nonacosadiene, predominantly produced by *melanogaster* females, appear to induce mating behaviors in males.⁶ In another study both (Z)7- and (Z)9-pentacosene appeared to stimulate copulation in *D. melanogaster*²⁵. Work focusing on *Drosophila virilis* identified the major stimulatory sex pheromone as (Z)11-pentacosene.

While many CHCs have been shown to evoke mating behavior, some appear to inhibit sexual courtship. For example, a male-specific CHC, (Z)7-tricosene, has been shown to hinder excitation of other males.⁹ An additional monoene pheromone, (Z)5-tricosene, has also been shown to hinder male courtship in *D. melanogaster*.²⁵ Similarly, individuals of the *D. simulans* with high levels of 7,11-dienes induce little to no courtship behaviors in males. Because these 7,11-dienes are found predominantly on *D. melanogaster*, and very small quantities can inhibit or prevent interspecies courtship, it is likely that they are involved in mate discrimination and subsequent sexual isolation between *D. simulans* males and *D. melanogaster* females.¹⁶

2. *Drosophila Athabasca*

Extensive studies have focused on CHCs found in various species of *Drosophila*, yet, a careful survey of the literature reveals only a single study discussing the role of CHCs in *Drosophila athabasca*.²⁶ *D. athabasca* is native to North America and exists in three, distinct behaviorally-isolated races. These races include WestNorthern (WN), Eastern A (EA), and Eastern B (EB).²⁷ While located primarily in differing geographical regions, there are some areas of sympatry, where the populations coexist. (Figure 1).²⁶

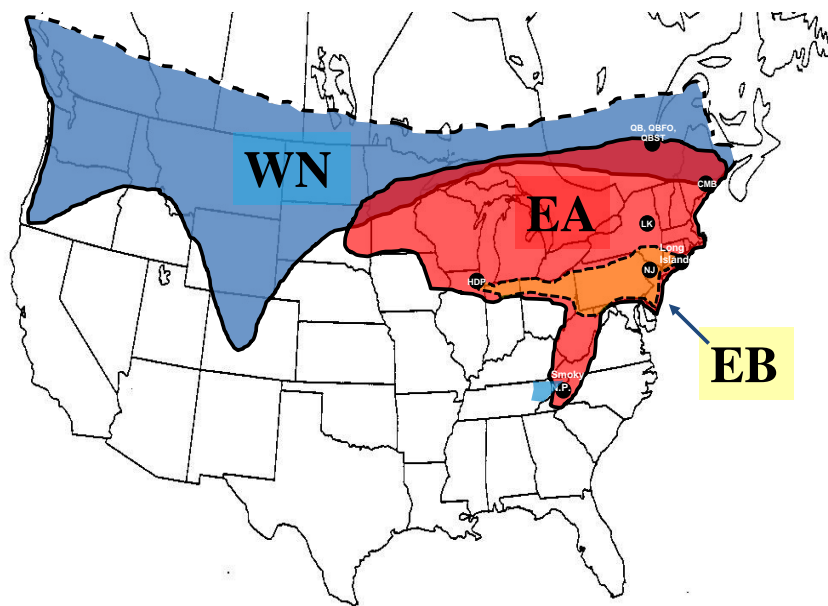


Figure 1. Geographical distribution of *D. Athabasca* races. WN is located in the blue region, EA in red, and EB in orange. ²⁶

The unique nature of the *D. athabasca* system arises from the lack of natural copulation between individuals of different races, though they exhibit small differences in morphology.²⁷⁻²⁹ This makes *D. athabasca* an ideal model system

particularly well suited to study nascent speciation.²⁶ While existing evidence supports CHCs exerting effects on sexual selection leading to sexual isolation,^{30,31} no clear explanation has arisen. Likewise, it has been reported that sexual isolation in *D. athabasca* may be controlled by other factors, including: male courtship song,²⁶ pigmentation, or genetic factors such as Y Chromosome type.²⁹ CHCs as anti-desiccants have also been explored in the *D. athabasca* system, though preliminary studies have suggested a negative correlation between CHC profile and desiccation resistance, further indicating unknown roles in this species.^{26,32}

To fully understand the role of CHCs in the *D. athabasca* system, comprehensive analyses of CHC profiles from each race must be performed. This is accomplished via thorough identification, synthesis, and quantification of all observed compounds. We assert that the complete analysis of natural profiles and preparation of synthetic composites can be used to gain a greater understanding of the role of CHCs in *D. athabasca*. Once synthesized, neat materials can be used to produce calibration curves for accurate measurement of CHCs in single fly samples. Knowledge of biologically relevant quantities allows for generation of complete synthetic CHC profiles to be used in behavioral studies. Exploring potential correlations between profile and behavioral response may elucidate the role of CHCs in *D. athabasca*.

3. Characterization and Identification

A complete understanding of the role of CHCs in the *D. athabasca* system requires complete identification of all CHCs from each race. Characterization and

identification are accomplished through a variety of analytical techniques coupled with derivatization reactions when necessary.

The most frequented method of identification is gas chromatography – mass spectrometry (GC-MS), which separates individual CHCs based upon boiling point and interactions with the stationary phase of an open column, and affords details about chemical structure. Successful resolution of compounds requires the development of temperature-programming methods in order to analyze standards as well as unknown extracts. Comparison to standard mass spectra and retention times, allows for elucidation of unknown structures. However, when CHCs possess unsaturation or branching sites, mass spectral interpretation can often lead to ambiguity and convoluted results, requiring derivatization reactions. For unsaturated compounds, DMDS derivatization is used while bromination is used to derivatize branched CHCs.

3.1. Gas Chromatography – Mass Spectrometry

Profiles from each race of *D. atabasca* are initially probed through GC-MS. GC allows for separation of individual components of a mixture, based upon boiling point and interaction with a stationary phase. After separation, electron ionization (EI) MS is performed to collect information about the structural properties of each analyte based on mass-to-charge ratios.

Typically, EI-MS analysis of saturated compounds affords unambiguous structural information. For branched hydrocarbons, branching positions and sizes are easily recognized through enhanced fragmentation at the alpha position.³³ Additionally, derivatizations of the branched CHCs can provide further evidence for

branch locations. However, molecules containing positions of unsaturation yield ambiguous fragmentation patterns in their mass spectra, preventing confirmation of structure without further derivatization. Because of this ambiguity in analysis, mass spectrometry is not a reliable method for identification of unsaturated CHCs. As a result, derivatization reactions must be performed on extracted hydrocarbon mixtures to determine sites of unsaturation.

3.2. Chemical Derivatization of Unsaturated CHCs

Various methods have been employed to derivatize unsaturations, including epoxidation (Figure 2a), and osmium tetroxide oxidation to the vicinal diol, followed by silylation (Figure 2b). While these methods proved efficient for mono-unsaturated alkenes, multiple unsaturated positions led to convoluted results, which could not be easily interpreted.³⁴

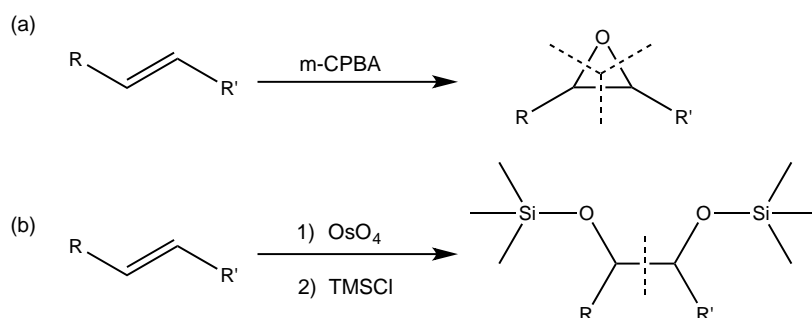


Figure 2. Alternate methods of locating positions of unsaturation in CHCs: (a) epoxidation of the double bond and (b) OsO₄ oxidation, followed by silylation. Dashed lines indicated possible fragmentation patterns when analyzed by EI-MS. However, these methods both lead to convoluted results when compounds contain multiple positions of unsaturation.³⁴

Another, more successful, method of derivatization involves the addition of dimethyl disulfide (DMDS) across a double bond. This produces unique thioether

adducts with predictable fragmentation locations (Figure 3). This derivatization method provides easily identifiable molecular ion (M^+) and fragment peaks in the resulting mass spectra of monoene CHCs.³⁴

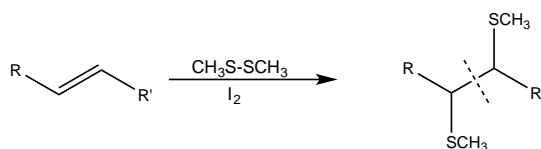


Figure 3. DMDS derivatization of mono-unsaturated CHCs results in a single adduct with a reliable fragmentation pattern, indicated by the dashed line.³⁴

CHCs possessing multiple double bonds afford more challenging mass spectra and require additional chemical strategies for analysis. Similar to monounsaturated CHCs, DMDS will react across a single pi bond and fragment at that location, resulting in two (or more) thioether adducts, depending upon the original number of pi bonds (Figure 4a). However, the resulting compounds are typically inseparable using common GC methods and result in one mass spectrum containing two sets of fragments.

CHCs with double bonds separated by two or three methylene group can form cyclic thioether adducts with unique fragmentation patterns (Figure 4b), in addition to reacting across each pi bond individually.³⁴ Cyclic thioether adducts fragment in predictable locations, allowing the locations of the original double bonds to be determined and compared to those from the mono-reacted adducts. Derivatizations of unsaturated CHCs provide structural information but give no insight into the geometric conformation and must be confirmed through synthesis.

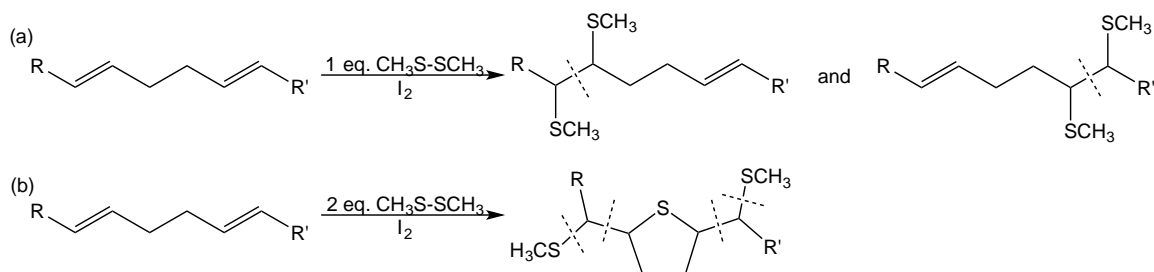


Figure 4. Adducts produced when dienes separated by three or fewer methylene groups are derivatized by DMDS. (a) Illustrates adducts formed when 1 eq. of DMDS is used and only one pi bond reacts, while (b) shows the cyclic thioether adduct formed with both double bonds react with 2 eq. of DMDS.

3.3. Chemical Derivatization of Saturated CHCs

Fully saturated CHCs cannot be identified through derivatization reactions that utilize pi bonds, such as DMDS derivatization. Instead, alternative reactions can be used that take advantage of the high selectivity of bromine radicals for tertiary positions. When these hydrocarbons are treated with a source of bromine radical, such as N-bromosuccinimide (NBS) or molecular bromine (Br_2), bromination is likely to occur at the branch site. Subsequent elimination of this brominated compound to produce the unsaturated olefin allows for DMDS derivatization. Using fragmentation patterns from the GC-MS analysis of the derivatized olefin, as well as the number of unsaturated products produced, the branching location can be identified (Figure 5). Additionally, the length of the branch can also be identified using this method.

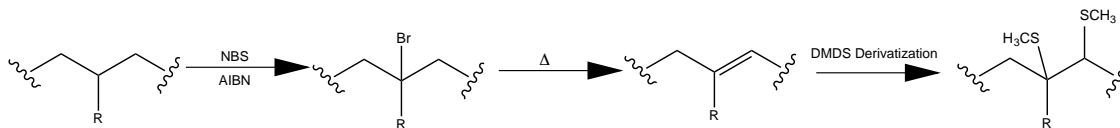


Figure 5. Bromination, elimination, and subsequent DMDS derivatization analysis of branched alkanes for determination of branching location and size.

3.4. Retention Indices for Literature Comparison

In addition to EI-MS and derivatization data, GC retention times (RTs) can be used to calculate a value for the Kováts Retention Index (KRI).³⁵ Equation (1) is used to calculate KRI values, where n is the chain length of the smaller n -alkane standard, $RT(n)$ is the RT of this compound and $RT(N)$ is the RT n -alkane immediately following the RT of the unknown CHC ($RT(\text{unknown})$).

$$\text{KRI} = 100 \times \left[n + \frac{RT(\text{unknown}) - RT(n)}{RT(N) - RT(n)} \right] \quad (1)$$

This value compares and normalizes the RT of the CHC of interest to an n -alkane standard. Once calculated, KRI values can then be used to examine elution patterns of CHCs and to compare to literature values observed on other GC instruments.

4. Synthesis of Identified CHCs

Upon successful identification, syntheses of each hydrocarbon must be accomplished in order to confirm retention times and geometric and stereochemical structure. Several CHCs from other insects are commercially available and can be used as standards for comparison to *D. athabasca* CHCs. However, not all of the compounds observed in this study are readily available and must be synthesized.

The variety of structural features of CHCs, including: monoenes, dienes, and branches requires multiple synthetic approaches.

4.1 Monoene Synthesis

A few identified CHCs from *D. atabasca* possess a single position of unsaturation. A *cis*-directed Wittig reaction³⁶ (Figure 6) had been previously attempted, however, low yields (24%) and unfavorable *cis*: *trans* ratios (80:20) led to arduous purification.³⁷

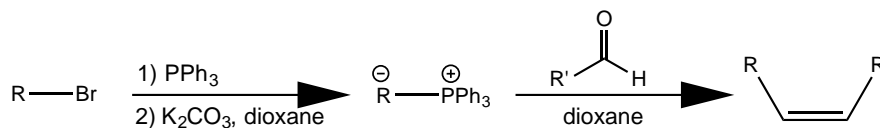


Figure 6. *Cis*-directed Wittig reaction initially utilized to produce monoene CHCs.³⁶ However, difficult geometric isomer separation resulted in exploration of other synthetic routes for these compounds.

As a result, a different synthetic procedure was employed. Initially, an internal alkyne was prepared via a substitution reaction using a deprotonated acetylene and a 1° alkyl halide.³⁸ Subsequent reduction to the *cis* isomer was accomplished using Lindlar catalyst (Figure 7).³⁹ This new synthesis has afforded greater *cis*:*trans* ratios (98:2) with virtually no side products, and much greater yields compared to the *cis*-directed Wittig reaction.

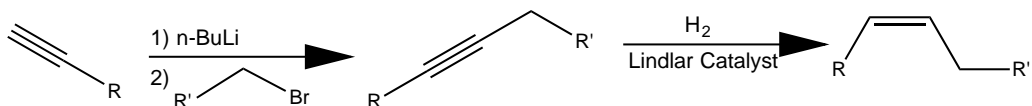


Figure 7. Production of cis-alkene CHCs with a single position of unsaturation is accomplished through nucleophilic substitution with a deprotonated acetylene and a primary alkyl halide, followed by hydrogenation to the cis isomer.^{38,39}

4.2. Dienes

CHCs containing multiple positions of unsaturation require a more complicated synthetic route than that used for monoenes. As illustrated in Figure 8, diene CHCs are produced through a substitution reaction of a deprotonated terminal acetylene with ethylene oxide, adding two methylene groups and forming a primary alcohol⁴⁰, mesylation of the resulting alcohol, followed by a second substitution reaction with another terminal acetylene afforded the diyne.⁴¹ This diyne was then subsequently reduced to the *cis*-diene via hydrogenation with Lindlar catalyst.³⁹

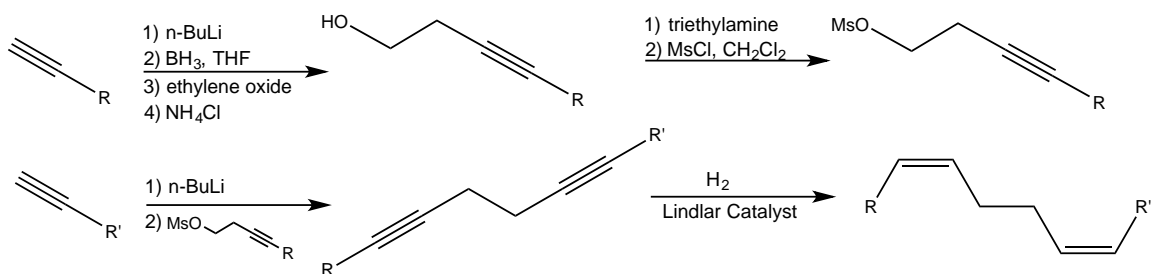


Figure 8. General synthetic route for the production of cis-diene CHCs.^{40,41}

4.3. Branched CHCs

Some CHCs observed in *D. atabasca* extracts are fully saturated but, unlike *n*-alkanes, possess branch sites. Many analogous branched CHCs have been identified in other species, including many of the compounds identified in this work. These compounds may be synthesized through a similar substitution reaction used for production of monoenes (Figure 9). However, complete reduction to the alkane is accomplished using 5% Pd/C, rather than Lindlar catalyst.⁴²

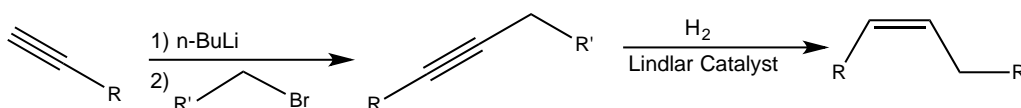


Figure 9. Synthetic scheme for the preparation of 2-methyl branched alkane CHCs via a nucleophilic substitution using a deprotonated terminal acetylene, followed by hydrogenation to the saturated alkane.

An alternate route for synthesis of 2-methyl branched alkanes is a Grignard reaction using an ester to afford a tertiary alcohol. Subsequent dehydration and hydrogenation affords the fully saturated alkane (Figure 10).⁴³

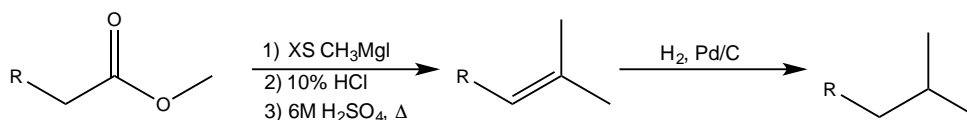


Figure 10. Alternative route for the production of 2-methyl branched CHCs using a Grignard reaction, followed by alcohol dehydration and hydrogenation.

5. Quantification

Synthetic CHC profiles must mimic natural samples, containing all observed compounds in appropriate biological ratios. Once identified and synthesized, quantification of CHCs on individual flies must be accomplished. While various studies utilize internal standards as a means on quantifying biological levels of CHCs^{15,44}, the volatility of the solvents used in these experiments can lead to increased uncertainty in concentrations. A known amount of a standard must be added to each analyzed sample of CHC extract.⁴⁵ Due to the high vapor pressure of the solvent (hexane) used to extract CHCs, an internal standard has the potential to change concentration from one experiment to another, decreasing the accuracy of its response factor. An inaccurate response factor would alter any calculated concentrations of CHCs. As a result, external standard calibration was chosen as a method for quantification. Using linear regression analysis allows for easy calculation of biological concentrations.⁴⁵ Additionally, a calibration curve can be produced for each identified and synthesized CHC. These curves will more accurately represent response factors for each individual analyte, without the inaccuracy of a changing internal standard.

Materials and Methods

Materials.

All reagents were purchased from Sigma-Aldrich unless otherwise noted. All starting materials were used without further purification.

Surveys. CHCs were extracted from a single fly of iso-female lines from a given race via maceration in 50 μL of purified hexanes (multiple flies were macerated in 250 μL), vortexed for 1 m, and then let sit for 2 m. Hexane solutions were then transferred into vial inserts, evaporated to dryness under $\text{N}_{2(\text{g})}$, and reconstituted in 10 μL of purified hexane. CHC extracts were subsequently analyzed via GC-MS using an Agilent 6890/5973 Gas Chromatograph tandem Mass Spectrometer fitted with a 30 m HP-35 column containing a (35%-Phenyl)-methyl siloxane stationary phase. A 5- μL sample was injected in splitless mode. Resolution of individual chromatogram peaks was achieved utilizing ramped temperature programming. The GC oven was held at 70 $^{\circ}\text{C}$ for 1 m, increased to 180 $^{\circ}\text{C}$ at a rate of 20 $^{\circ}\text{C}/\text{m}$, held for 5 m, and finally increased to 250 $^{\circ}\text{C}$ (at 4 $^{\circ}\text{C}/\text{min}$) and held for an additional 15 m.

Synthesis.

Safety Notes. *Caution!* Dimethyl disulfide vapors may form explosive mixtures with air and should be handled with extreme care. Proper personal protective equipment should be used.

Identification.

An array of analytical standards were subjected to GC-MS analysis to obtain retention time and characterization data. Fully saturated, n-alkane hydrocarbons (C₇ – C₃₀; Supelco and C₇ – C₄₀; Supelco) were analyzed, and retention times used to calculate KRIs for observed *D. atabasca* CHCs using the formula derived by Kováts.³⁵ CHCs previously identified in other insects were commercially available, including: (Z)7-pentacosene (Cayman Chemical Company), (Z)7-tricosene (Cayman Chemical Company), (Z)9-tricosene (TCI), (Z,Z)7,11-pentacosadiene (Cayman Chemical Company), (Z,Z)7,11-heptacosadiene (Cayman Chemical Company), and (Z,Z)7,11-nonacosadiene (Cayman Chemical Company) and were used as standards to optimize DMDS derivatization methodology.

DMDS Derivatization.

For compounds containing positions of unsaturation that cannot be identified unambiguously using electron ionization (EI) mass spectrometry, dimethyl disulfide derivatization was employed using a procedure adapted from Carlson et al.³⁴ Prepared CHC extracts from 50 to 100 flies were added to hexane (200 µL). An iodine solution (100 µL of 60 mg/mL in Et₂O) was added, followed by reagent grade DMDS (200 µL). The solution was held at 40 °C for 4 h or overnight. The reaction was quenched with 5% aqueous sodium thiosulfate, dried over MgSO₄, filtered, and the organic phase was analyzed by GC-MS.

Bromination.

Fully saturated, branched CHCs present a different challenge and no current literature examples of derivatization exist. However, bromination of tertiary positions allows for successful, and selective, derivatization of branched alkanes.

Thus, a useful method was developed to successfully and reproducibly identify crucial structural information regarding branched hydrocarbons including: branch size and location.

Bromination with Molecular Bromine.

A hexane fly extract was evaporated to dryness under $N_{2(g)}$ and reconstituted in dichloromethane (100 μ L). Two to three drops of molecular bromine were added and the solution was stirred at 40 °C for 3-4 h. The reaction was quenched with 5% aqueous sodium thiosulfate (100 μ L), dried with $MgSO_4$ and filtered. The organic layer was analyzed using GC-MS.

Synthesis of Identified CHCs.

All characterized CHCs were subsequently synthesized to confirm retention time, structure, stereochemistry, and geometric isometry.

Synthesis of 2-methylhexacosane.

Preliminary synthesis of branched alkanes was completed using the reaction scheme outlined in Figure 10. To a stirred mixture of Mg° in anhydrous THF (0.5 g in 4 mL) was added iodomethane (2.5 mL), dropwise over 30 m. Once added, the mixture was refluxed for 30 m and then cooled to room temperature. A solution of methyl pentacosanoate (50 mg) in anhydrous THF (4 mL) was added dropwise over 30 m and then refluxed for 4 h. The solution was poured off the remaining Mg° and Mg salts and quenched with 10% HCl (10 mL). The solution was extracted with MTBE (20 mL), washed with bicarbonate, and concentrated *in vacuo*. The resulting residue was resuspended in hexane (25 mL). To this suspension, 5% Pd-C (0.75g) was added and the reaction mixture was hydrogenated to completeness under H_2

balloons. The mixture was filtered through Celite, concentrated *in vacuo*, reconstituted in hexane and analyzed by GC-MS.

Quantification of CHCs using External Standard Curves.

Calibration curves were produced using multiple standard solutions of varying concentration of synthetic CHCs. Standard solutions of known concentrations were analytically prepared and analyzed sequentially by GC-MS. The concentration of each standard was plotted against its respective peak area from the GC chromatogram to afford external standard curves. Linear regression analyses were performed to determine quantities of material in each single-fly CHC extract.

Results

Full characterization of CHCs in *D. athabasca* is crucial to further understanding of their biological roles in this organism. Single individuals from each race were analyzed using established GC-MS methods described in the Methods Section. Both concentrated, pooled samples and individuals were analyzed by GC-MS. Over 20 individual compounds were present in each race. Branched, saturated, mono- and di-unsaturated compounds ranging from C15-C30 were identified using a combination of chemical derivatization and mass spectral analysis approaches.

Analysis of Linear Alkane Standards

Mass spectra and retention times of purchased *n*-alkane standards (C7-C40; see Appendix B – C39 and C40 were not observed due to low vapor pressure) were compared to observed fly profiles to identify any potential saturated CHCs. Mass spectra from fly samples were analyzed and M⁺ peaks also confirmed saturation. One fly CHC, located at 22.90 m, was identified as *n*-tricosane and its mass spectrum is illustrated in Figure 11.

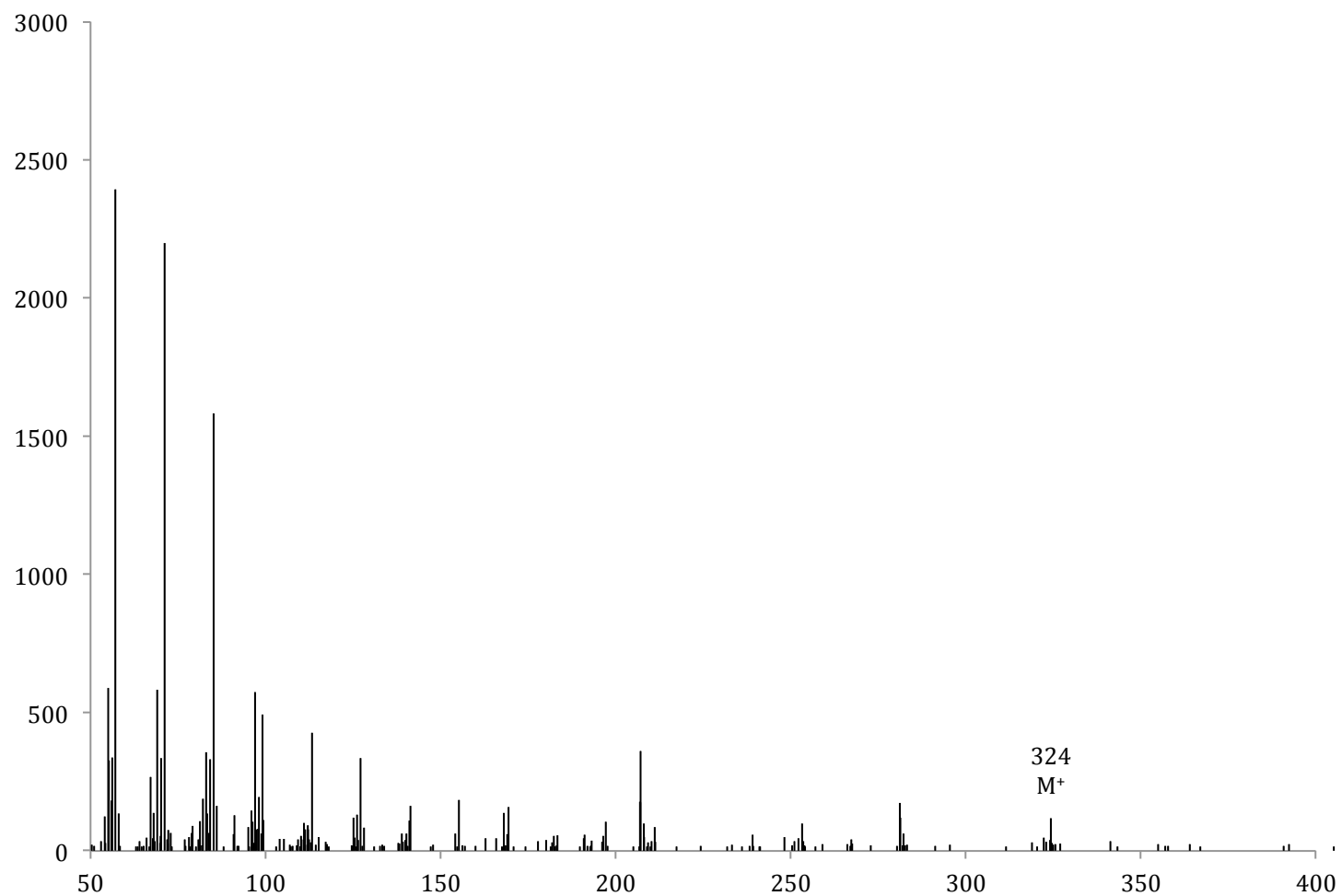


Figure 11. Mass spectrum of CHC located at 22.90 m. Compared to mass spectra of n-alkanes, this CHC was determined to be *n*-tricosane.

Identification of Branched Alkanes.

Unlike linear alkanes that display a continuously increasing abundance from high to low m/z ratios, each branched spectrum will contain high abundance fragments corresponding to alpha cleavage points, disrupting the continuum. For proposed 2-methyl branched alkanes, two major peaks exist with mass-to-charge ratios of $[M-15]^+$ and $[M-43]^+$. The loss of 15 m/z corresponds to the cleavage of a methyl group from the second carbon, while the fragment with a loss of 43 m/z results from the loss of a propyl group (See Figure 12).

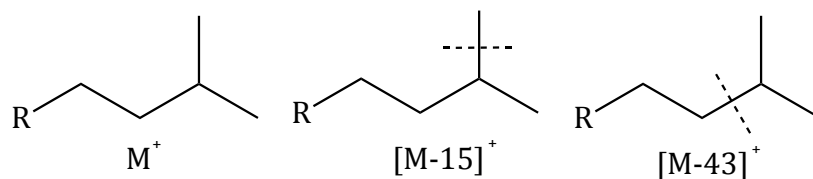


Figure 12. Fragmentation pattern of 2-methyl branched alkanes. A loss of 43 m/z is indicative of the loss of a propyl group, while $[M-15]^+$ corresponds to loss of a single methyl group.

The fragmentation pattern illustrated in Figure 12 was considered and carefully compared to CHC mass spectra flagged as resulting from saturated CHCs to identify any 2-methyl branched alkanes. Figure 13 shows the mass spectrum of the CHC at RT 30.12 m.

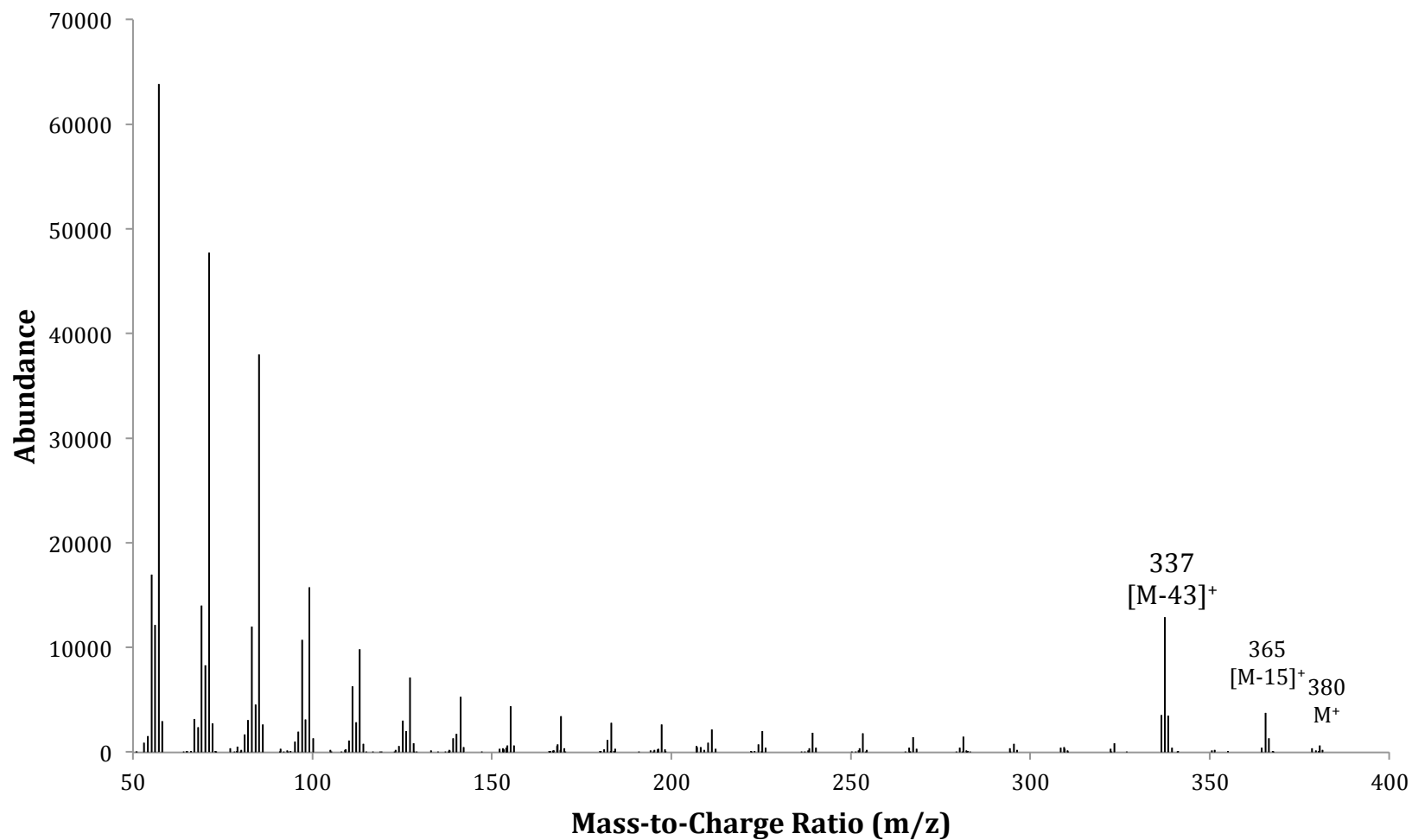


Figure 13. Mass spectrum of CHC observed at 30.12 m in all three races of *D. athabasca*. Peaks at 337, 365, and 380, are indicative of a methyl branch at the second carbon of a C26-chain, or 2-methylhexacosane, based on the fragmentation pattern in Figure 12.

Additional 2-methyl branched alkanes were also identified, including: 2-methyldocosane (2-Me-C22), 2-methyltetracosane (2-Me-C24), 2-methylpentacosane (2-Me-C25), 2-methylheptacosane (2-Me-C27), 2-methyloctacosane (2-Me-C28), and 2-methyltriacontane (2-Me-C30). The mass spectra additional 2-methyl CHCs are illustrated in Figures C1 through C6, respectively (Appendix C) and identities are listed in Table 1 (see Appendix A).

Derivatization of Branched Alkanes Using Molecular Bromine.

Unlike CHCs with more reactive functional groups (i.e. saturations, esters, etc.), branched alkanes contain no obvious reactive functional groups. Currently, no derivatization method has been described to confirm identities of branched, saturated CHCs. A bromination protocol was developed to locate positions of branching. A CHC extract containing 25 EB flies was first analyzed using GC-MS and then subjected to free radical bromination conditions. The resulting chromatograms, pre- and post- bromination, are illustrated in Figure 14.

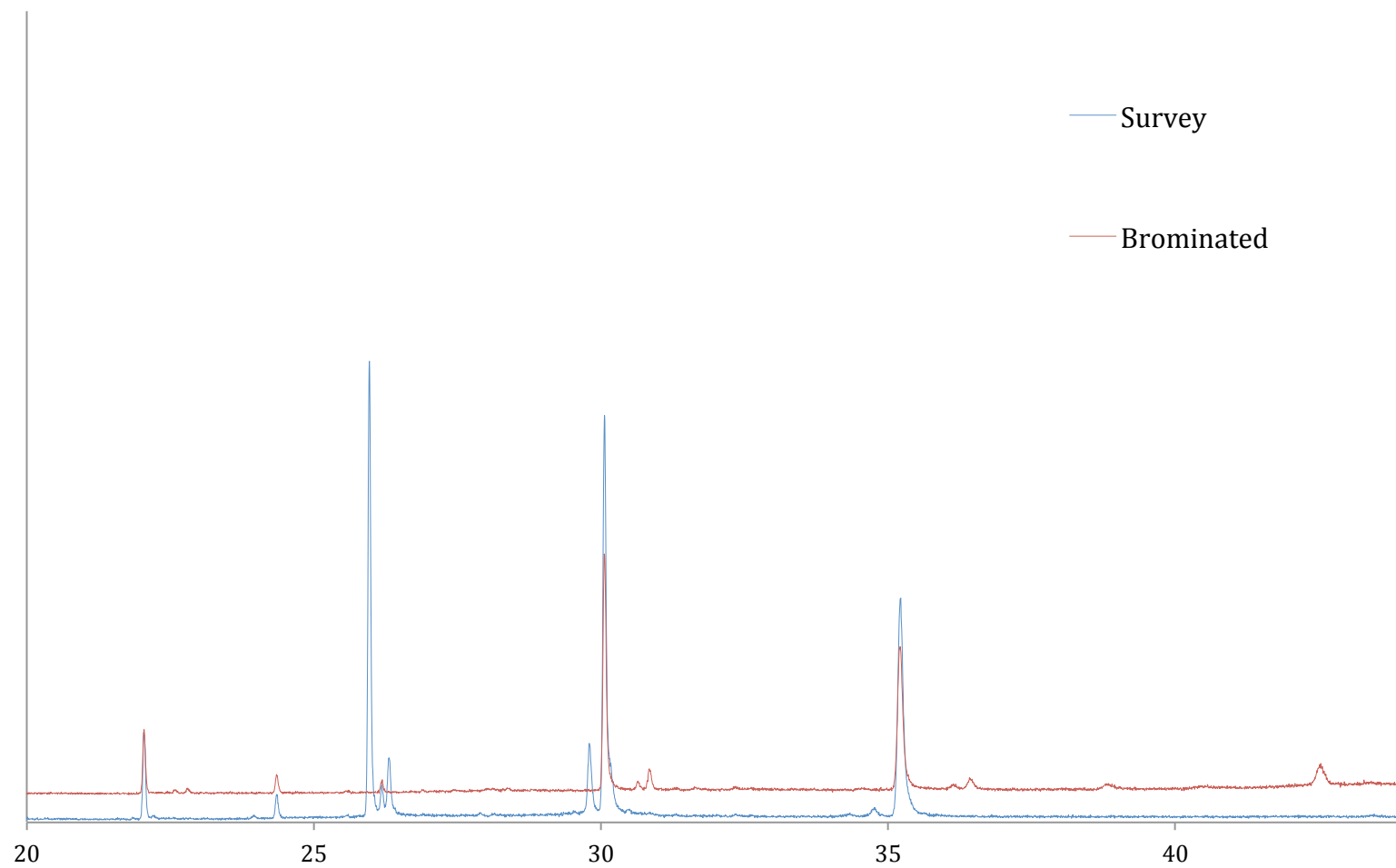


Figure 14. An extract of 25 EB flies (blue) was subjected to brominating conditions. Post-bromination, the sample was analyzed by identical GC-MS methods to afford the spectrum in red.

Post-bromination, the CHC extract was analyzed to search for characteristic bromine fragments in the mass spectrum. Immediately following each peak predicted to be a branched alkane, were two novel signals, with M^+ showing a loss of two m/z units relative to the natural CHC mass spectrum. A loss of two mass-to-charge ratio units indicated an elimination reaction occurred, following the bromination of each branched alkane. Mass spectra of non-brominated 2-methylhexacosane, and identified branched CHC, and the corresponding elimination product(s) are illustrated in Figure 15. Mass spectra comparing pre-and post-bromination/elimination CHCs are shown in Figures D1 through D3 in Appendix D.

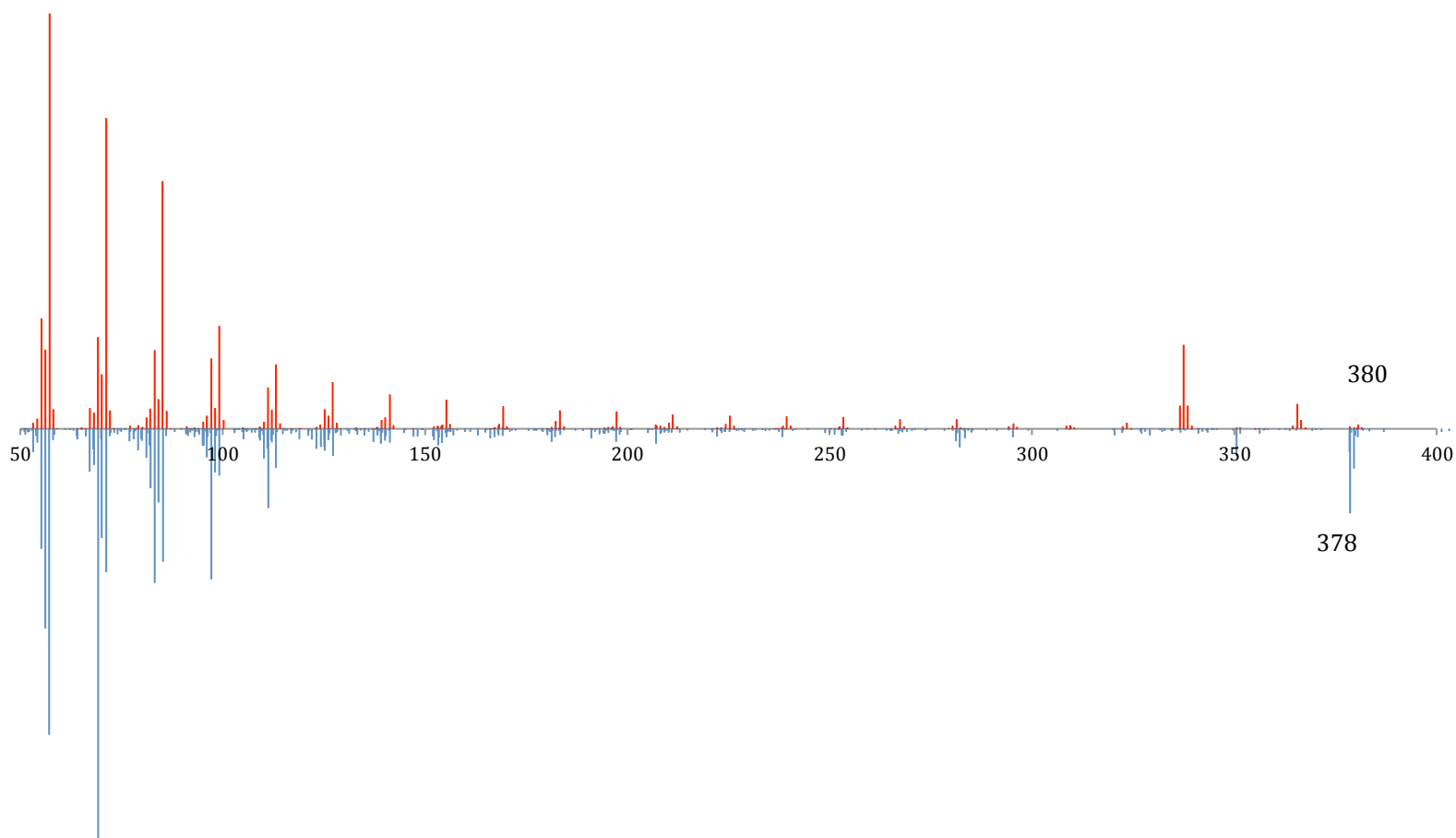


Figure 15. 2-methylhexacosane mass spectrum pre-bromination (top, red) and post-bromination (bottom, blue). A loss of two m/z in the post-bromination mass spectrum is indicative of an elimination reaction, and not bromination.

Further, synthetic materials were generated to confirm the identity of branched CHCs. Figure 16 shows a comparison between a fly-obtained mass spectrum of 2-methylhexacosane (**red**), a proposed branched alkane, and material synthesized (**blue**) using the Grignard reaction scheme outlined in Figure 10.

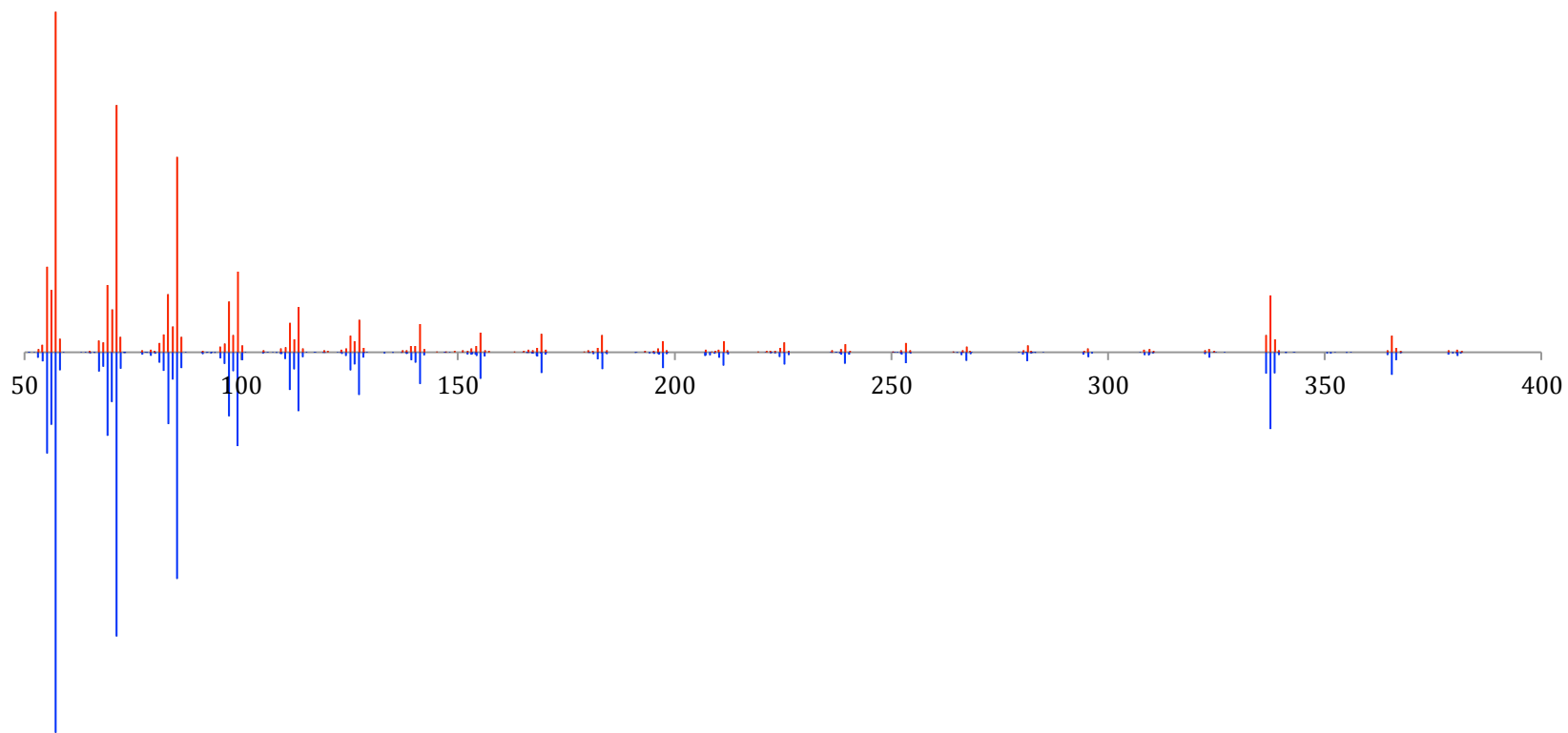


Figure 16. Mass spectral comparison of fly 2-MeC26 (red) and synthetic 2-Me-C26 (blue). Identical mass spectra confirm the identity of 2-methylhexacosane as a branched alkane located at ~30.12 m.

In a similar manner to 2-methyl, other branched alkanes can be identified using mass spectrum fragmentation analysis. One CHC, noted exclusively in EB, presented with a mass spectrum consistent with a branched alkane but the fragmentation pattern consistent with a 2-methyl branching as shown in Figure 12 was not observed. The fragmentation pattern illustrated in Figure 18 was considered and carefully reconstructed to identify the compound as 3-methyltricosane. Peaks at $[M-15]^+$, $[M-29]^+$ and $[M-57]^+$ were predominant in this mass spectrum, consistent with 3-methyl branching (Figure 17). However, no M^+ peak was observed.

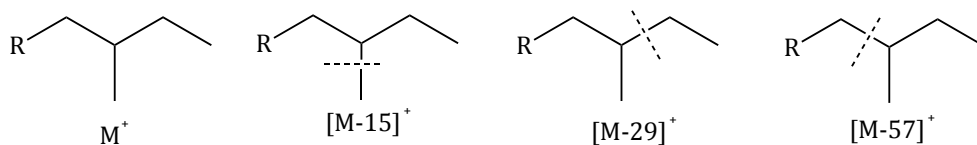


Figure 17. Fragmentation pattern of 3-methyl branched CHCs. A loss of 15 m/z corresponds to a loss of a methyl group, loss of 29 m/z corresponds to loss of an ethyl, and loss of 57 m/z corresponds to a loss of a sec-butyl group.

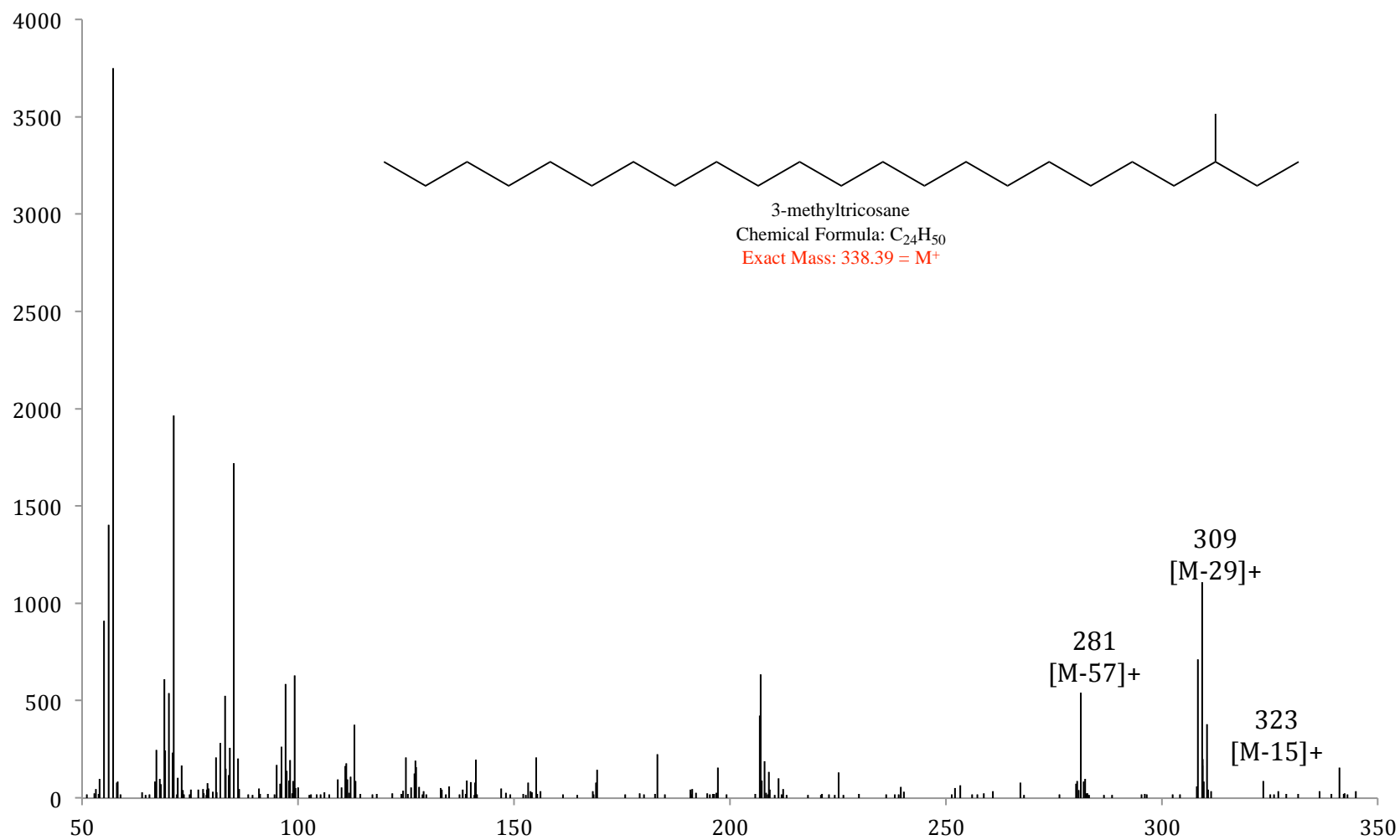


Figure 18. Mass spectrum of CHC at 24.42 m in EB flies. Fragments at $[M-15]^+$, $[M-29]^+$ and $[M-57]^+$ are indicative of a methyl branch at the 3rd carbon of a C23-chain, or 3-methyltricosane.

Identification of Monoenes.

Interpretation of mass spectra from compounds containing positions of unsaturation often leads to ambiguity. Thus, derivatization reactions must be utilized. In these experiments, DMDS was used as an electrophile to add across the double bond, generating thioether adducts.

Typically, chromatograms of DMDS-derivatized mixtures contain unchanged signals from unreactive compounds such as methyl branched and linear alkanes. Signals that disappear upon reaction with DMDS were deemed reactive and considered for further analysis. New signals appeared at longer retention times (~20 m; see Figure 19) with mass spectra containing M^+ and characteristic fragments indicative of thioether DMDS adducts.

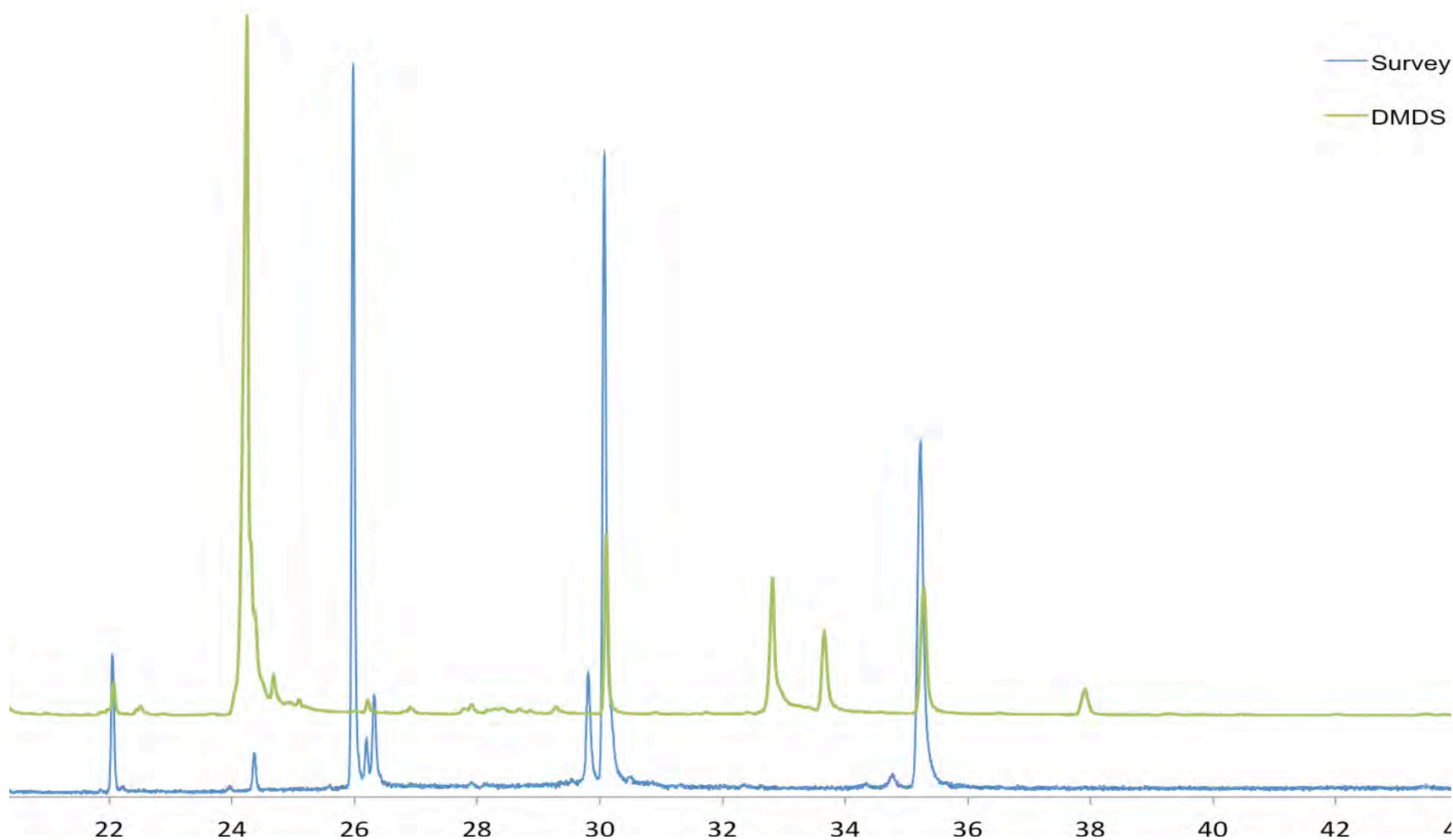


Figure 19. DMDS-derivatized (green) versus unreacted survey (blue) of a 25-fly CHC extract from EB flies. Peaks that disappear upon reaction with DMDS are classified as unsaturated and further investigated. New peaks in the DMDS chromatogram are also investigated.

DMDS derivatization was performed on 100-fly extracts, affording spectra elucidating isomeric mixtures of alkenes. For example, Figure 20 illustrates the mass spectrum observed for GC signal post-DMDS derivatization. Two sets of fragments (243 and 201 m/z; 215 and 229 m/z), along with a single M⁺ peak of 444 m/z are indicative of a mixture of pentacosenes with unsaturations at the 11th and 12th carbons. Thus, these spectra correspond to 11-pentacosene and 12-pentacosene.

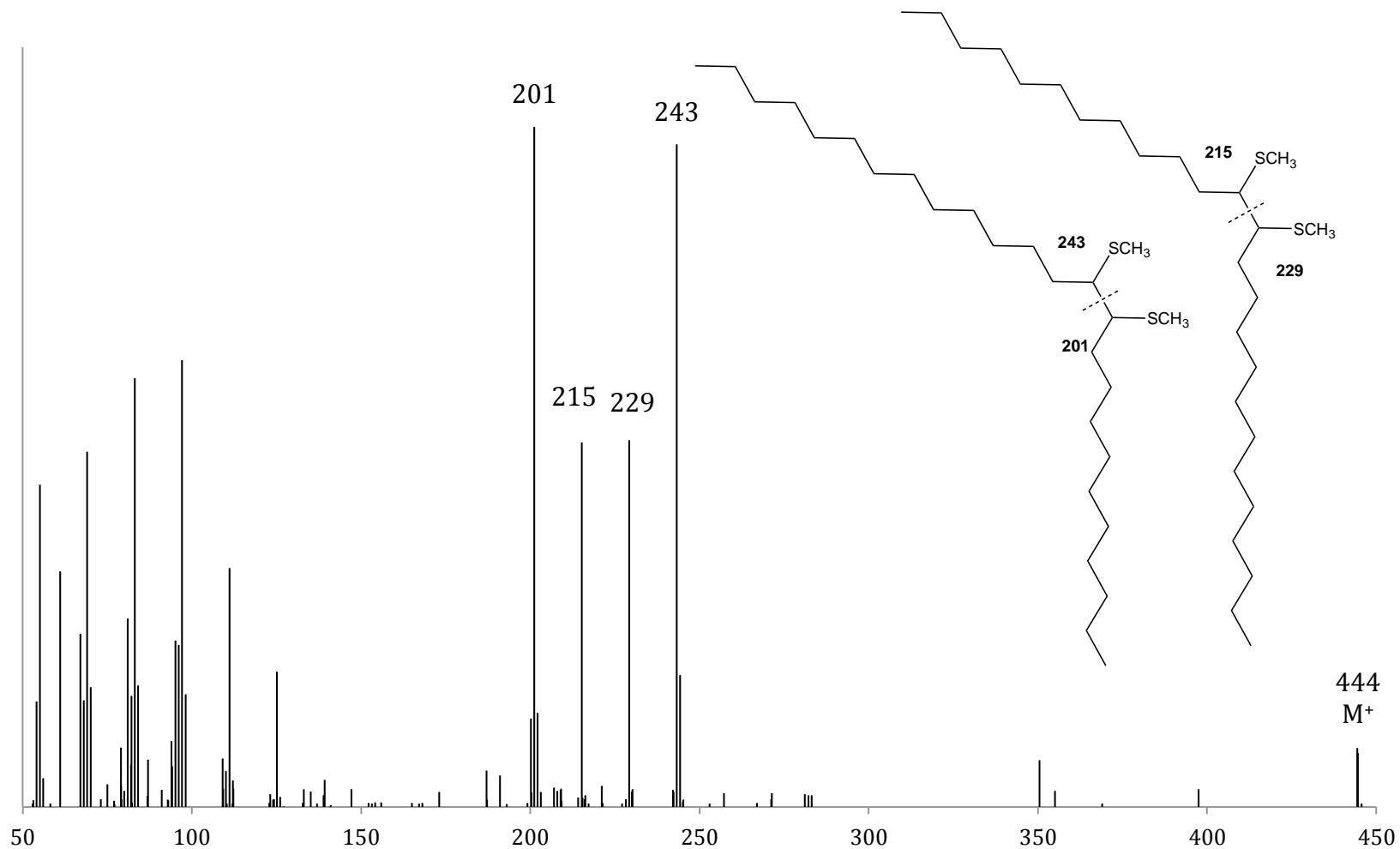


Figure 20. DMS-derivatized mass spectrum containing two sets of fragments corresponding to 11- and 12-pentacosene. Insets are fragmentation patterns of the identified pentacosene DMS adducts.

Both geometric isomers of 11-pentacosene and 12-pentacosene were synthesized to confirm identity and geometric isometry of the observed CHC.

An additional mixture of DMDS derivatized CHCs were observed in both EA and WN. Illustrated in Figure 21, three individual sets of fragments (173 and 243; 187 and 229; 201 and 215 m/z) were observed in the mass spectrum of the DMDS-derivatized CHC mixture. With an M^+ peak of 416 m/z, the fragments were reconstructed to identify the original CHCs as tricosenes (C23:1) with unsaturations at the ninth, tenth, and eleventh carbons.

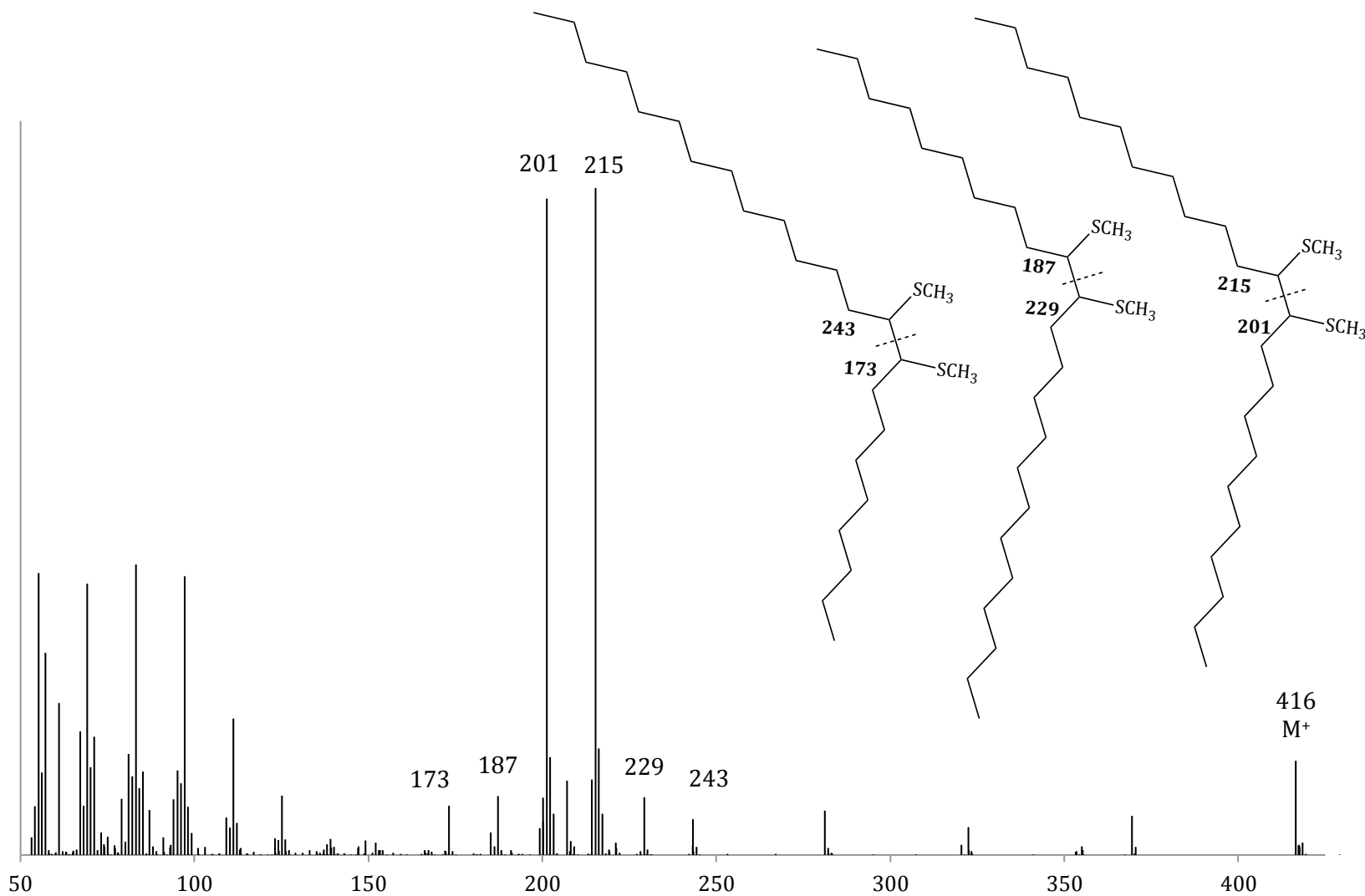


Figure 21. Mass spectrum of DMDS derivatized CHCs. A total mass of 416 m/z , along with three sets of fragments indicates three different tricosene (C₂₃:1) isomers with unsaturations at the 9th, 10th, and 11th carbons.

An additional monoene CHC was identified at 24.39 m (see Table 1). The molecular ion of this peak was 336 m/z, indicative of a tetracosene (C₂₄:1; see Figure 5 in Appendix E). Upon treatment with DMDS, a new peak appeared in the chromatogram. The mass spectrum corresponding to this signal is shown in Figure 22. An M⁺ of 430 m/z confirms an addition of DMDS to a tetracosene. However, two fragments were not observed in the mass spectrum, but rather, one major peak appeared at 215 m/z. Upon reconstruction of two fragments, each equivalent to 215 m/z, the CHC was determined to be 12-tetracosene. The existence of a single fragment is due to the symmetric nature of this compound.

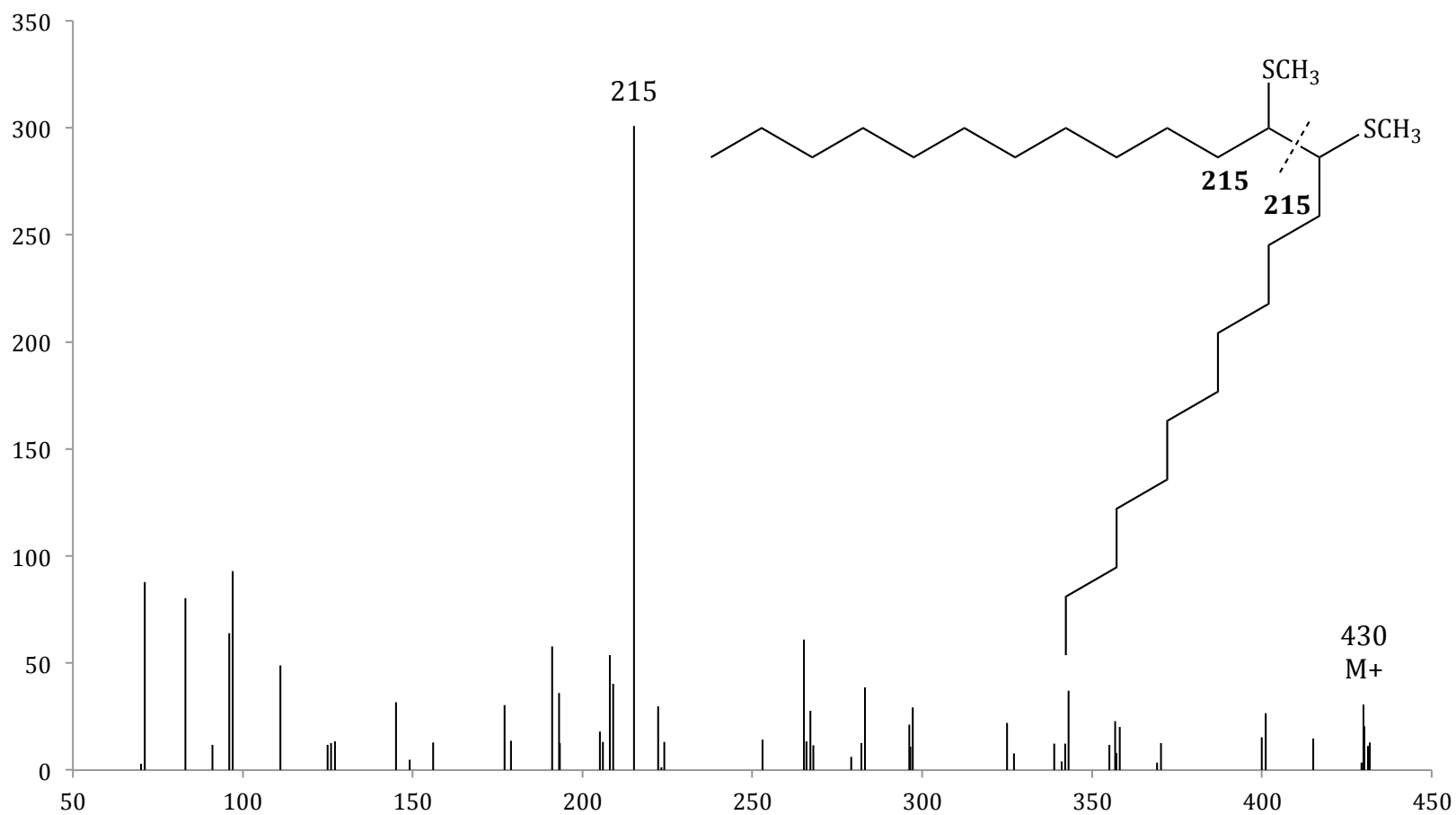


Figure 22. Mass spectrum of DMDS-derivatized 12-tetracosene. The symmetry of 12-tetracosene results in the observation of only a single peak.

Identification of Dienes.

Similarly to monoenes, dienes can be characterized using DMDS derivatization. Unlike their monounsaturated counterparts, dienes can generate multiple thioether adducts following reaction with DMDS. For instance, only one of the two unsaturations can react with DMDS, yielding half-reacted adducts observable in the mass spectrum (Figure 23), as described in Figure 4. Dienes might also fully react to generate multiple vicinal thioethers at each unsaturated position. However, when the unsaturated positions are within a certain distance, cyclic thioether products are possible further complicating the analysis of mass spectra of DMDS derivatized samples. Though convoluted, the mass spectra of these cyclic adducts provide further evidence confirming the identity of the dienes. For example, confirmation of 10,14-pentacosadiene utilized cyclic DMDS adducts mass spectrum data illustrated in Figure 24.

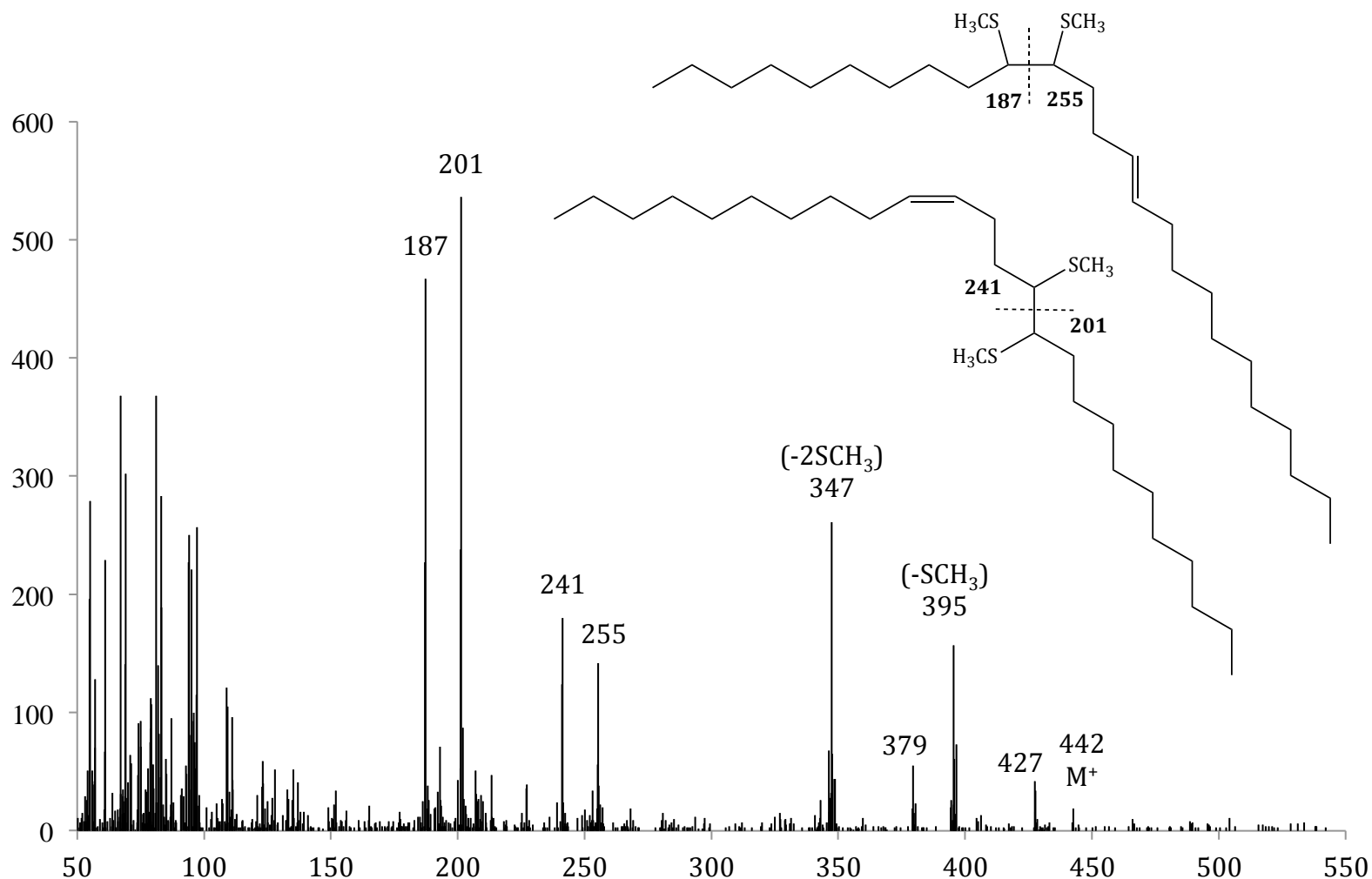


Figure 23. Mass spectrum of DMS-derivatized 10,14-pentacosadiene with one equivalent of DMS. Inset is the fragmentation patterns of the thioether adducts of this derivatization. Signals at 395 and 347 m/z correspond to cleavage of one SCH₃ group and two SCH₃ groups, respectively. Signals at 427 m/z and 379 m/z correspond to small amounts of cyclic adduct shown in Figure 24.

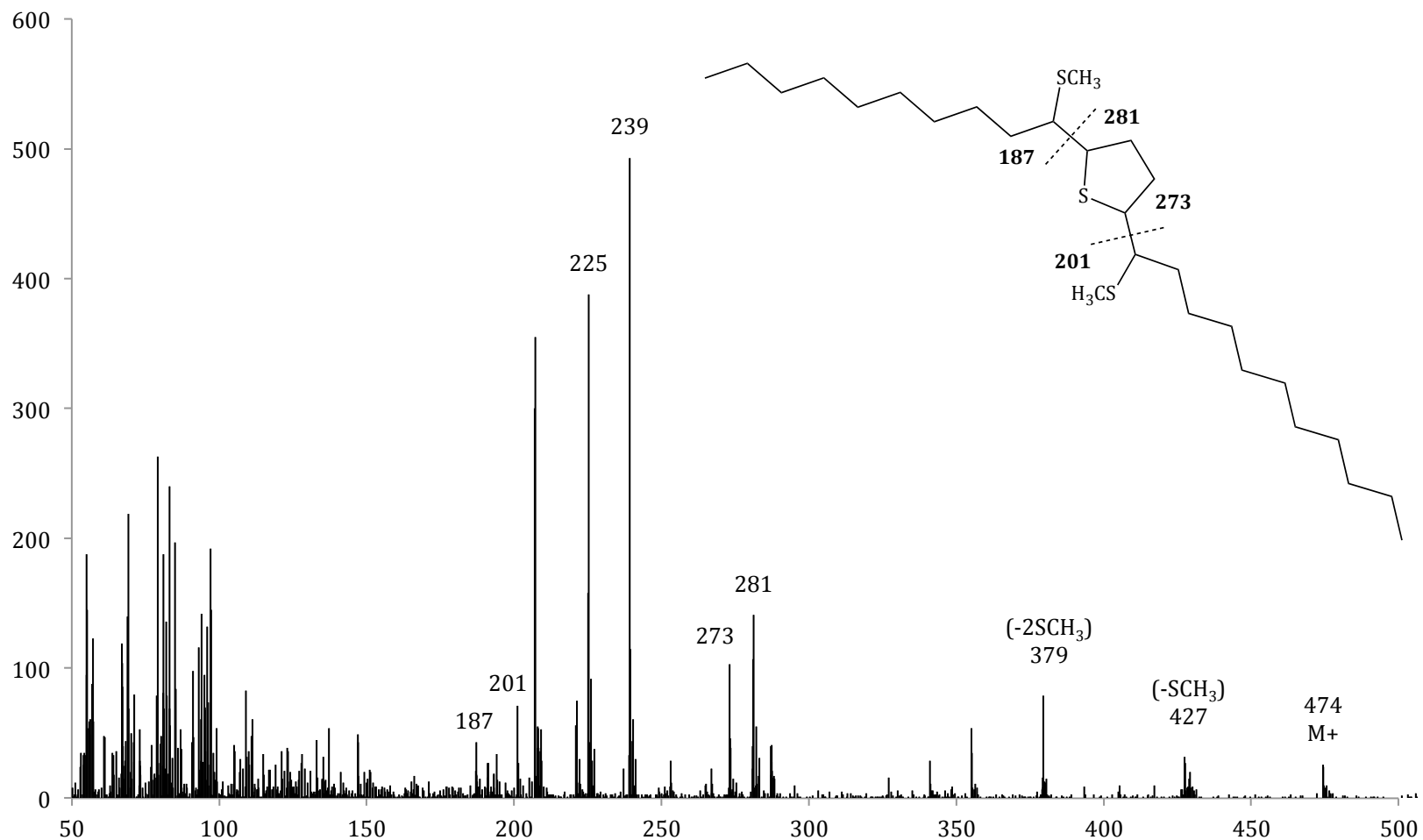


Figure 24. Mass spectrum of DMDs-derivatized 10,14-pentacosadiene, cyclic adduct. Inset is the fragmentation patterns of the thioether adducts of this derivatization. (2 molar equivalents of DMDS reagent). The signal at 207 m/z is due to column bleed.

Identification of *cis*-Vaccenyl Acetate

Several CHCs were identified exclusively using mass spectral analysis and comparison to both literature data and synthetic standards. These compounds displayed varying functionalities including: acetates, methyl esters, and carboxylic acids. Figure 25 illustrates the mass spectrum of a CHC located at 20.50 m, observed solely in male profiles. This mass spectrum was predicted to be (Z)11-octadecn-1-yl acetate, or *cis*-Vaccenyl acetate (cVA) based upon literature data published by Ray et al.⁴⁶

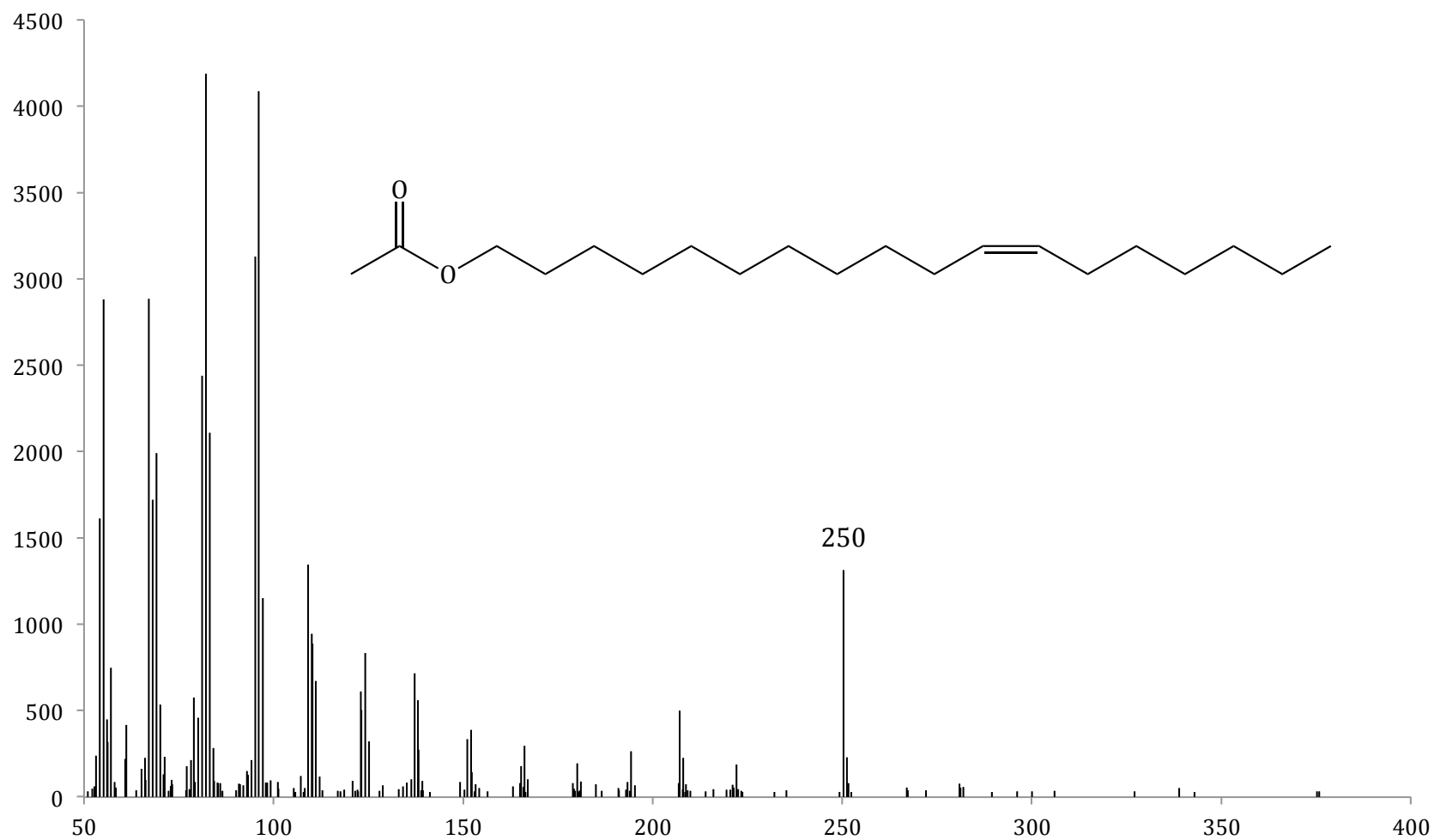


Figure 25. Mass spectrum of the CHC at 20.5 m, identified as cVA, exclusively found in males from all races of *D. athabasca*. As reported, no molecular ion was observed in this spectrum.⁴⁶ Inset is the chemical structure of cVA.

Identification of Saturated and Unsaturated Carboxylic Acids

Identification of unsaturated carboxylic acids was accomplished using the fragmentation pattern outlined in Figure 26. Presence of a peaks in the mass spectrum equivalent to $[M-18]^+$ and $[M-60]^+$ are indicative of a carboxylic acid. $[M-18]^+$ corresponds to the cleavage of the hydroxyl portion of the carboxylic acid while $[M-60]^+$ is a result of a cleavage proximal to the alpha carbon. The number of unsaturations is subsequently determined by comparing the M^+ to the M^+ peaks of the linear alkanes shown in Figures B1 through B32 (Appendix B).

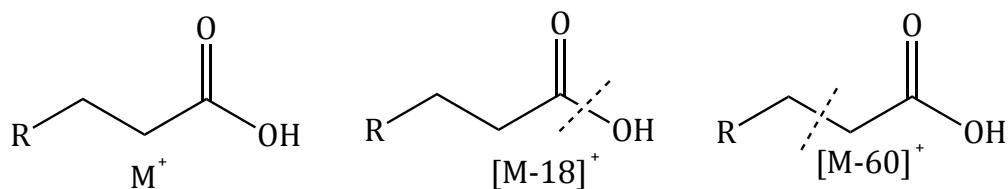


Figure 26. Fragmentation pattern of unsaturated carboxylic acids analyzed by EI-MS.

Saturated carboxylic acids, such as hexadecanoic acid illustrated in Figure 28, were identified by comparison to literature mass spectra compiled in the NIST Mass Spectral Library.

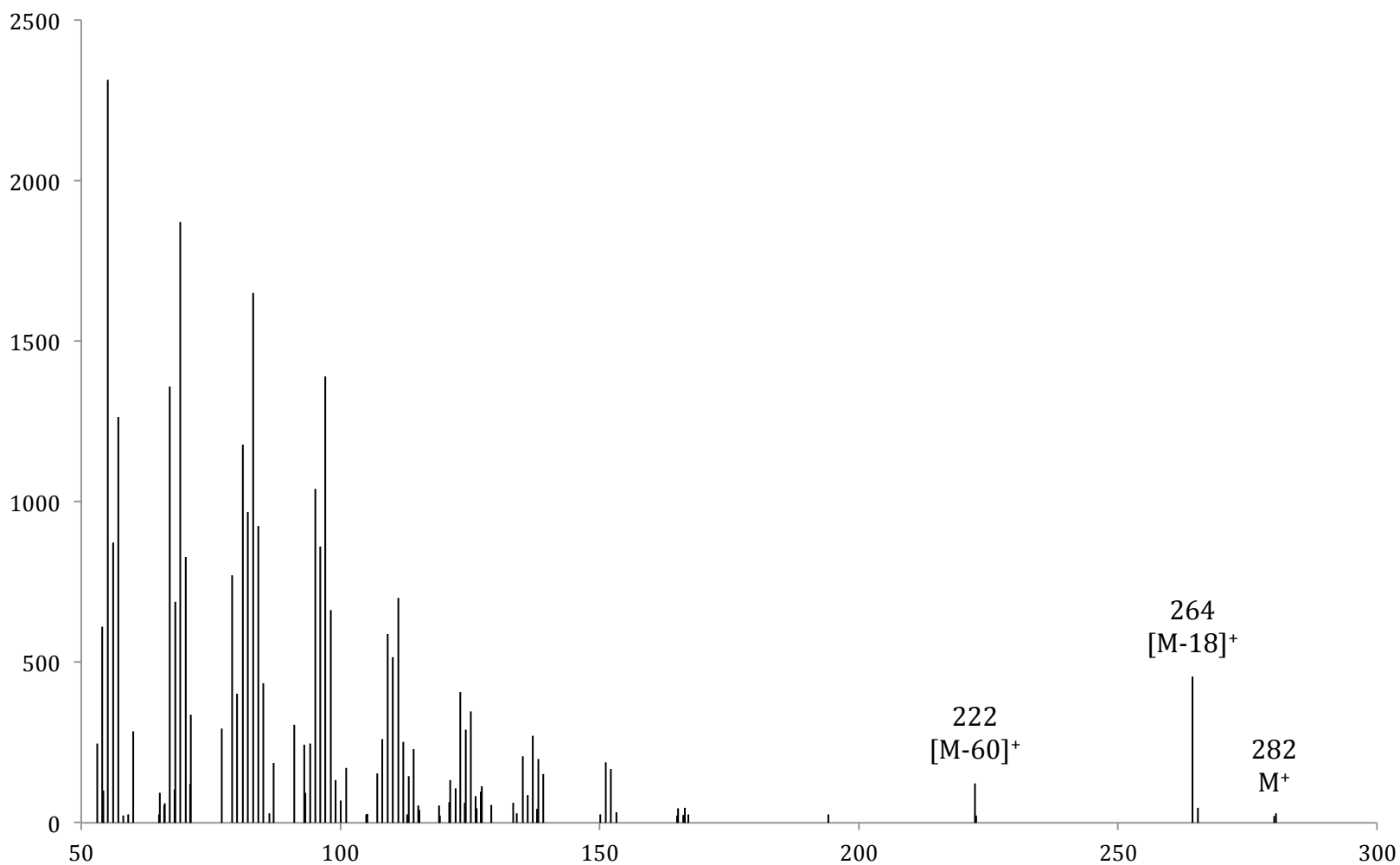


Figure 27. Mass spectrum of a CHC at 19.32 m in all races. The fragmentation pattern of this CHC was compared to literature spectra and determined to be oleic acid. Synthetic oleic acid was subsequently analyzed via GC-MS to confirm this identification (see overlay in Figure G7 in Appendix G).

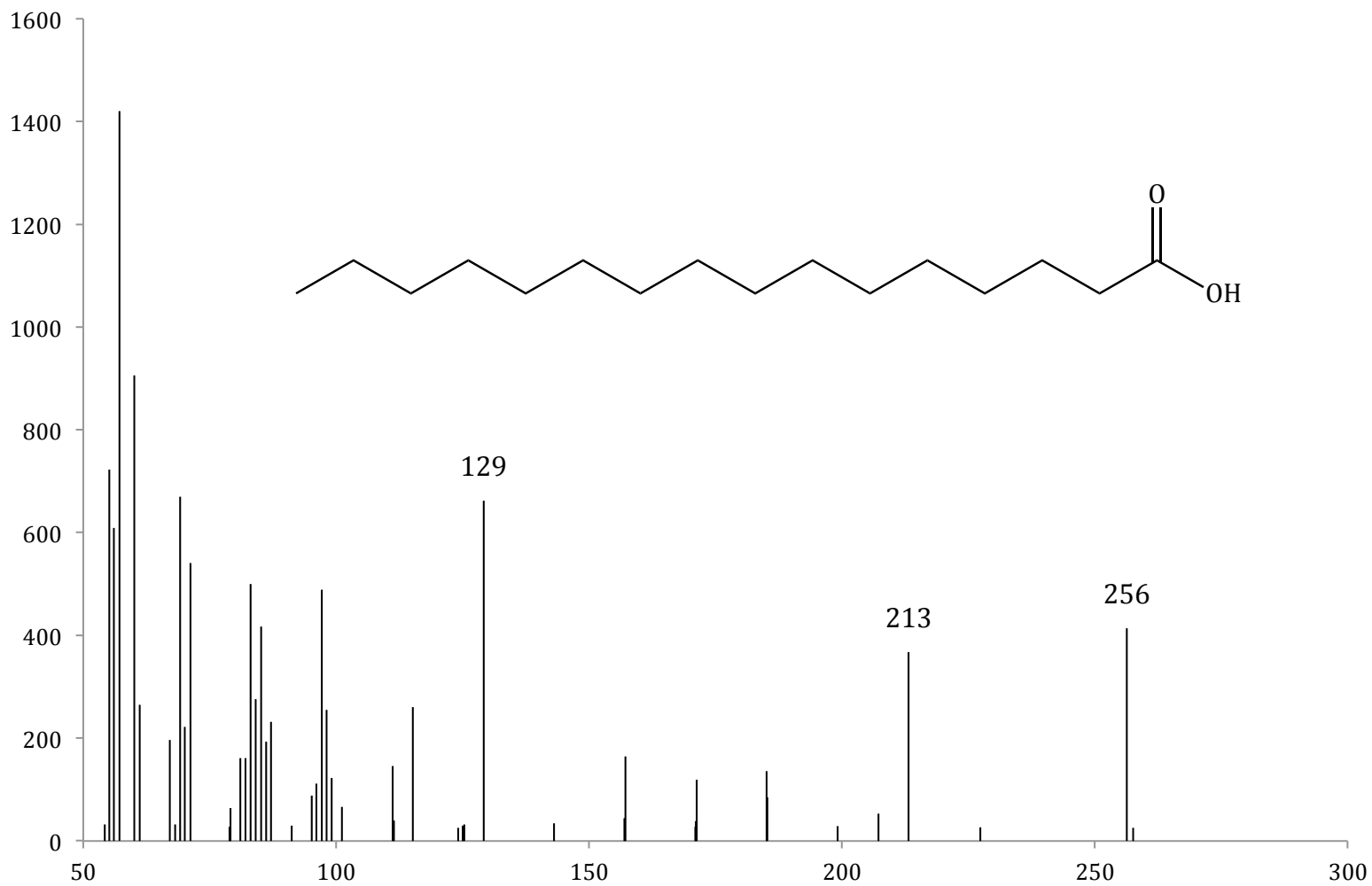


Figure 28. Mass spectrum of a CHC at 15.19 m. Using the NIST 14 Mass Spectral Library, this compound was identified as hexadecanoic acid.

Identification of Methyl Esters

Several CHCs exhibit mass spectra that are characteristic of methyl esters. One distinguishable fragment occurs at $[M-31]^+$, indicative of the cleavage of the methoxy group (Figure 29). Figure 30 illustrates a mass spectrum collected from a CHC extract with a noticeable $[M-31]^+$ peak. Based upon this fragmentation pattern, this CHC was identified as methyl hexadecanoate, a C16 methyl ester.

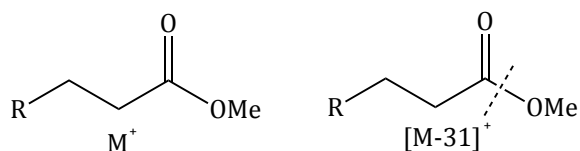


Figure 29. Mass spectral fragmentation pattern of methyl esters.

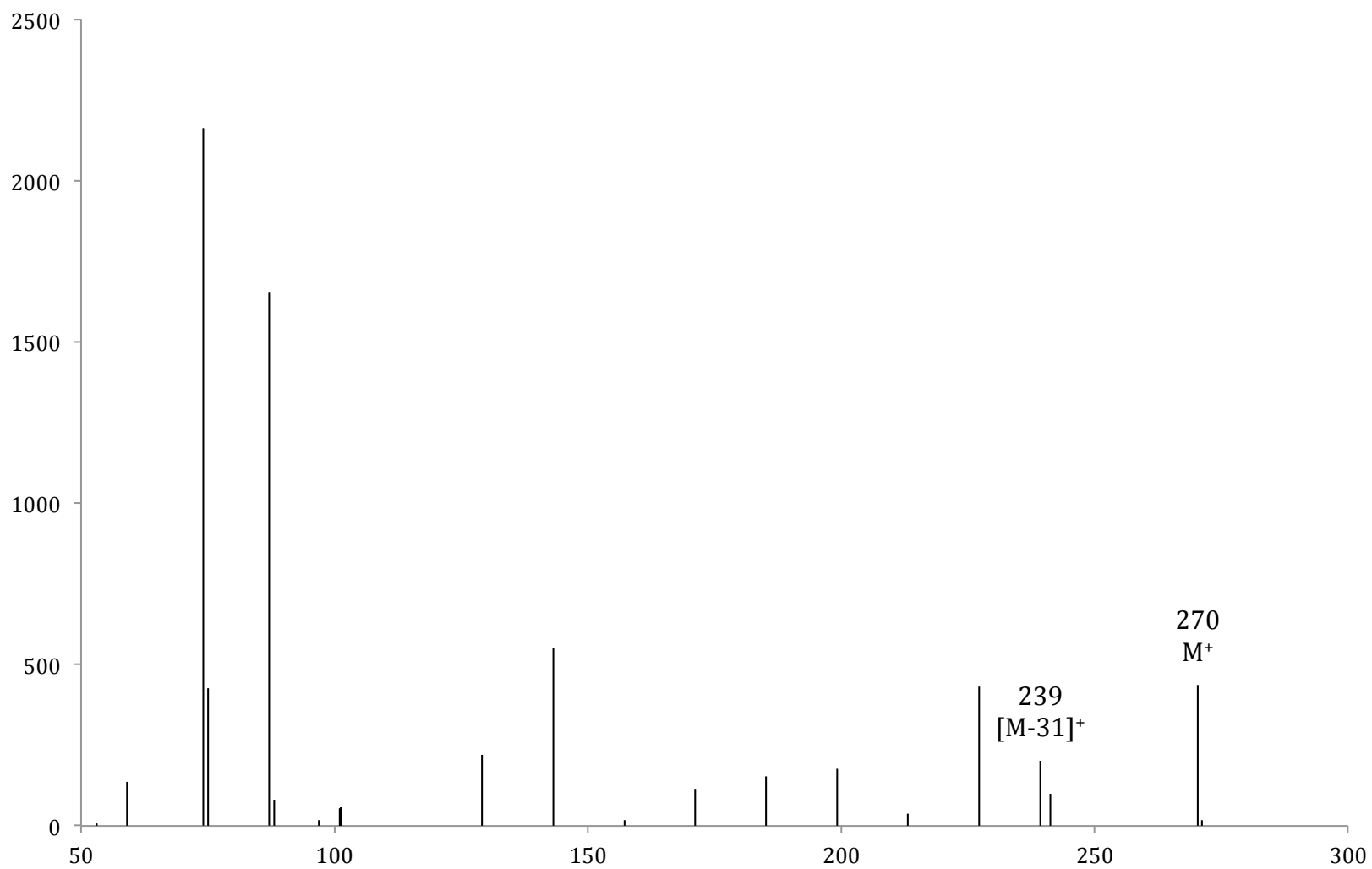


Figure 30. Mass spectrum of a CHC at 14.36 m. The fragmentation pattern illustrated in Figure 29 was used to identify this compound as methyl hexadecanoate.

Quantification of CHCs Using External Standard Curves

Six calibration curves have been developed using external solutions of known CHC concentration. Figure 31 shows the standard curve for synthetic (Z)11-tricosene. Additional standard curves are illustrated in Appendix G.

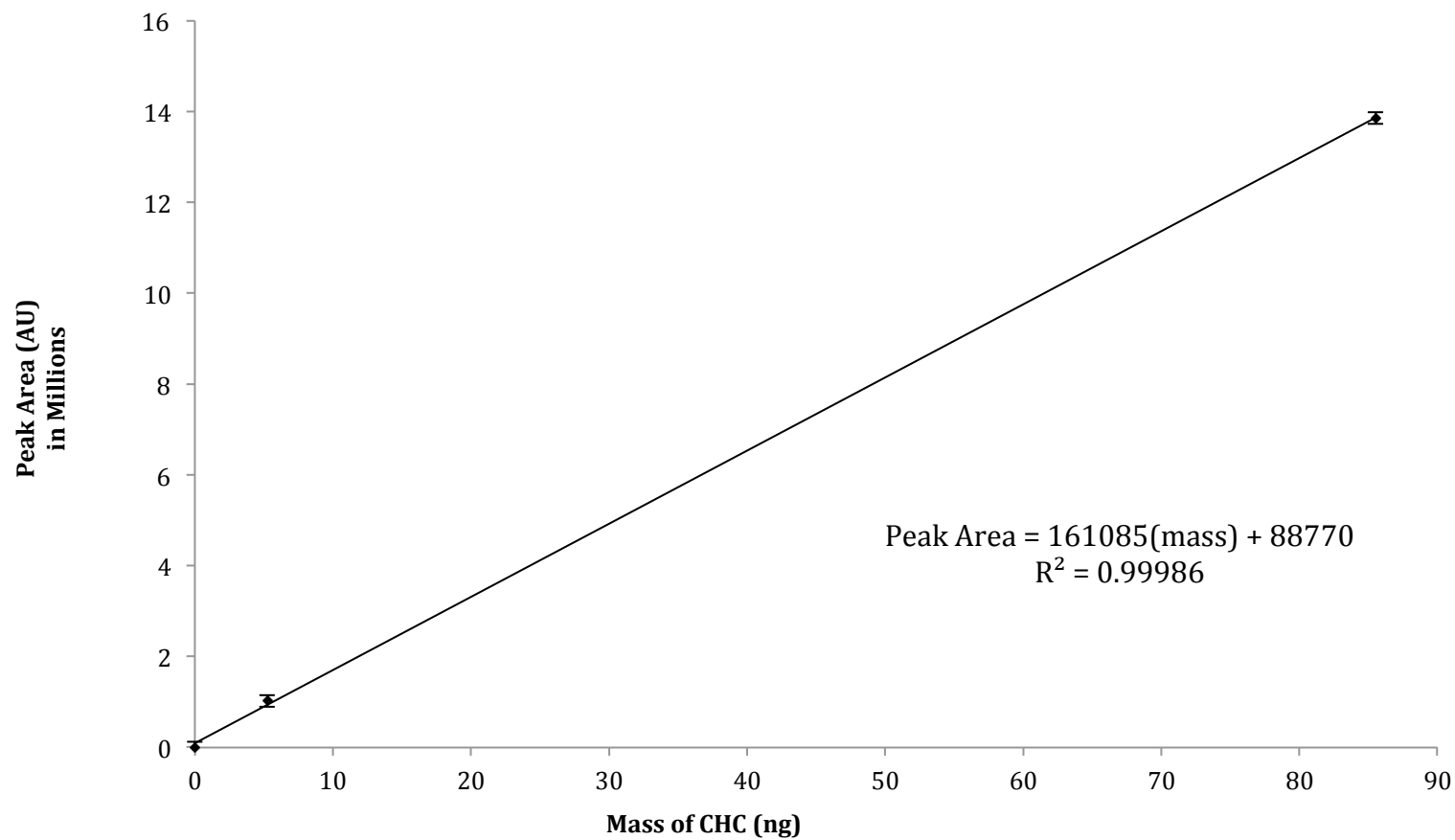


Figure 31. External calibration curve generated from standards of known concentrations of synthetic (Z)11-tricosene. Linear regression analysis using this curve allowed for quantification of CHCs in single fly samples.

Intra-racial Variability

A complete understanding of the roles that CHCs may play in in *D. athabasca* requires extensive evaluation of the variation that occurs both within each race and between the two races. GC-MS analysis of single-fly extracts from multiple lines of a given race allowed for compilation of CHC profiles to observe and note any potential intra-racial variation. All three races were compared individually, with profiles randomly chosen and overlaid to compare CHC variation.

Eastern A. Figure 32 illustrates four overlaid CHC profiles of single EA flies. Qualitative differences in CHC profiles were determined using overlay figures like this while quantitative data were collected from the percent of the total CHC content in each profile. Figure 33 was utilized to determine differences between sexes of the same fly line, LK1.

Eastern B. CHC profiles from single EB flies were compared to depict variation within the race. Figure 34 illustrates eight overlaid single fly CHC profiles used to identify any potential variation within the EB race. The chromatograms have been standardized by peak area to note any quantitative and qualitative differences. Additionally, single male and female chromatograms were overlaid (Figure 35) to detect any variation between the sexes.

WestNorthern. Similarly to EA and EB, CHC profiles from WN flies were overlaid to look for intra-racial variation. Figure 36 illustrates ten overlaid single fly CHC profiles from different lines of the WN race. The chromatograms have been standardized by peak area to note any quantitative and qualitative differences. A single male and female chromatograms was overlaid (Figure 37) to detect any variation between the sexes.

Inter-racial Variability

Ultimately, differences between each race of *D. athabasca* must be well understood to produce the most accurate non-natural profiles possible. To compare CHC variability between EA, EB and WN, chromatograms from 100-fly extracts were overlaid (Figure 38). Both qualitative and quantitative differences in this figure were subsequently analyzed to search for any variation between the races.

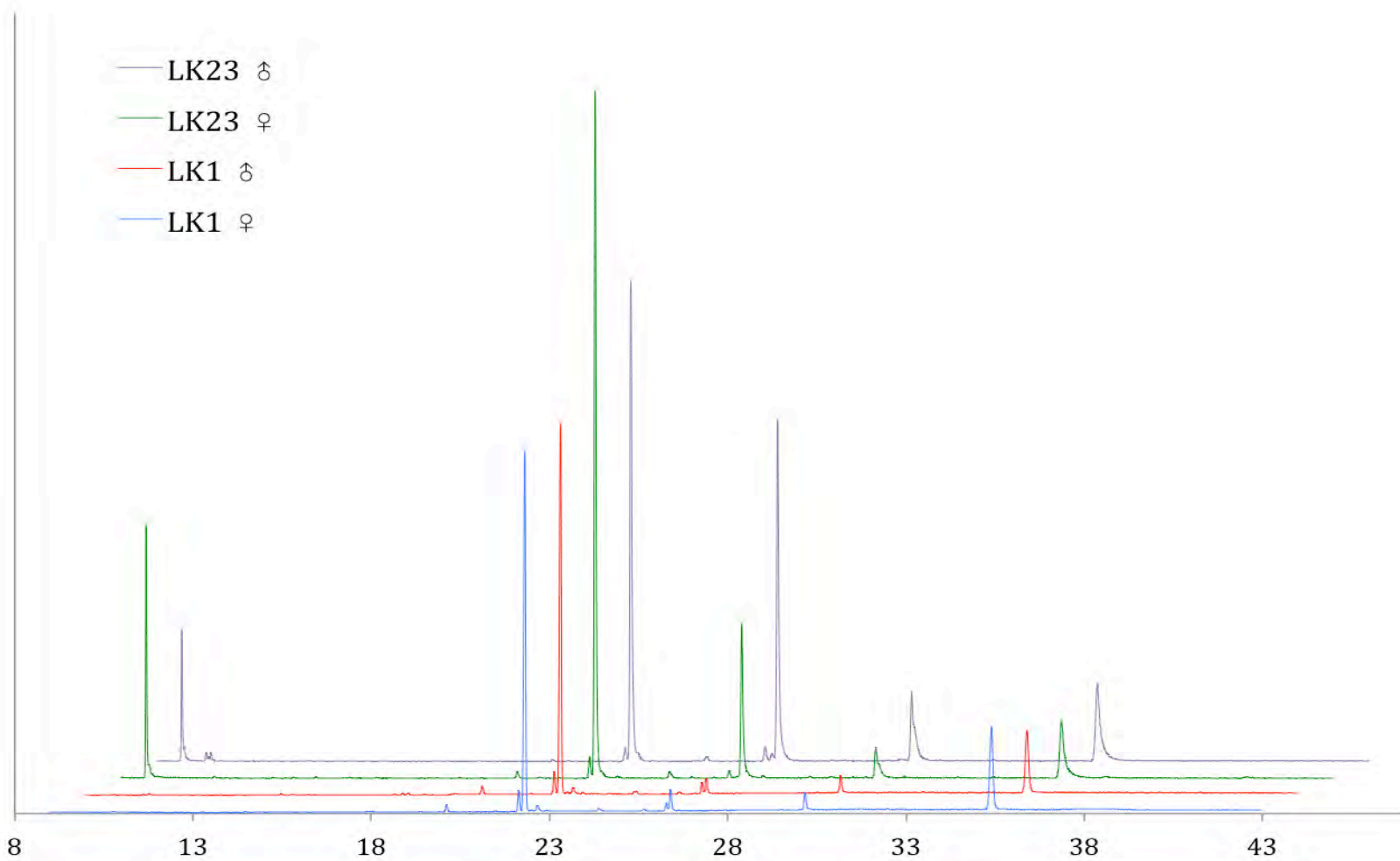


Figure 32. Overlaid CHC profiles for four individual flies of EA race. LK1 and LK23 are two isofemale lines of EA, labeled according to original field collection. CHC profiles have been standardized by peak area to reveal both qualitative and quantitative differences between lines.

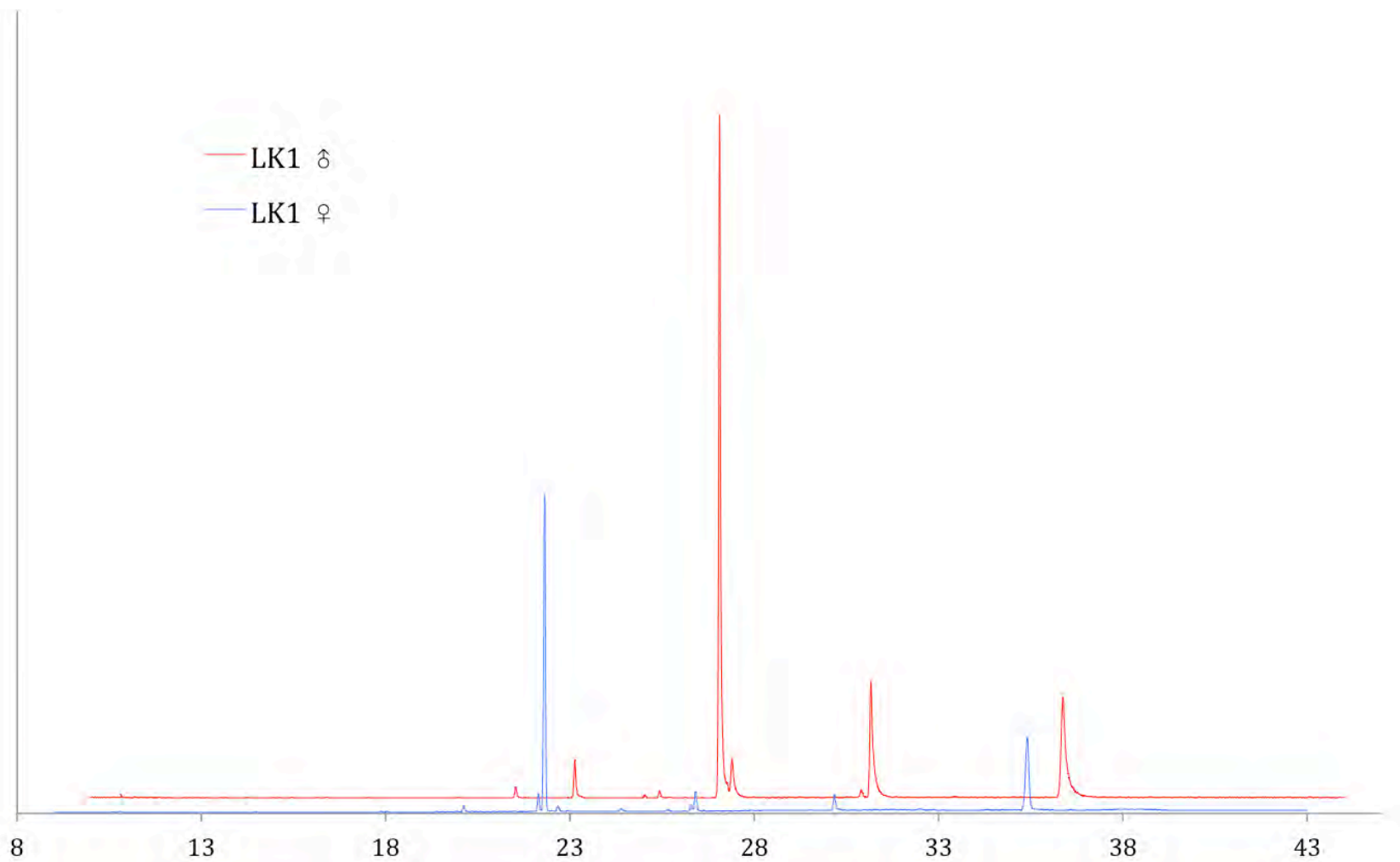


Figure 33. Area standardized CHC profiles of an EA female (blue) and male (red).

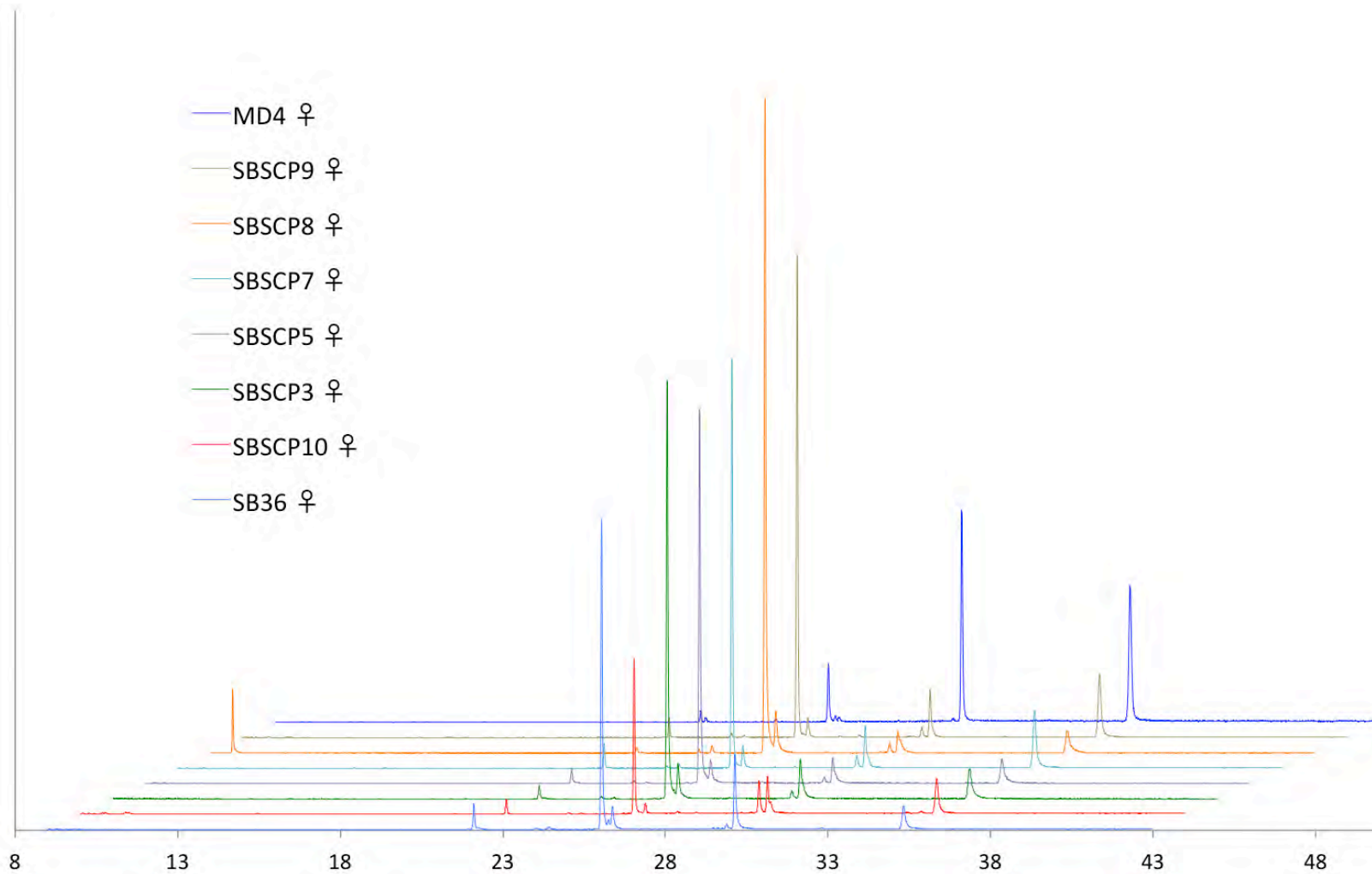


Figure 34. Overlaid CHC profiles for eight individuals of different isofemale lines from the EB race. CHC profiles have been standardized by area to reveal both qualitative and quantitative differences between lines.

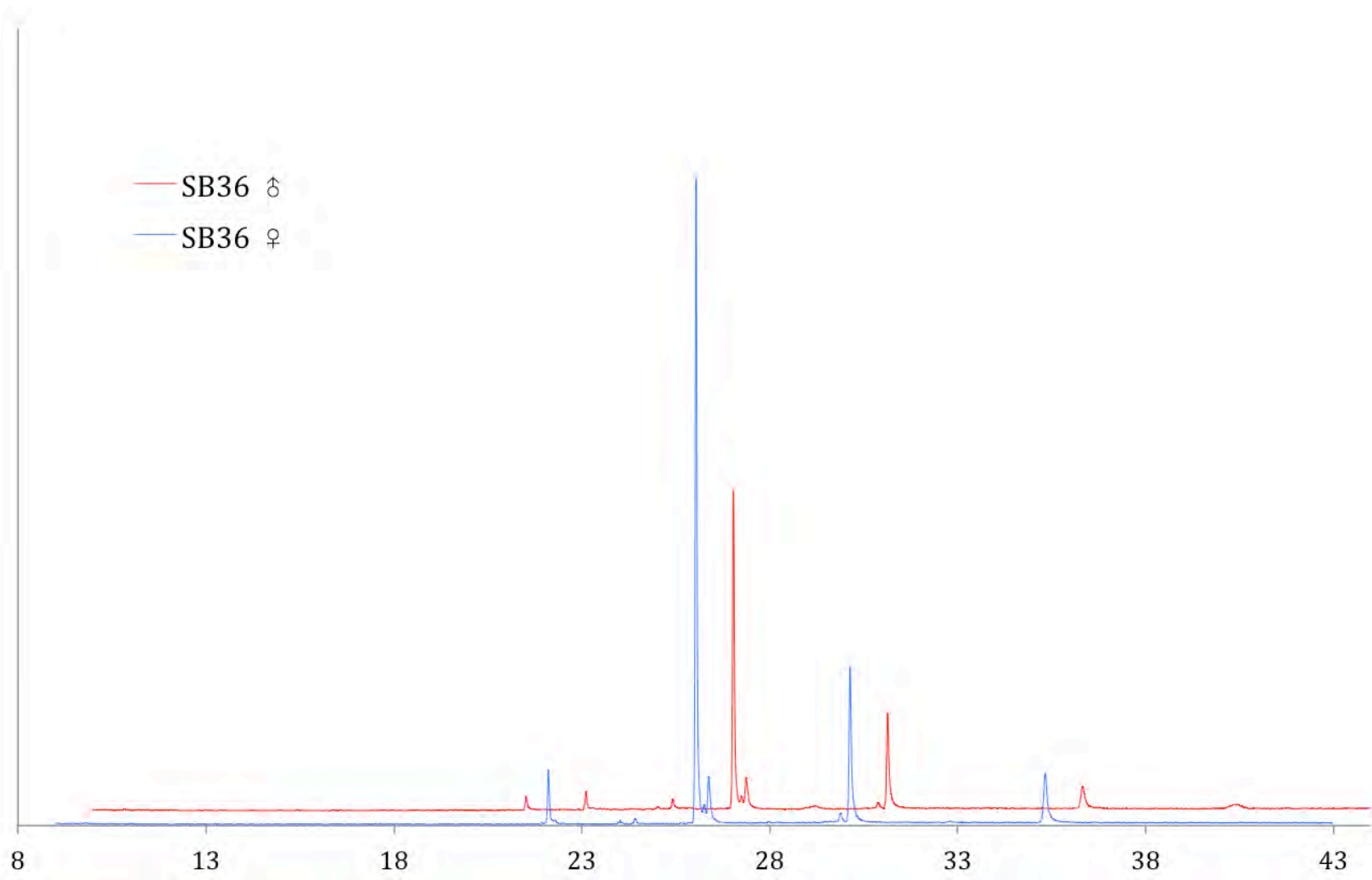


Figure 35. Area standardized CHC profiles of an EB female (blue) and male (red).

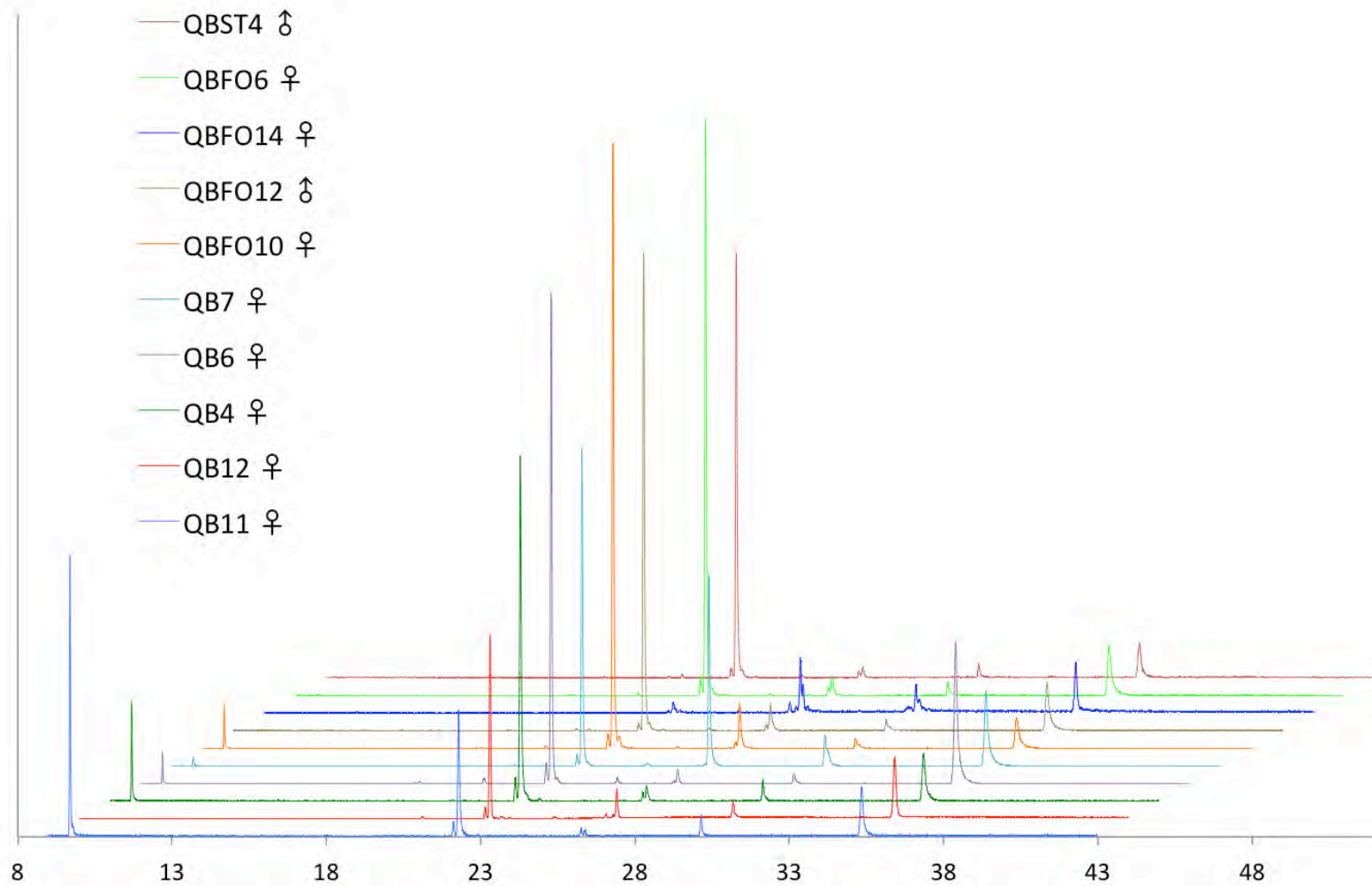


Figure 36. Overlaid CHC profiles for ten individuals of different isofemale lines from the WN race. CHC profiles have been standardized by area to reveal both qualitative and quantitative differences between lines.

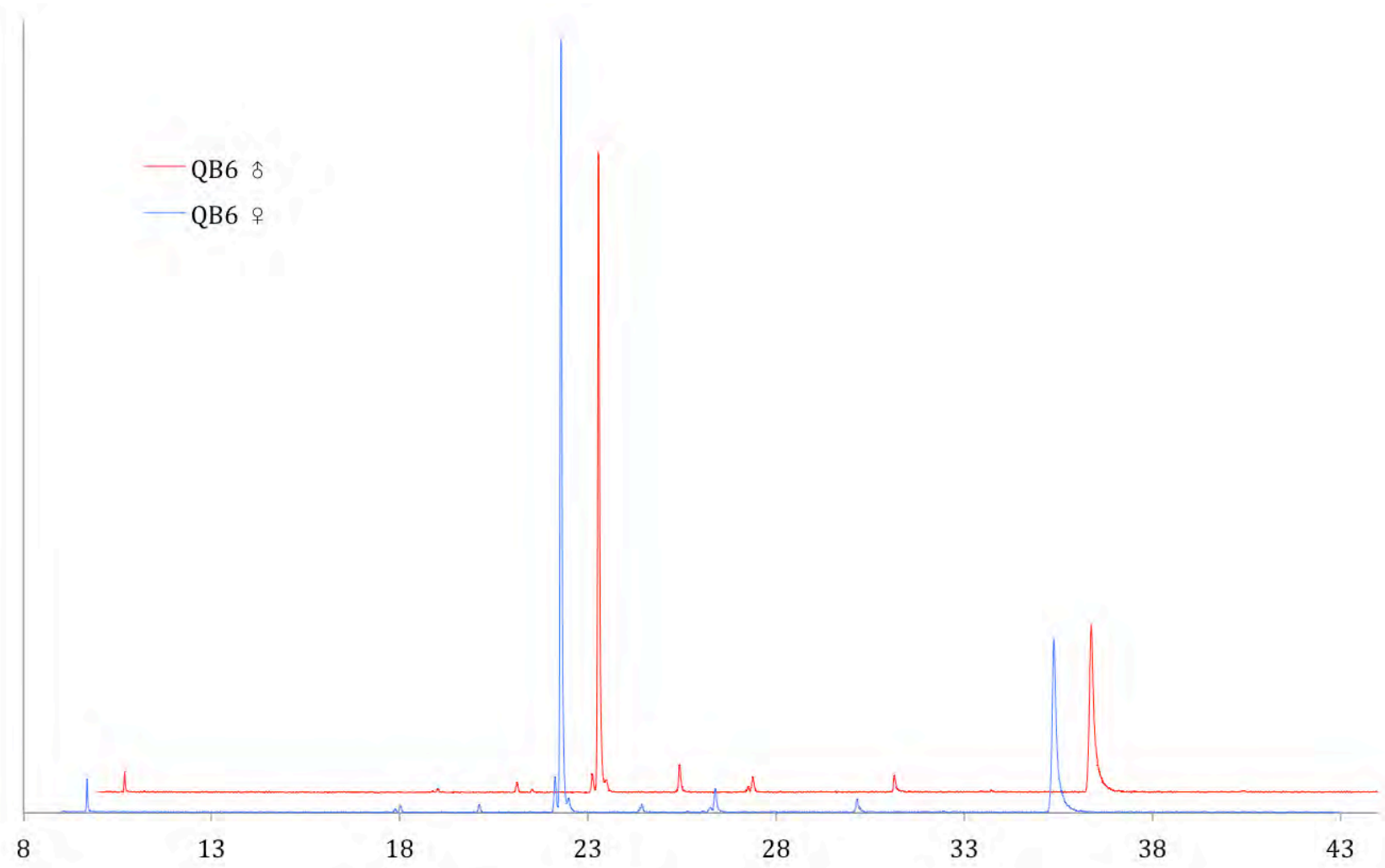


Figure 37. Area standardized CHC profiles of a WN female (blue) and male (red).

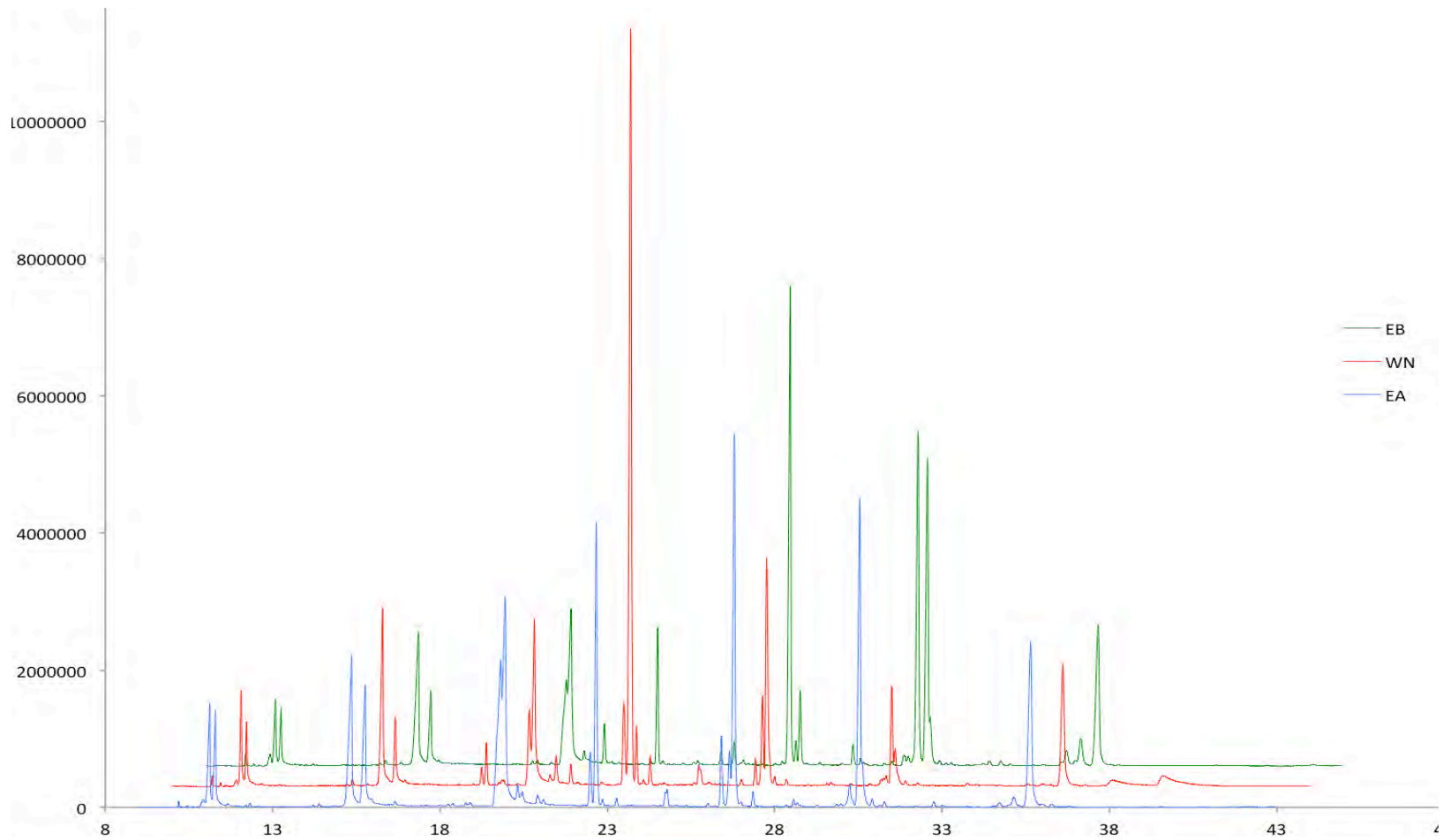


Figure 38. Overlaid chromatograms from 100-fly CHC extracts of EA (blue), WN (red), and EB (green), standardized by peak area. 100-fly extracts were used to eliminate random variability that may occur in single fly samples.

Discussion

Established methods for identification, derivatization, and synthesis have proven successful in the continued exploration of *D. athabasca* CHCs. In total, 33 unique CHCs have been identified using GC-MS, chemical derivatization, and literature comparison (see Table 1).

Identification of Linear Alkanes

Mass spectra of linear alkanes possess characteristic fragment patterns displaying an exponential decay in abundance with increasing m/z ratio. Figure 11 has a M^+ of 324 m/z with a fragmentation pattern similar to that of synthetic *n*-tricosane (Figure B17, Appendix B). The abundances of saturated compounds were lower, compared to monoenes, dienes, and oxygen-containing CHCs, and were only observed in 100-fly extracts. Linear alkanes have been implicated in anti-desiccation, though, evidence of this theory is lacking in the *D. athabasca* system.²⁶ The low abundance of these saturated alkanes may imply that they are not as relevant to sexual selection and may be bound up in the epicuticular layer to prevent water loss.

Identification of Branched Alkanes

Taken together, the mass spectral data and analysis of bromination/elimination data suggest several observed alkanes are branched at the two position. In total, eight CHCs were identified as methyl branched alkanes using mass spectral analysis and/or chemical derivatization approaches. Six of these methyl branched CHCs were observed in all races of *D. athabasca*. Two compounds, 2-Me-

C25 and 3-Me-C23 were observed exclusively in EA and EB, respectively. Hence, these branched compounds demonstrate distinct profile differences among races. The likelihood of the ubiquitous 2-methyl branched alkanes participating in mate stimulating behavior is slim, due to similarities in profile composition. However, the race specificity of 2-Me-C25 and 3-Me-C23 could imply a potential role in the evolution leading to subspecies. Experimental approaches aimed toward understanding the function of 2-Me-C25 and 3-Me-C23 are dependent upon successful synthesis and behavioral studies.

The synthesis of 2-Me-C25 is plausible using the route outlined in Figure 10. However, the presence of a methyl group on the third carbon provides stereochemical complexity. Using solely EI-MS, the absolute configuration of 3-methyltricosane cannot be determined. Previous research has shown that the stereochemistry of these asymmetrical CHCs can actually hinder or inhibit responses in insects.^{47,48} Stereoselective synthesis can be employed and synthetic RTs can be compared to the naturally occurring counterparts. However, the likelihood of enantiomers being separated by GC on a non-chiral column is minimal. As a result, future research would require separation of 3-methyltricosane from CHC extracts followed by analysis via polarimetry.

Identification of Monoenes

Five monoenes have been fully characterized, including: (*Z*)11-pentacosene, (*Z*)12-pentacosene, (*Z*)11-tricosene, (*Z*)9-tricosene, and (*Z*)12-tetracosene, using DMDS derivatization (shown in Figures 20-22). Geometry of one tricosene (10-tricosene) remains unconfirmed. Additionally, two monoenes (C22:1 and C27:1)

remain uncharacterized, although collected mass spectra indicate a single unsaturation.

Analysis of DMDS-derivatized mass spectra provides additional information on the relative abundances of isomeric CHCs, such as 11- and 12-pentacosene. The greater abundance of the DMDS fragments for 11-pentacosene indicates the presence of larger quantities of 11-pentacosene in the CHC extract. Similarly, the abundance of 11-tricosene is significantly greater than 10- and 9-tricosene based upon the ratios of DMDS fragments in Figure 21.

The geometry of 11-pentacosenes, 12-pentacosene, 11-tricosene, and 9-tricosene was determined using synthetic material or purchased standards. Complete characterization of 10-tricosene is ongoing. Successful quantification of these CHCs can be accomplished using external standard curves (Appendix I) and additional curves must be generated once all isomers of identified monoenes have been synthesized. Further optimization of the GC method will also allow complete separation and quantification of isomeric mixtures (i.e. pentacosenes and tricosenes).

Identification of Dienes

Two dienes have been identified in *D. athabasca*, with one CHC being completely characterized. As illustrated in Figures 23, a diene at 26.03 m was identified as 10,14-pentacosadiene. DMDS derivatization using a diene standard, (Z,Z)7,11-heptacosadiene, was used to optimize reaction conditions for selectivity yielding mono-derivatization or yielding cyclic derivatization. The mass spectrum illustrated in Figure 23 showing mono-derivatization was used to predict a 10,14-

pentacosadiene, while the mass spectrum in Figure 24 showing cyclization confirmed identity. The synthesis of 10,14-pentacosadiene, in all geometric isomers, is ongoing.

An additional heptacosadiene (C27:2) was identified at 29.89 min (see Figure 8 in Appendix E) but current lack of successful DMDS derivatization prevents complete identification of this CHC. Further DMDS derivatization is necessary to successfully elucidate the structure of this CHC.

With increasing chemical complexity arises increased potential for information storage, thus dienes may likely be involved in communication within the *D. athabasca* system. The potential for chemical communication must be explored through synthesis and behavioral testing of these CHCs.

Identification of *cis*-Vaccenyl Acetate

As illustrated in Figure 25, a mono-unsaturated acetate, cVA, was identified in the CHC profiles of male *D. athabasca*. This compound has been suggested to be an aggregation pheromone, luring females to increase the likelihood of successful copulation.⁴⁹ Typically, this CHC is secreted prior to courtship, although, small quantities of material may exist on an individual at any given time.

The presence of cVA in male CHC profiles is in agreement with previous observations in *Drosophila*.⁵⁰ In contrast, Ray et al.⁴⁶, identify cVA as a female-produced CHC in *D. melanogaster*. Discrepancies between sex-based compounds may result from the method of fly rearing. Female flies matured in the presence of male flies are likely to have CHCs transferred between individuals. Because flies in these studies were raised in a sexually segregated environment it is unlikely that

material was transferred to male flies. We do not observe cVA in the CHC profiles of females. Biological testing in this system would be necessary to explore its sex-specific role.

Identification of Carboxylic Acids and Methyl Esters

Carboxylic acids and methyl esters were observed in all three races of *D. atabasca* (see Table 1). The mass spectra of identified carboxylic acids are shown in Appendix F. These CHCs were characterized using the fragmentation pattern outlined in Figure 26. Oleic acid, or (*Z*)-9-octadecenoic acid was fully characterized by comparison to synthetic material (Figure 7 in Appendix F). All other CHCs with additional sites of unsaturation must be further characterized using DMDS derivatization.

Like carboxylic acids, methyl esters display unique fragmentation patterns in their mass spectra (Figure 29). This fragmentation pattern was used to identify methyl tetradecanoate (Figure 1 in Appendix F) and methyl hexadecanoate (Figure 30).

The biosynthetic pathway of CHC synthesis is well understood, with CHCs being derived from fatty acids (carboxylic acids). A variety of methyl esters and fatty acids/carboxylic acid are commercially available, so further investigation of their chemical and biological function in this system should be straightforward.

Quantification of CHCs Using External Standard Curves

Nearly all papers exploring the role of CHCs in biological systems utilize an internal standard as a means of quantifying the amount of material present.

However, it was noted during these investigations that internal standards are difficult to maintain at a known concentration using hexanes. The high vapor pressure of hexane prevents a constant concentration of the internal standard, ultimately affecting the calculated concentration of material present in a CHC extract. To combat this issue, six standard curves have been successfully generated using synthetic material (Figure 31 and Figures G1 through G5 in Appendix G) and have been used to quantify biologically relevant amounts on a single fly. Linear regression analyses have calculated quantities as low as 3 nanograms of (Z)11-tricosene on a single fly. This value is in agreement with a multitude of sources claiming the quantities of CHCs vary between 10-20 nanograms.

Intra-racial Variability

Eastern A. From Figure 31, the most abundant CHC observed in all lines of EA is located at 22.28 m. This peak was previously identified as (Z)11-tricosene, however, recent data have shown that this peak actually contains three isomers of tricosene: (Z)11-tricosene, (Z)9-tricosene, and 10-tricosene (see Figure 21). However, comparison of a single male and a single female reveals differences in major CHCs based upon sex (see Figure 32). The major CHC in females is a mixture of tricosenes, while the major CHC in males is the mixture of pentacosenes. A 100-fly CHC extract of EA flies (see Figure 38) also indicates the major CHC of EA to be the mixture of pentacosenes, contradictory to what is observed in Figure 31. Discrepancies in major CHCs are likely populational, and comparison of single fly and 100-fly extracts accounts for variation within individuals. It is also possible that the 100-fly extract

consisted primarily of male flies, as the sex of each fly was not identified prior to extraction.

Aside from discrepancies in the identity of the major CHC of EA, the ratio of CHCs is constant. From analysis of Figure 32, it is apparent that most CHCs are consistently observed intra-racially. The ratio of 2-Me-C26 to 2-Me-C28 is constant between each profile, although the overall quantities of CHCs do change.

The limited sample size of EA CHC profiles does limit complete and successful characterization of the intra-racial variation, however. Further analysis of EA extracts is required before conclusions about major CHCs and ratios can be made.

Eastern B. Single fly CHC extracts from multiple isofemale lines of EB were analyzed and overlaid in Figure 34. This figure displays intra-racial variation, specifically in regard to major CHCs. The major CHC of all but one line of EB is located at 26.03 min, or 10,14-pentacosadiene. The MD4 line of EB has a major CHC at 30.13 min, 2-Me-C26. It is necessary to further explore the MD4 fly line due to observed differences from other EB lines. The major CHC of the 100-fly CHC extract of EB flies was 10,14-pentacosadiene, providing some evidence that the variation in MD4 may be due to some random variation and not significant CHC differences.

Single fly CHC extracts from one male and one female were also overlaid and compared to search for variation within the EB race. The major CHC, as well as ratios between all compounds were consistent to that observed in Figure 34.

WestNorthern. Ten single fly CHC extracts from isofemale lines of WN were overlaid and compared in Figure 36. The major CHC in nine of these individuals is (Z)11-tricosene, although the major CHC in QBFO14 is (Z)11-pentacosene. This variation must be further explored by surveying additional QBFO14 profiles. Similarly to EB, the major CHC of the 100-fly extract was concurrent with the major CHC of the majority of individuals. In the case of WN, the major CHC in the 100-fly CHC extract was also (Z)11-tricosene.

Additionally, one male and one female CHC profile were compared (Figure 36) to observe any potential variation between the sexes. The major CHC in this comparison was still (Z)11-tricosene, although it can be noted that the female fly has a larger abundance than the male. This is the case for all races and is likely due to the fact that females are larger than males, therefore they secrete more CHCs overall. Normalization to fly mass would also be necessary to observe any small variation between males and females and could be done in the future.

Inconsistent Fly Lines. Two fly lines, MD4 and QBFO14, had been proposed to be members of EB and WN races, respectively. CHC profile comparisons of these lines to other individuals of the same race afforded inconsistencies in CHC composition. As previously mentioned, the major CHC in MD4 was determined to be 2-Me-C26 (Figure 34), though the major CHC of all other EB lines is 10,14-pentacosadiene (Figures 34 and 38). It may be suggested that MD4 may have been incorrectly identified as an EB line. However, susceptibility to CHC evolution is dependent upon rearing and laboratory conditions.⁵¹ Likewise, it has been found that CHCs may vary

for up to five years post-collection from the field.⁵² As a result, MD4 flies may have evolved their CHC profiles to better suit the conditions of their rearing, though the likelihood of lines evolving differently, when exposed to the same lab conditions is slim.

The major CHC of QBF014 was identified as 3-Me-C23 (Figure 36), while the major CHC of other WN lines was (Z)11-tricosene. Similarly to MD4, QBF014 individuals may have evolved CHC profiles in the laboratory. CHC profiles of both MD4 and QBF014 should be further explored to deduce racial identity.

Inter-racial Variability

CHC profiles, extracted from 100-fly samples, have been standardized by peak area to provide insight into quantitative differences among the EA, EB, and WN races. As illustrated in Figure 37, the major CHC for each race appears as the most abundant peak. EA, shown in blue, has a major signal at approximately 26.3 m, identified as a mixture of (Z)11- and (Z)12-pentacosene. The major CHC in WN is seen around 22.2 m, or (Z)11-tricosene. These two races have the most similar profiles in terms of ratios and notable signals. For example, the signal at 26.3 m ((Z)11-pentacosene) is bordered to the left and right by additional signals. These compounds are found in similar ratios relative to (Z)11-pentacosene in both EA and WN.

Unlike EA and WN, EB exhibits a differing CHC profile with a major signal at approximately 26.0 m. This CHC was identified as 10,14-pentacosadiene, and is observed solely in EB, making it a characteristic identifier of EB flies. The ratios of methyl branched alkanes also differs in EB, compared to EA and WN. At

approximately 22.4 m, 2-Me-C22 appears in much larger ratios in EB relative to the major compounds of EA and WN.

Similarly, a hexacosene at 29.9 m, immediately to the left of 2-Me-C26, is observed in all three races. However, it is evident that the concentration of this CHC is significantly greater in EB, as it exceeds the amount of 2-Me-C26, while EA and WN have much smaller amounts relative to the same branched alkane.

Conclusions and Future Work

In total, 33 CHCs have been completely identified in *D. athabasca*. Observed differences among the profiles of the three races establish EA and WN as having the most closely related profiles, while EB is more diverse in chemical space. Comparing individuals from the same race, we see slight variation in ratios between profile constituents. For example, some lines (MD4 and QBFO14) display profiles that are different from their assigned race. Future research will be directed at further characterizing the major CHCs of these isofemale lines. Determining differences within the races is crucial to understand the potential for divergence of *D. athabasca*.

Three identified CHCs have been fully synthesized, and afforded comparable mass spectra, confirming identities. Continued synthesis of characterized CHCs is crucial for development of non-natural profiles. With synthetic CHC profiles in hand, an in-depth biological assay can begin that will correlate CHC profile to behavioral response in *D. athabasca* flies.

References

- (1) Ferveur, J. F. Cuticular hydrocarbons: Their evolution and roles in *Drosophila* pheromonal communication. *Behav. Genet.* **2005**, *35* (3), 279–295.
- (2) Drijfhout, F. P.; Kather, R.; Martin, S. J. The Role of Cuticular Hydrocarbons in Insects. In *Behavioral and Chemical Ecology*; 2010; pp 91–114.
- (3) Akino, T. Cuticular hydrocarbons of *Formica truncorum* (Hymenoptera: Formicidae): Description of new very long chained hydrocarbon components. *Appl. Entomol. Zool.* **2006**, *41* (4), 667–677.
- (4) Hunt, J.; Snook, R. R.; Mitchell, C.; Crudgington, H. S.; Moore, A. J. Sexual selection and experimental evolution of chemical signals in *Drosophila pseudoobscura*. *J. Evol. Biol.* **2012**, *25* (11), 2232–2241.
- (5) Grillet, M.; Dartevelle, L.; Ferveur, J.-F. A *Drosophila* male pheromone affects female sexual receptivity. *Proc. Biol. Sci.* **2006**, *273* (1584), 315–323.
- (6) Ishii, K.; Hirai, Y.; Katagiri, C.; Kimura, M. T. Sexual isolation and cuticular hydrocarbons in *Drosophila elegans*. *Heredity (Edinb.)* **2001**, *87* (4), 392–399.
- (7) Perera, M. A. D. N.; Qin, W.; Yandea-Nelson, M.; Fan, L.; Dixon, P.; Nikolau, B. J. Biological origins of normal-chain hydrocarbons: A pathway model based on cuticular wax analyses of maize silks. *Plant J.* **2010**, *64* (4), 618–632.
- (8) Drijfhout, F. P.; Kather, R.; Martin, S. J. The Role of Cuticular Hydrocarbons in Insects. In *Behavioral and Chemical Ecology*; pp 91–114.
- (9) Rouault, J. D.; Marican, C.; Wicker-Thomas, C.; Jallon, J. M. Relations between cuticular hydrocarbon (HC) polymorphism, resistance against desiccation and breeding temperature; a model for HC evolution in *D. melanogaster* and *D. simulans*. *Genetica* **2004**, *120* (1–3), 195–212.
- (10) Chung, H.; Carroll, S. B. Wax, sex and the origin of species: Dual roles of insect cuticular hydrocarbons in adaptation and mating. *BioEssays* **2015**, 822–830.
- (11) Martin, S.; Drijfhout, F. A Review of Ant Cuticular Hydrocarbons. *J. Chem. Ecol.* **2009**, *35*, 1151–1161.
- (12) Wang, L.; Han, X.; Mehren, J.; Hiroi, M.; Billeter, J.-C.; Miyamoto, T.; Amrein, H.; Levine, J. D.; Anderson, D. J. Hierarchical chemosensory regulation of male-male social interactions in *Drosophila*. *Nat. Neurosci.* **2011**, *14* (6), 757–762.
- (13) Blows, M. W.; Allan, R. a. Levels of mate recognition within and between two *Drosophila* species and their hybrids. *Am. Nat.* **1998**, *152* (6), 826–837.
- (14) Everaerts, C.; Lacaille, F.; Ferveur, J. F. Is mate choice in *Drosophila* males guided by olfactory or gustatory pheromones? *Anim. Behav.* **2010**, *79* (5), 1135–1146.
- (15) Jennings, J. H.; Etges, W. J.; Schmitt, T.; Hoikkala, A. Cuticular hydrocarbons of *Drosophila montana*: Geographic variation, sexual dimorphism and potential roles as pheromones. *J. Insect Physiol.* **2014**, *61* (1), 16–24.
- (16) Marcillac, F.; Houot, B.; Ferveur, J. F. Revisited roles of *Drosophila* female pheromones. *Chem. Senses* **2005**, *30 SUPPL.* (suppl 1), 273–274.
- (17) Niehuis, O.; Buellesbach, J.; Gibson, J. D.; Pothmann, D.; Hanner, C.; Mutti, N. S.; Judson, A. K.; Gadau, J.; Ruther, J.; Schmitt, T. Behavioural and genetic analyses of *Nasonia* shed light on the evolution of sex pheromones. *Nature* **2013**, *494* (7437), 345–348.

- (18) Pavković-Lučić, S.; Todosijević, M.; Savić, T.; Vajs, V.; Trajković, J.; Andelković, B.; Lučić, L.; Krstić, G.; Makarov, S.; Tomić, V.; et al. "Does my Diet Affect my Perfume?" Identification and Quantification of Cuticular Compounds in Five *Drosophila melanogaster* Strains Maintained over 300 Generations on Different Diets. *Chem. Biodivers.* **2016**, *13* (2), 224–232.
- (19) Singer, T. L. Roles of Hydrocarbons in the Recognition Systems of Insects
Author (s): Theresa L. Singer Published by: Oxford University Press Stable URL: <http://www.jstor.org/stable/4620153> REFERENCES Linked references are available on JSTOR for this article: You. *Am. Zool.* **2016**, *38* (2), 394–405.
- (20) Smadja, C.; Butlin, R. K. On the scent of speciation: the chemosensory system and its role in premating isolation. *Heredity (Edinb.)*. **2009**, *102* (1), 77–97.
- (21) South, A.; LeVan, K.; Leombruni, L.; Orians, C. M.; Lewis, S. M. Examining the role of cuticular hydrocarbons in firefly species recognition. *Ethology* **2008**, *114* (9), 916–924.
- (22) Torres, C. W.; Brandt, M.; Tsutsui, N. D. The role of cuticular hydrocarbons as chemical cues for nestmate recognition in the invasive Argentine ant (*Linepithema humile*). *Insectes Soc.* **2007**, *54* (4), 363–373.
- (23) Ralph W. Howard, C. A. McDaniel, G. J. B. Chemical Mimicry as an Integrating Mechanism: Cuticular Hydrocarbons of a Termitophile and Its Host. *Science (80-.)*. **1980**, *210* (4468), 431–433.
- (24) Howard, R. W.; Blomquist, G. J. Ecological, Behavioral, and Biochemical Aspects of Insect Hydrocarbons *. *Annu. Rev. Entomol* **2005**, *50*, 371–393.
- (25) Farine, J. P.; Ferveur, J. F.; Everaerts, C. Volatile *Drosophila* cuticular pheromones are affected by social but not sexual experience. *PLoS One* **2012**, *7* (7).
- (26) Yukilevich, R.; Harvey, T.; Nguyen, S.; Kehlbeck, J.; Park, A. The search for causal traits of speciation: Divergent female mate preferences target male courtship song, not pheromones, in *Drosophila athabasca* species complex. *Evolution (N. Y.)*. **2016**, *70* (3), 526–542.
- (27) Miller, D. D. Sexual Isolation and Variation in Mating Behavior within *Drosophila athabasca*. *Evolution (N. Y.)*. **1958**, *12* (1), 72–81.
- (28) Miller, D. D. ; Goldstein, R. B. ; Patty, R. A. Semispecies of *Drosophila athabasca* Distinguishable by Male Courtship Sounds. *Evolution (N. Y.)*. **2009**, *29* (3), 531–544.
- (29) Miller, D. D.; Westphal, N. J. Further Evidence on Sexual Isolation Within *Drosophila athabasca*. *Evolution (N. Y.)*. **1967**, *21* (3), 479–492.
- (30) Wicker-Thomas, C. Evolution of insect pheromones and their role in reproductive isolation and speciation. *Ann. la Soc. Entomol. Fr.* **2011**, *47* (1–2), 55–62.
- (31) Zhang, B.; Xue, H. J.; Song, K. Q.; Liu, J.; Li, W. Z.; Nie, R. E.; Yang, X. K. Male mate recognition via cuticular hydrocarbons facilitates sexual isolation between sympatric leaf beetle sister species. *J. Insect Physiol.* **2014**, *70*, 15–21.
- (32) Harvey, T. R. Latitude, Body Size, and Cuticular Hydrocarbons as Factors of Desiccation Resistance in, 2016.
- (33) Brown, W. V.; Jaisson, P.; Taylor, R. W.; Lacey, M. J. Novel Internally Branched, Internal Alkenes as Major Components of the Cuticular Hydrocarbons of the

- Primitive Australian Ant *Nothomyrecia macrops* Clark (Hymenoptera: Formicidae). *J. Chem. Ecol.* **1990**, *16* (9), 2623–2635.
- (34) Carlson, D. A.; Roan, C. S.; Yost, R. A.; Hector, J. Dimethyl disulfide derivatives of long-chain alkenes, alkadienes, and alkatrienes for gas-chromatography mass-spectrometry. *Anal. Chem.* **1989**, *61* (14), 1564–1571.
- (35) Kováts, E. Gas-chromatographische Charakterisierung organischer Verbindungen. Teil 1: Retentionsindices aliphatischer Halogenide, Alkohole, Aldehyde und Ketone. *Helv. Chim. Acta* **1958**, *41* (7), 1915–1932.
- (36) Le Bigot, Y.; Delmas, M.; Gaset, A. Direct Synthesis of Dipteran Sex Pheromones by the Wittig Reaction in a Heterogeneous Medium. *J. Agric. Food Chem.* **1983**, *31* (5), 1096–1098.
- (37) Piotrowski, P. K. Identification, characterization and synthesis of *Drosophila athabasca* cuticular hydrocarbons, Union College, 2014.
- (38) Schwarz, M.; Waters, R. M. Insect Sex Attractant: XII. An Efficient Procedure for the Preparation of Unsaturated Alcohols and Acetates. *Synthesis (Stuttg.)*. **1972**, 567–568.
- (39) Heath, R. R.; Coffelt, J. A.; Sonnet, P. E.; Proshold, S. I.; Dueben, B.; Tumlinson, J. H. Identification of Sex Pheromone Produced by Female Sweetpotato Weevil, *Cylas formicarius elegantulus*. *J. Chem. Ecol.* **1986**, *12* (6), 1489–1503.
- (40) Murphy, G. K.; Shirahata, T.; Hama, N.; Bedermann, A.; Dong, P.; McMahon, T. C.; Twenter, B. M.; Spiegel, D. A.; McDonald, I. M.; Taniguchi, N.; et al. Toward the synthesis of phomoidride D. *J. Org. Chem.* **2013**, *78* (2), 477–489.
- (41) Crossland, R. K.; Servis, K. L. A Facile Synthesis of Methanesulfonate Esters. *J. Org. Chem.* **1970**, *35* (9), 3195–3196.
- (42) Hoover, K.; Keena, M.; Nehme, M.; Wang, S.; Meng, P.; Zhang, A. Sex-Specific Trail Pheromone Mediates Complex Mate Finding Behavior in *Anoplophora glabripennis*. *J. Chem. Ecol.* **2014**, *40* (2), 169–180.
- (43) Shi, B.; Wu, L.; Liao, Y.; Jin, C.; Montavon, A. Explanations of the Formation of Branched Hydrocarbons During Fischer–Tropsch Synthesis by Alkylidene Mechanism. *Top. Catal.* **2013**, *57* (6–9), 451–459.
- (44) Howard, R. W.; Jackson, L. L.; Banse, H.; Blows, M. W. Cuticular hydrocarbons of *Drosophila birchii* and *D-serrata*: Identification and role in mate choice in *D-serrata*. *J. Chem. Ecol.* **2003**, *29* (4), 961–976.
- (45) Robinson, J. W.; Skelly Frame, E. M.; Frame, G. M. *Undergraduate Instrumental Analysis*, 7th ed.; CRC Press, 2014.
- (46) Ray, A. M.; Žunič, A.; Alten, R. L.; McElfresh, J. S.; Hanks, L. M.; Millar, J. G. cis-Vaccenyl Acetate, A Female-Produced Sex Pheromone Component of *Ortholeptura valida*, A Longhorned Beetle in the Subfamily Lepturinae. *J. Chem. Ecol.* **2011**, *37* (2), 173–178.
- (47) Ablard, K.; Gries, R.; Khaskin, G.; Schaefer, P. W.; Gries, G. Does the Stereochemistry of Methylated Cuticular Hydrocarbons Contribute to Mate Recognition in the Egg Parasitoid Wasp *Ooencyrtus kuvanae*? *J. Chem. Ecol.* **2012**, *38* (10), 1306–1317.
- (48) Bello, J. E.; McElfresh, J. S.; Millar, J. G. Isolation and determination of absolute configurations of insect-produced methyl-branched hydrocarbons. *Proc. Natl. Acad. Sci. U. S. A.* **2015**, *112* (4), 1077–1082.

- (49) Landolt, P. J. Sex Attractant and Aggregation Pheromones of Male Phytophagous Insects. *Am. Entomol.* **1997**, *43* (1), 12–22.
- (50) Butterworth, A. F. M. Lipids of *Drosophila* : A Newly Detected Lipid in the Male Author (s): F . M . Butterworth Published by : American Association for the Advancement of Science Stable URL : <http://www.jstor.org/stable/1726406> . **2013**, *163* (3873), 1356–1357.
- (51) Singer, T. L. Roles of Hydrocarbons in the Recognition Systems of Insects Author (s): Theresa L . Singer Published by : Oxford University Press Stable URL : <http://www.jstor.org/stable/4620153> REFERENCES Linked references are available on JSTOR for this article : You. **2016**, *38* (2), 394–405.
- (52) Houot, B.; Svetec, N.; Godoy-Herrera, R.; Ferveur, J.-F. Effect of laboratory acclimation on the variation of reproduction-related characters in *Drosophila melanogaster*. *J. Exp. Biol.* **2010**, *213* (13), 2322–2331.

Appendix A. Table of All Identified Compounds.

Table 1. Retention times, KRI values, and identities of all identified CHCs.

Retention Time (min)	KRI ^a	Molecular Formula	Identification	Method ^b
10.13	N/A	C15:0	Methyl tetradecanoate	MS, L, St
10.61	N/A	C14:1	X-Tetradecenoic acid	MS, St
10.76	N/A	C14:0	Tetradecanoic acid	MS, L, St
14.36	N/A	C16:0	Methyl hexadecanoate	MS, L, St
14.82	N/A	C16:1	(Z)9-hexadecenoic acid	MS, L, St
15.19	N/A	C16:0	Hexadecanoic acid	MS, L, St
19.18	N/A	C18:2	X,X-octadecadienoic acid	MS
19.32	N/A	C18:1	(Z)9-octadecenoic acid	MS, L, St
19.80	N/A	C18:0	Octadecanoic acid	MS, L, St
19.90	N/A	C22:1	X- docosene	MS
20.50	2192	C20:1	11-Octadecen-1-yl acetate	MS, L
22.12	2266	2-Me-C22	2-methyl docosane	MS, St, B
22.28	2270	C23:1	(Z)11-tricosene	MS, D
22.29	N/A	C23:1	10-tricosene	D
22.30	N/A	C23:1	9-tricosene	D
22.48	N/A	C23:1	7-tricosene	D
22.90	N/A	n-C24	<i>n</i> -tricosane	MS, St
24.03	2352	C24:2	x,x-tetracosadiene*	MS
24.39	2374	C24:1	12-tetracosene*	MS, D
24.42	2375	3-Me-C23	3-methyltricosane*	MS, St
26.05	2452	C25:2	10,14-pentacosadiene*	MS, D
26.23	2461	2-Me-C24	2-methyltetracosane	MS, St, B
26.36	2472	C25:1	(Z)12-pentacosene	MS, D
26.38	2473	C25:1	11-pentacosene*	MS, D
26.40	N/A	C25:1	10-pentacosene	D
28.06	N/A	2-Me-C25	2-methylpentacosane	MS, St
29.89	2646	C27:2	x,x-heptacosadiene*	MS
30.12	2663	2-Me-C26	2-methylhexacosane	MS, St, B
30.30	2672	C27:1	x-heptacosene	
32.40	2776	2-Me-C27	2-methylheptacosane	MS, St
35.29	2862	2-Me-C28	2-methyloctacosane	MS, St, B
43.45	3061	2-Me-C30	2-methyltriacontane	MS, St

Appendix B – Linear Alkane Standard Mass Spectra.

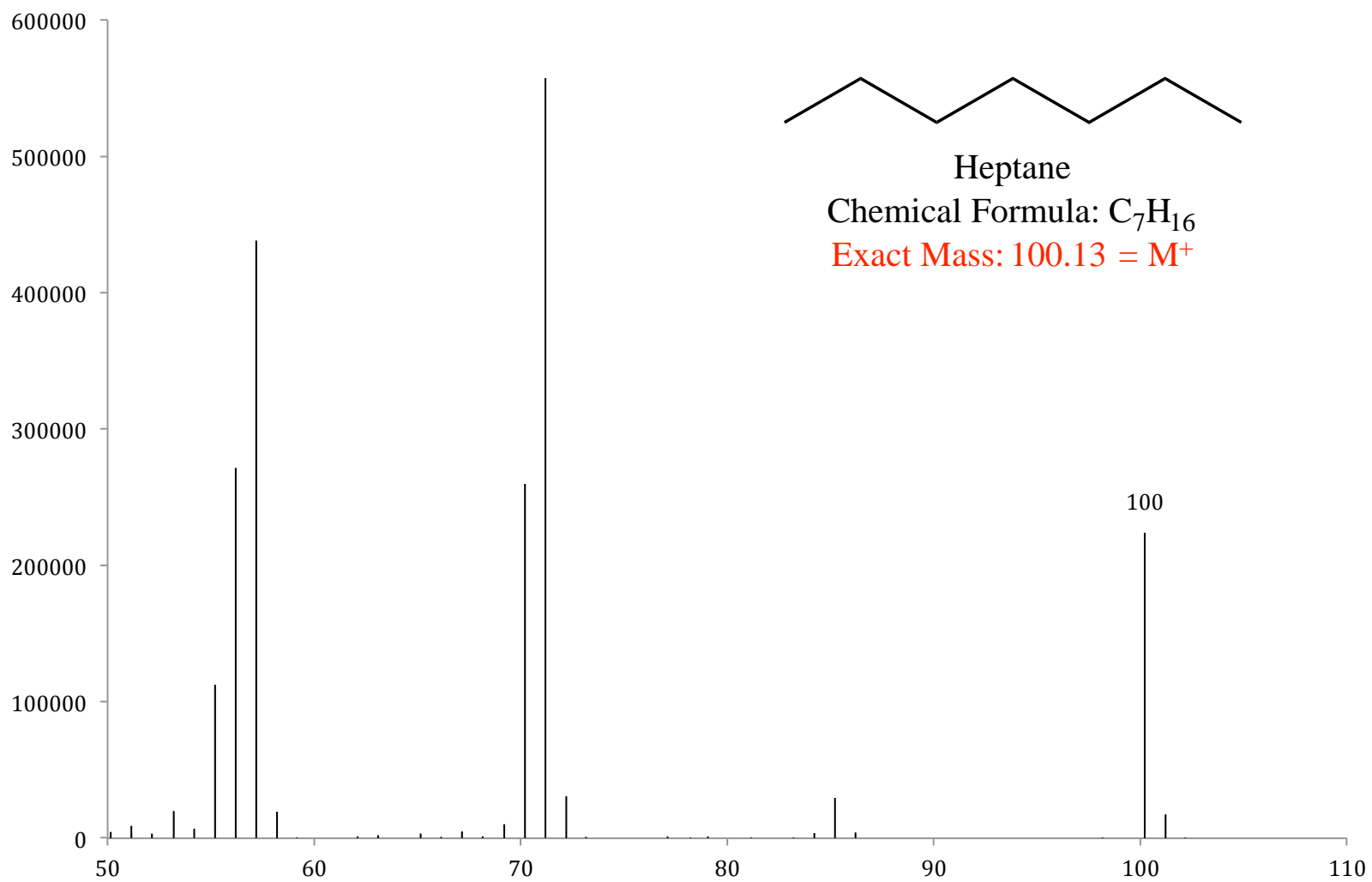


Figure B1. Mass spectrum of C7, or n-heptane, a purchased standard. The structure, chemical formula and expected M^+ are inset.

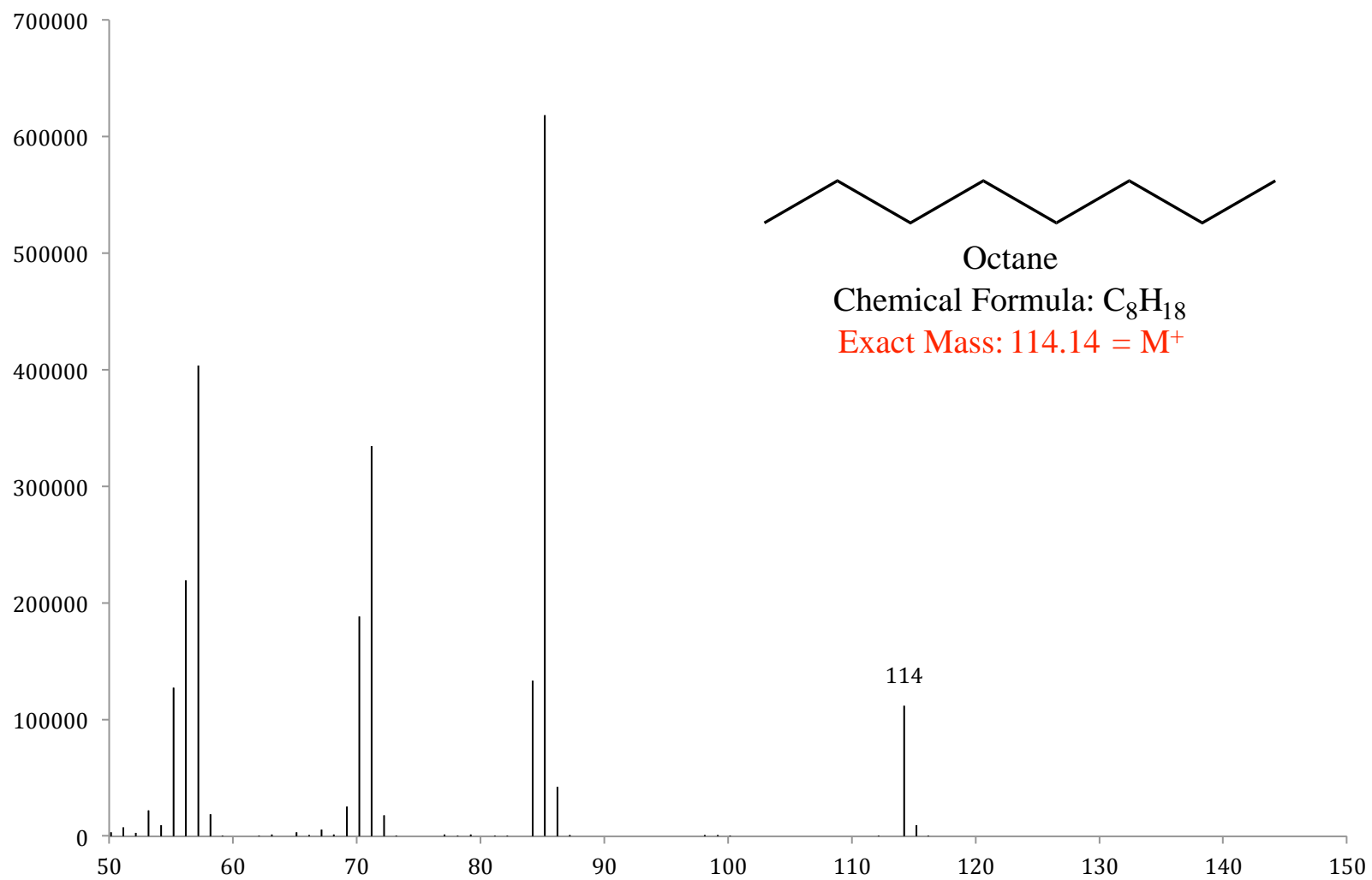


Figure B2. Mass spectrum of C₈, n-octane, a purchased standard. The structure, chemical formula and expected M⁺ are inset.

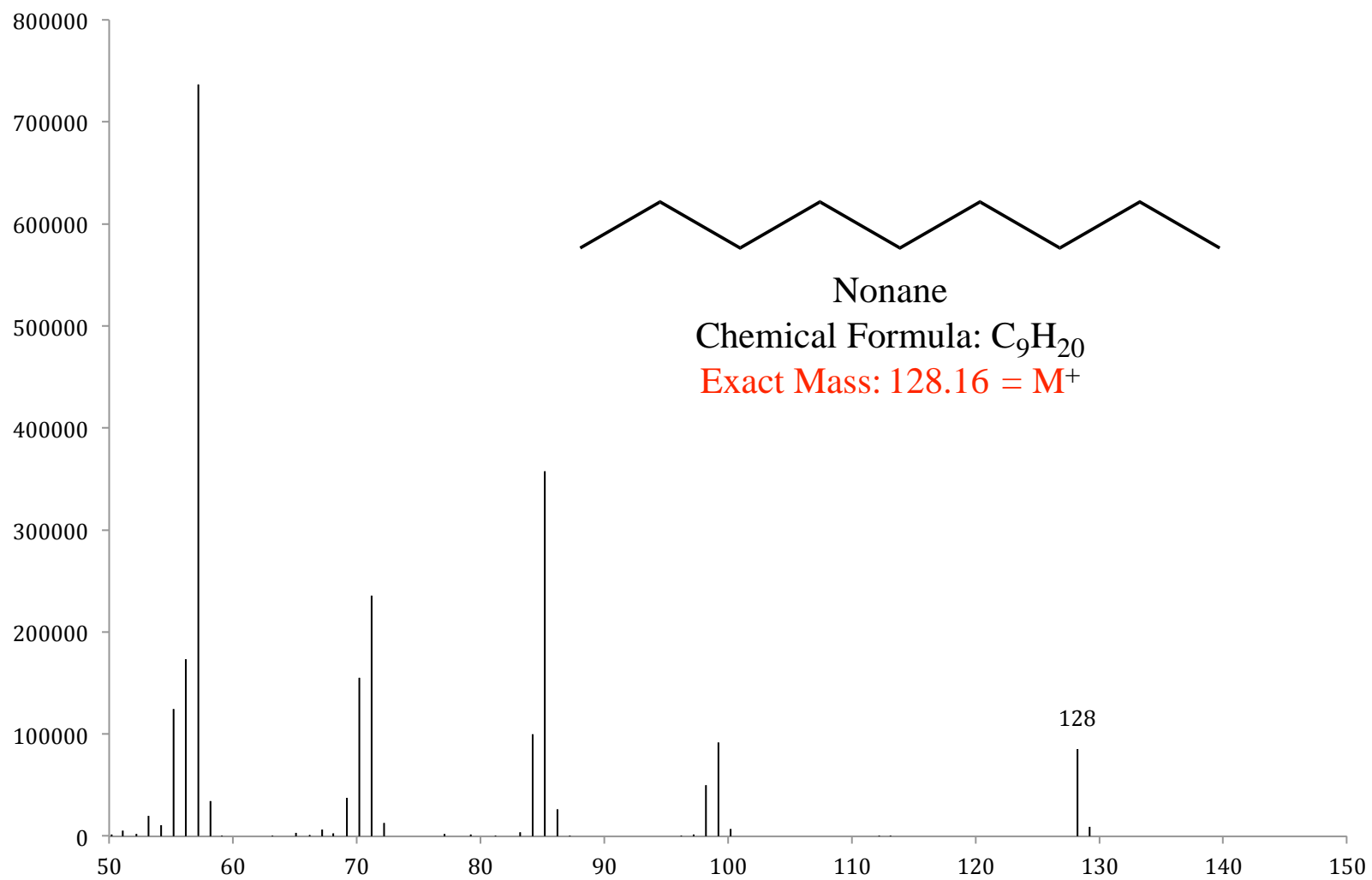


Figure B3. Mass spectrum of C₉, or n-nonane, a purchased standard. The structure, chemical formula and expected M⁺ are inset.

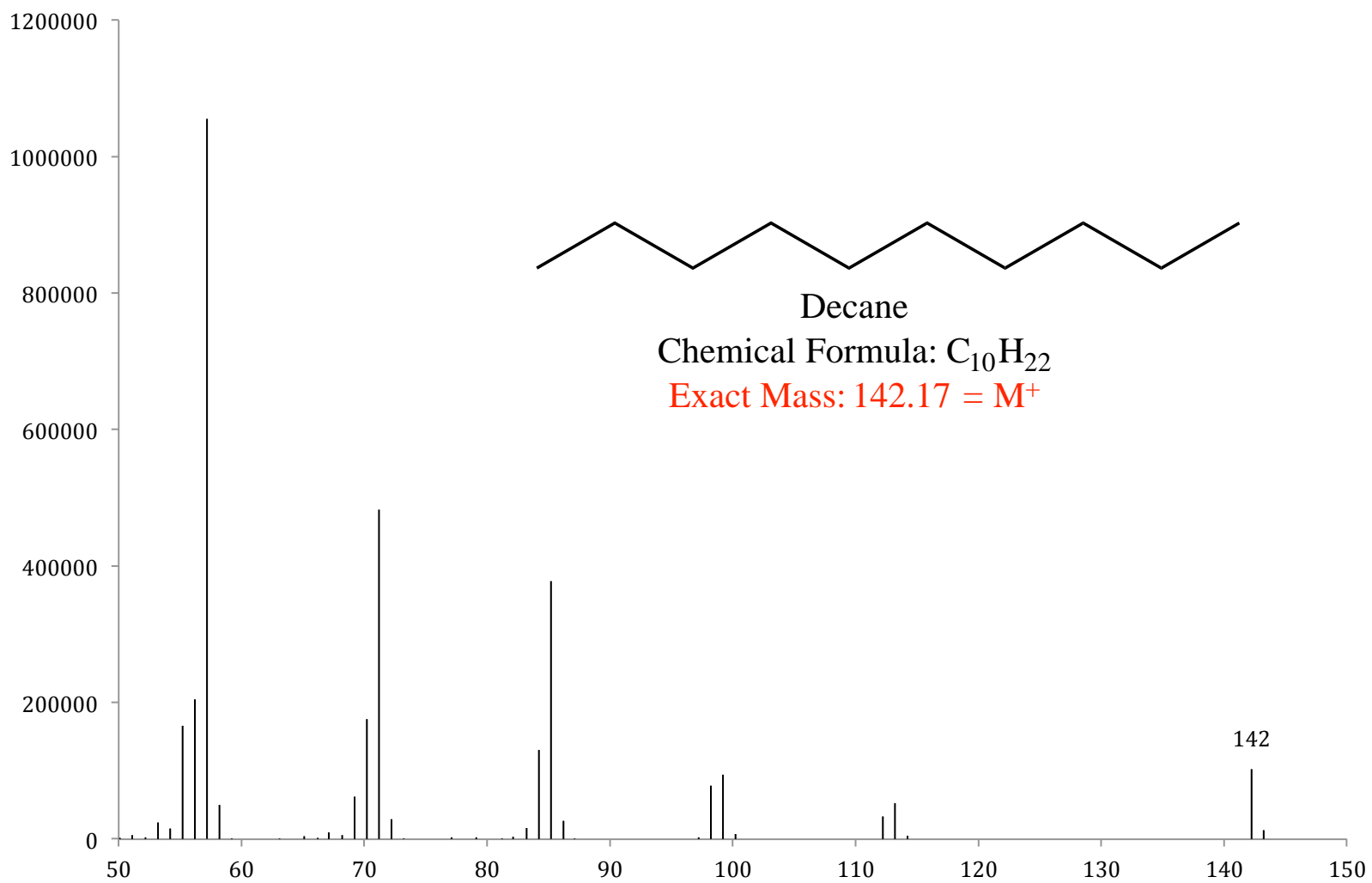


Figure B4. Mass spectrum of C10, or n-decane, a purchased standard. The structure, chemical formula and expected M^+ are inset.

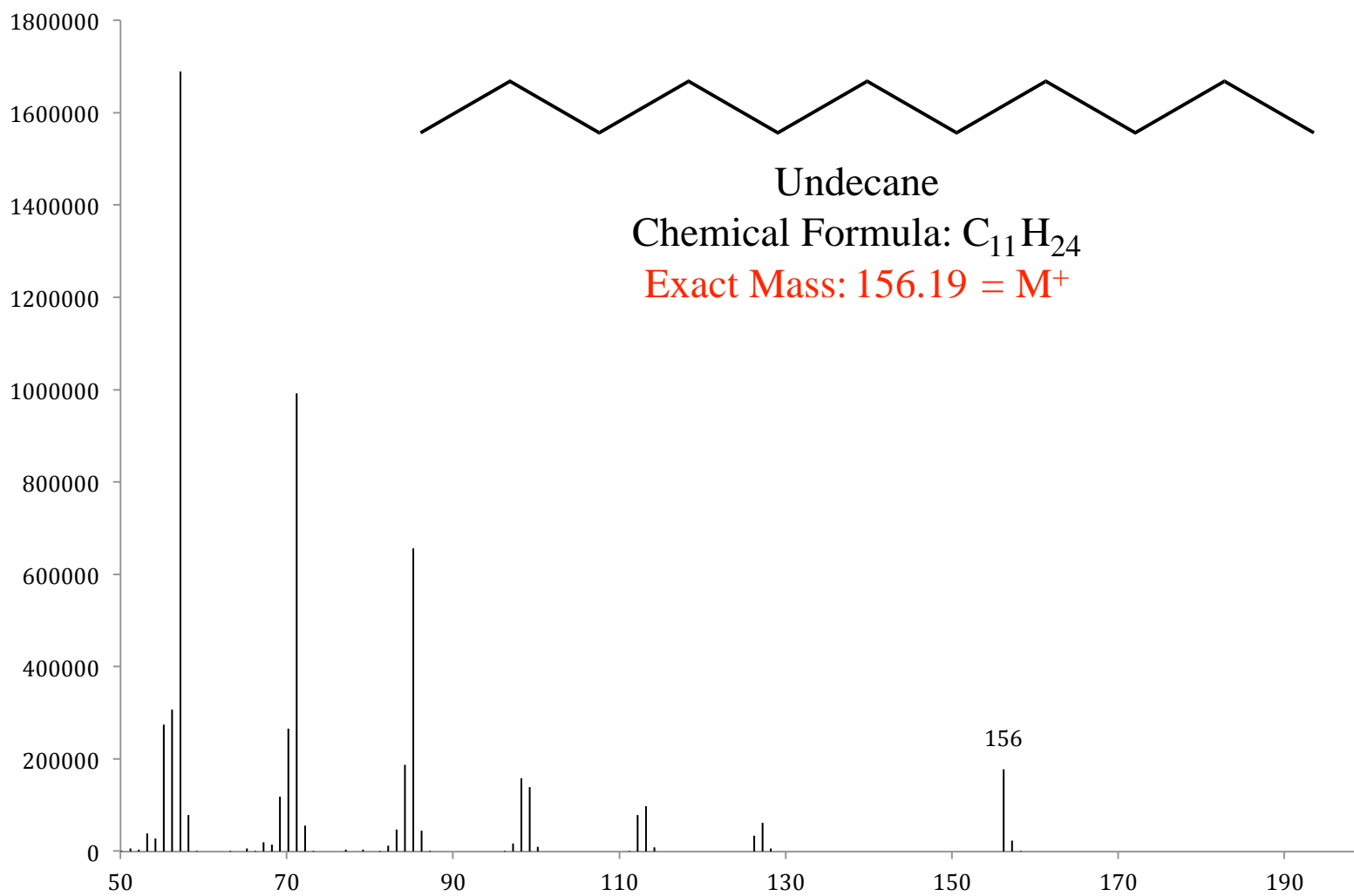


Figure B5. Mass spectrum of C11, or undecane, a purchased standard. The structure, chemical formula and expected M^+ are inset.

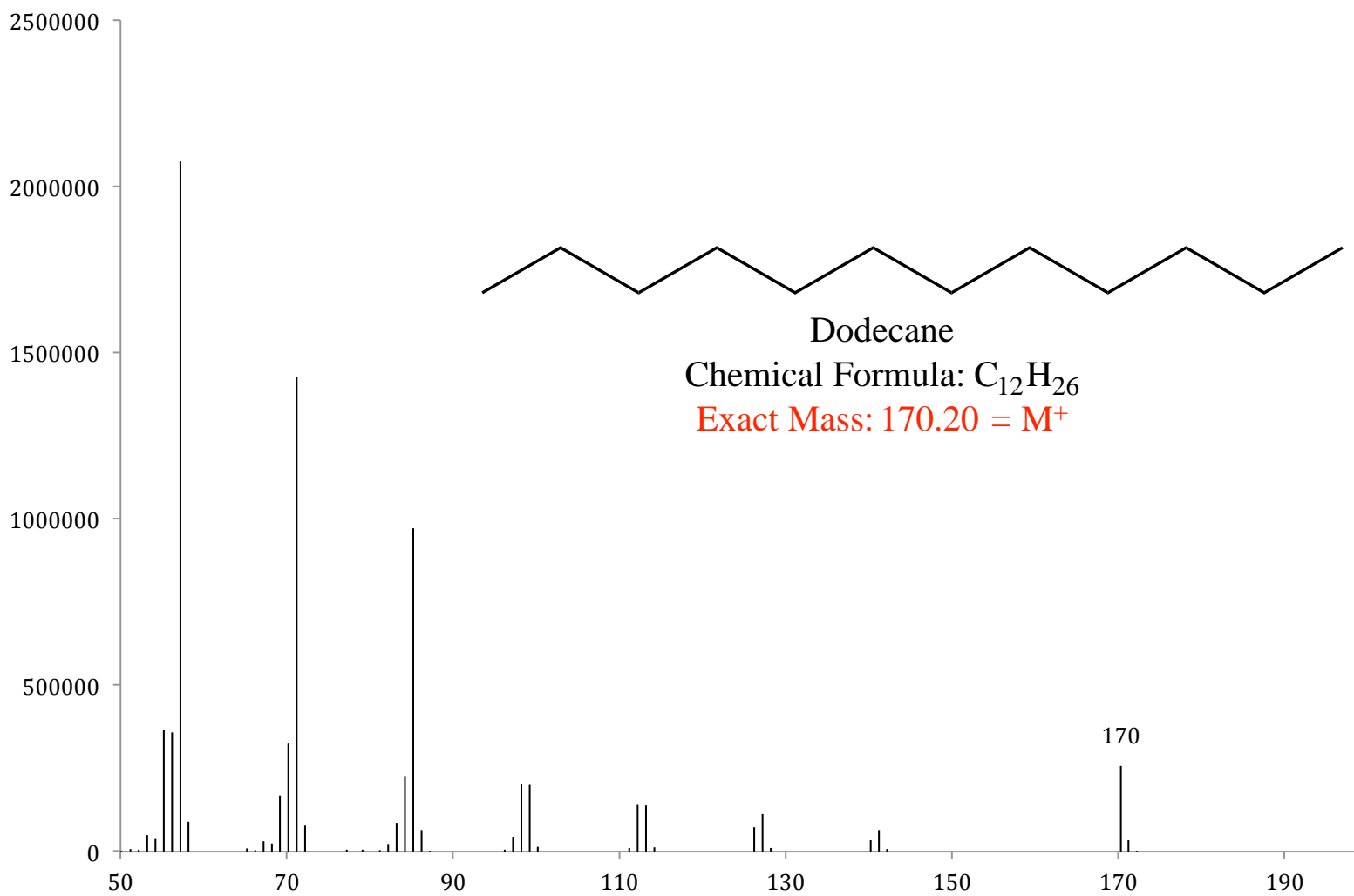


Figure B6. Mass spectrum of C12, or n-dodecane, a purchased standard. The structure, chemical formula and expected M⁺ are inset.

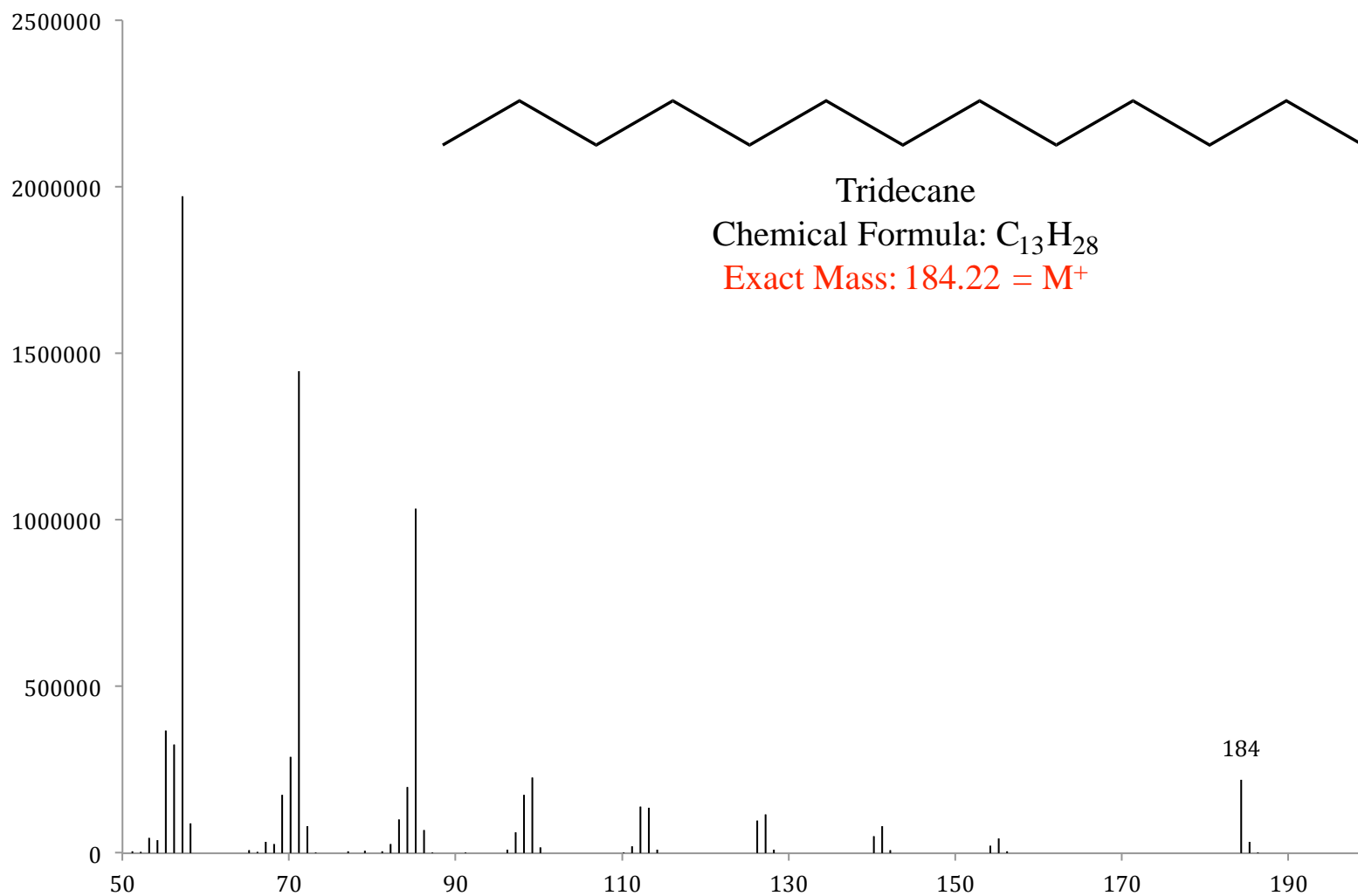


Figure B7. Mass spectrum of C13, or n-tridecane, a purchased standard. The structure, chemical formula and expected M^+ are inset.

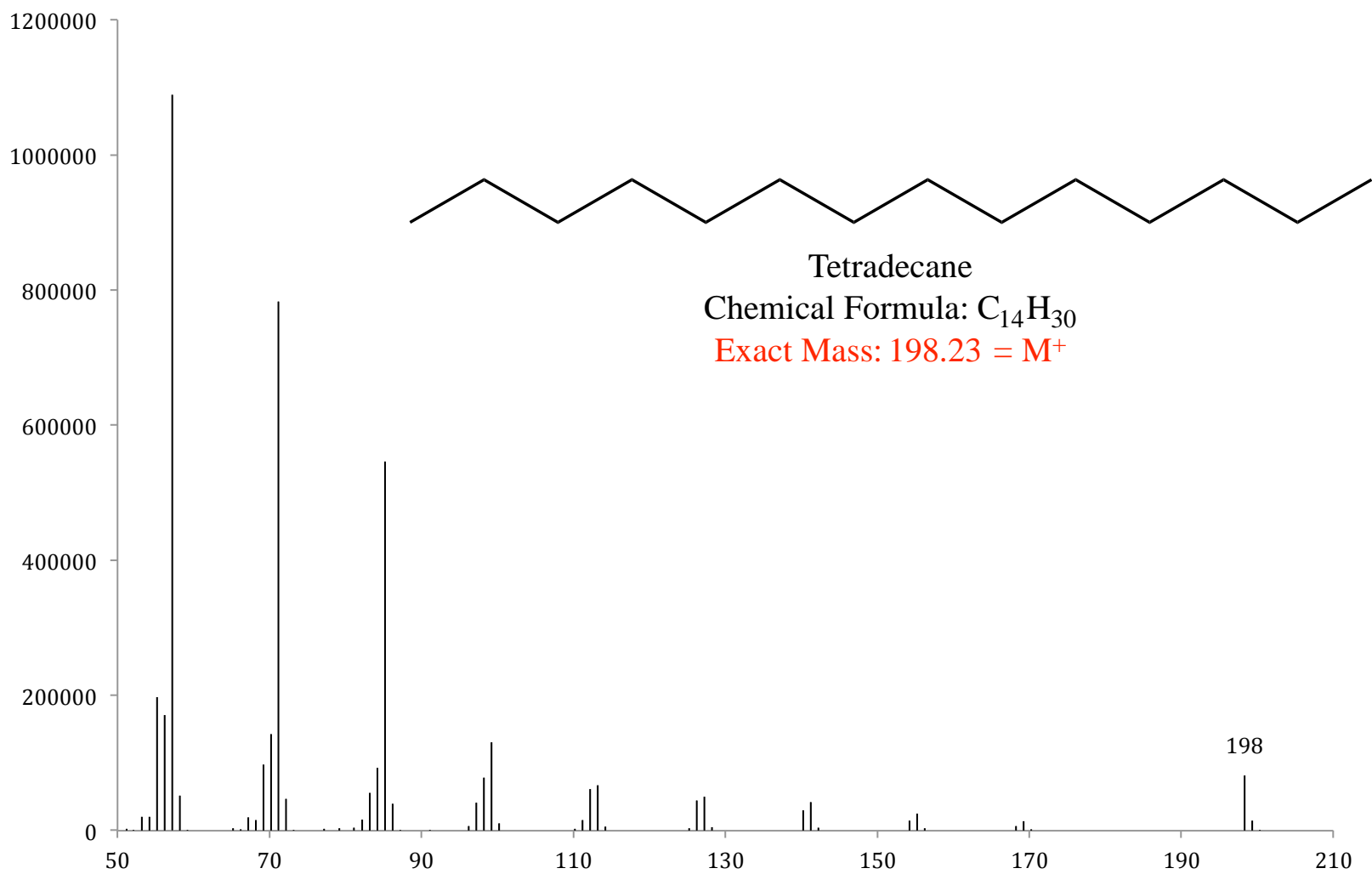


Figure B8. Mass spectrum of C14, or n-tetradecane, a purchased standard. The structure, chemical formula and expected M^+ are inset.

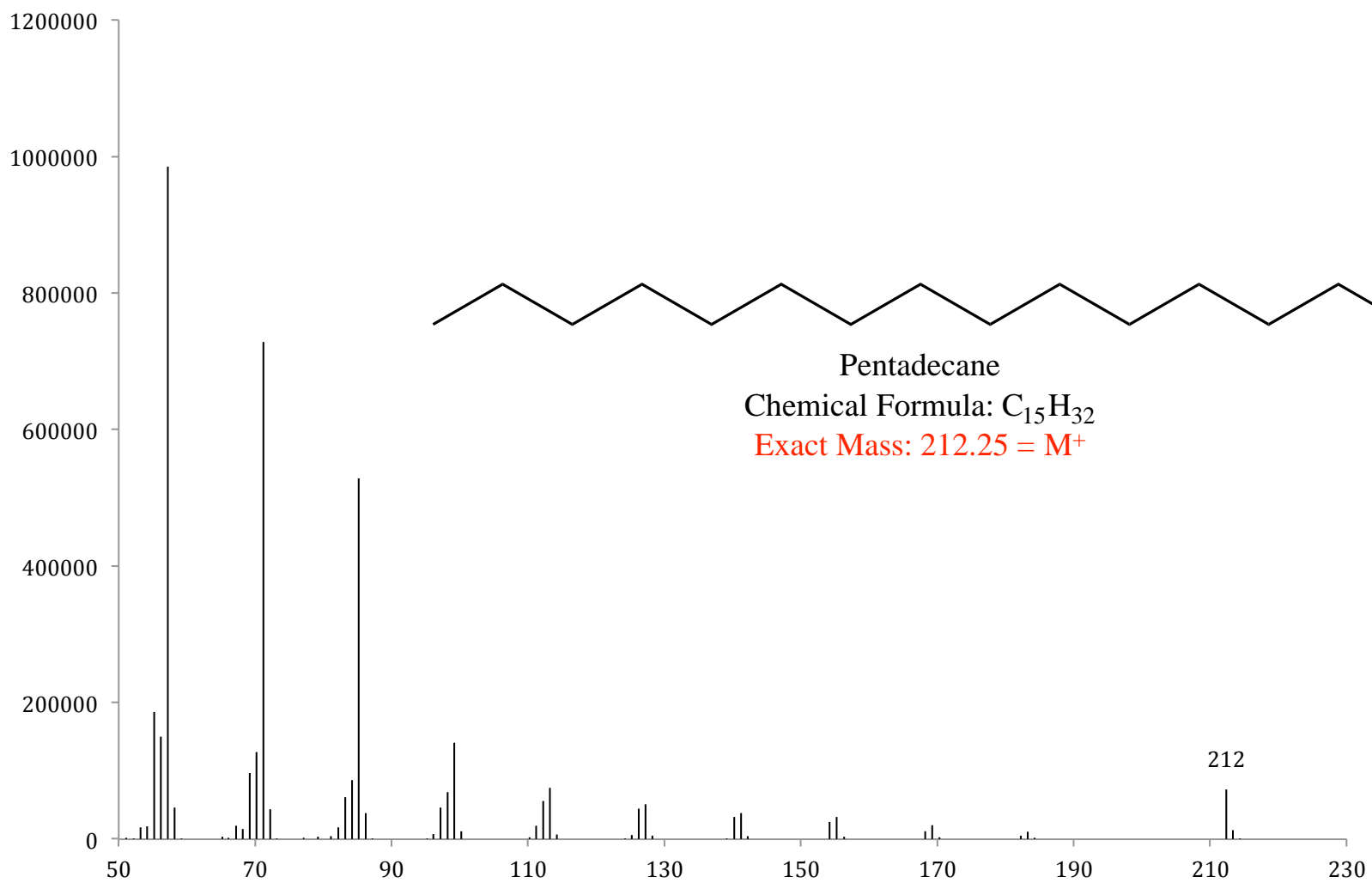


Figure B9. Mass spectrum of C15, or n-pentadecane, a purchased standard. The structure, chemical formula and expected M^+ are inset.

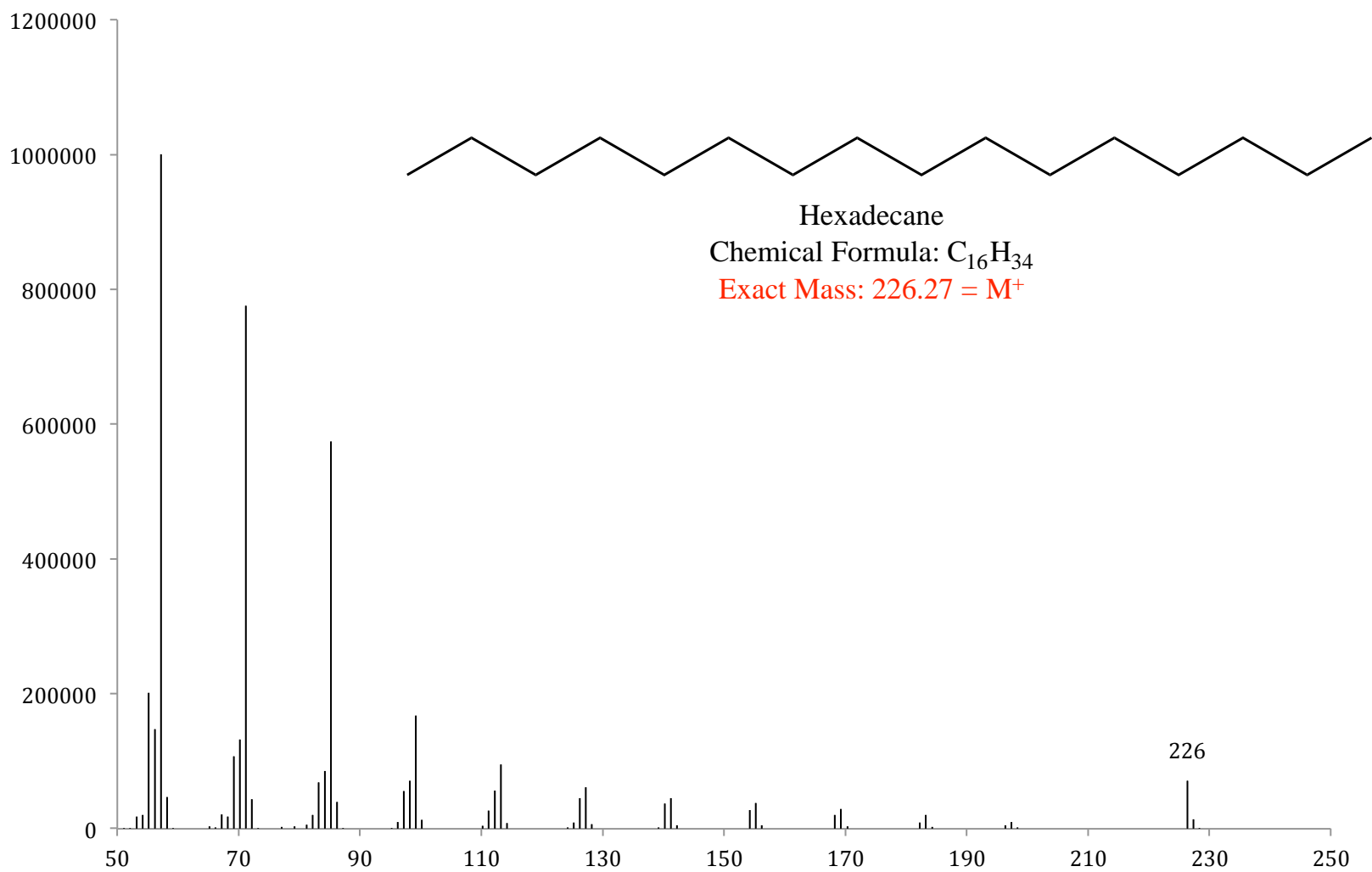


Figure B10. Mass spectrum of C16, or n-hexadecane, a purchased standard. The structure, chemical formula and expected M^+ are inset.

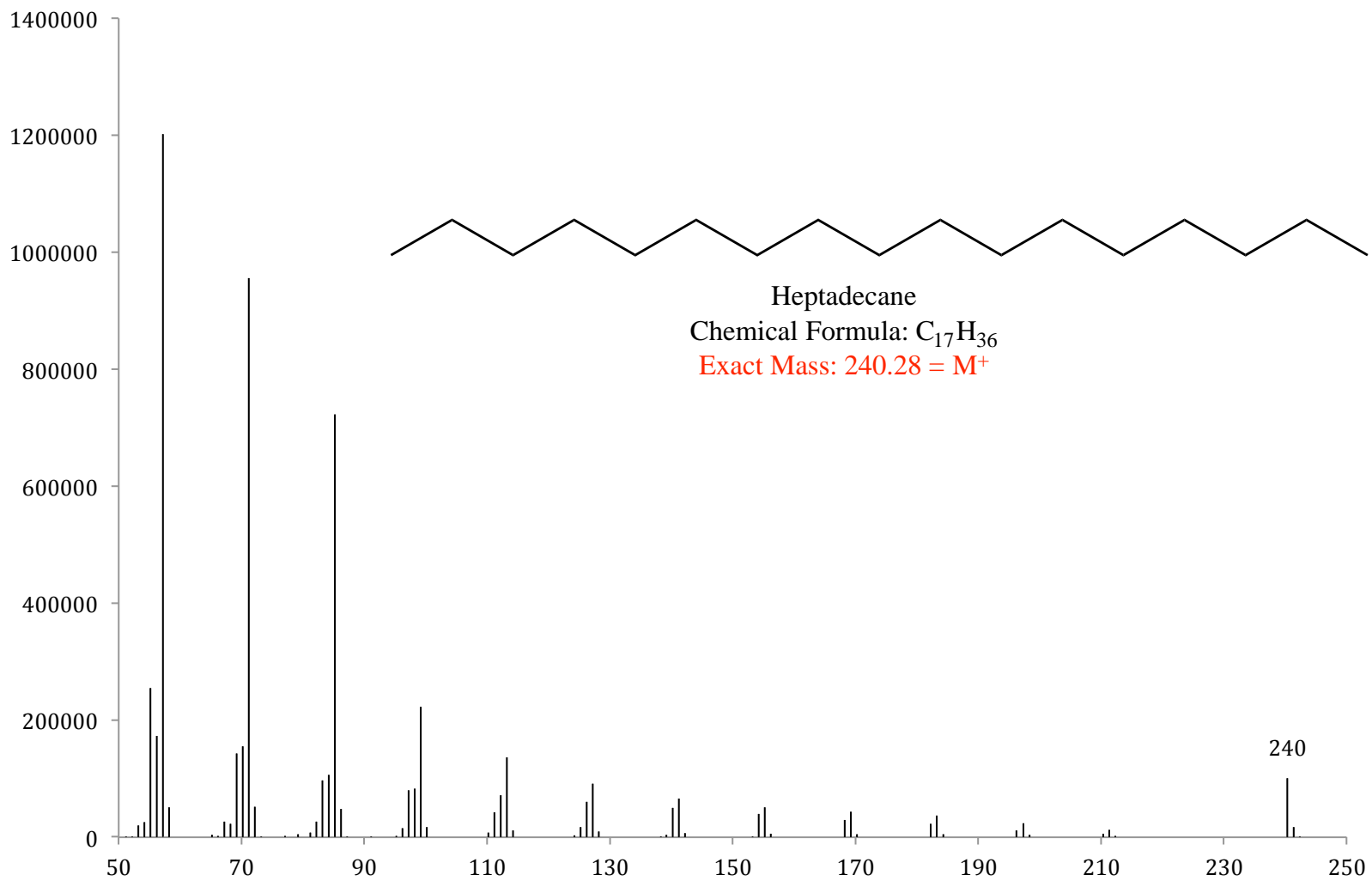


Figure B11. Mass spectrum of C17, or n-heptadecane, a purchased standard. The structure, chemical formula and expected M^+ are inset.

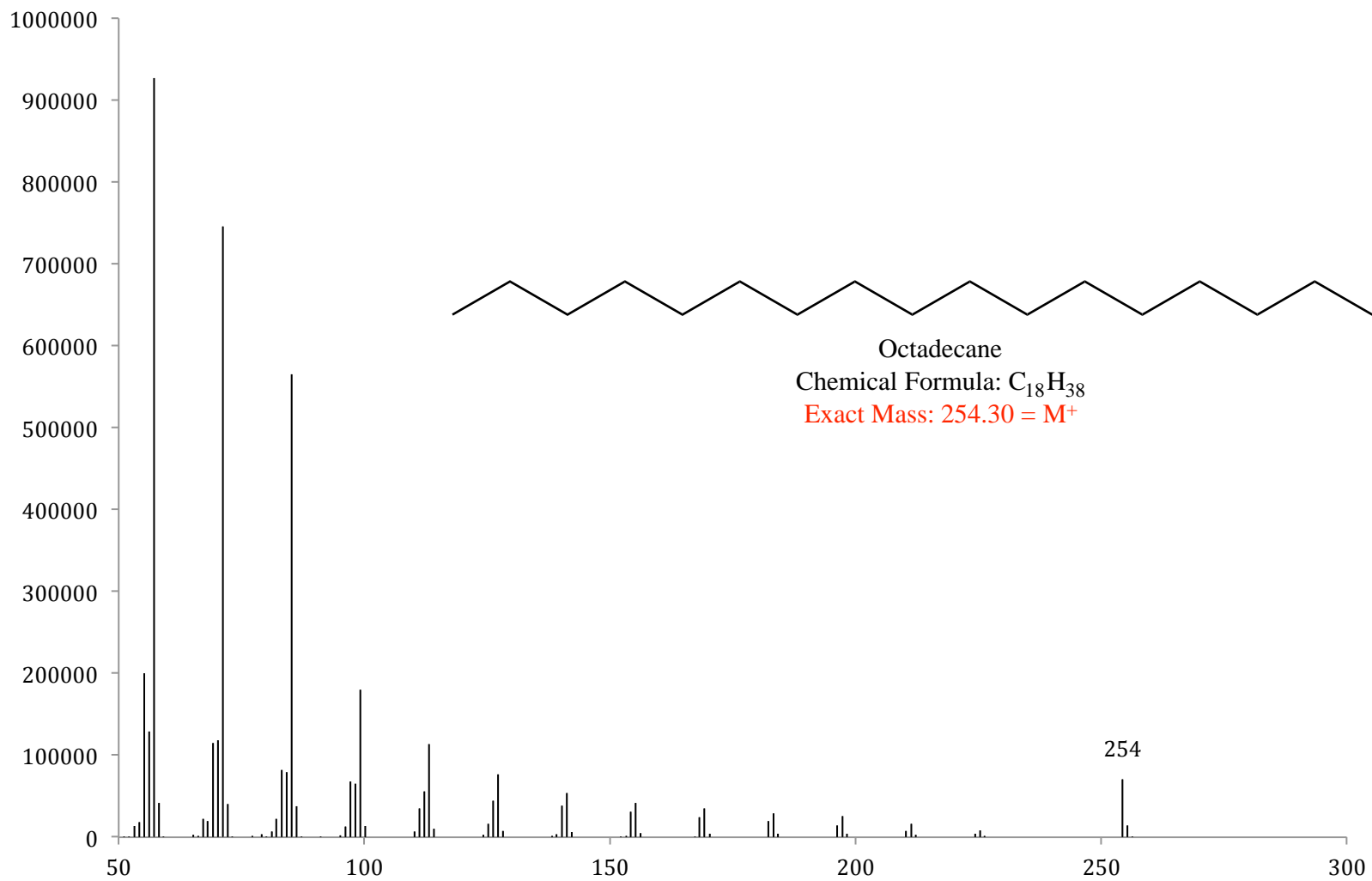


Figure B12. Mass spectrum of C18, n-octadecane, a purchased standard. The structure, chemical formula and expected M^+ are inset.

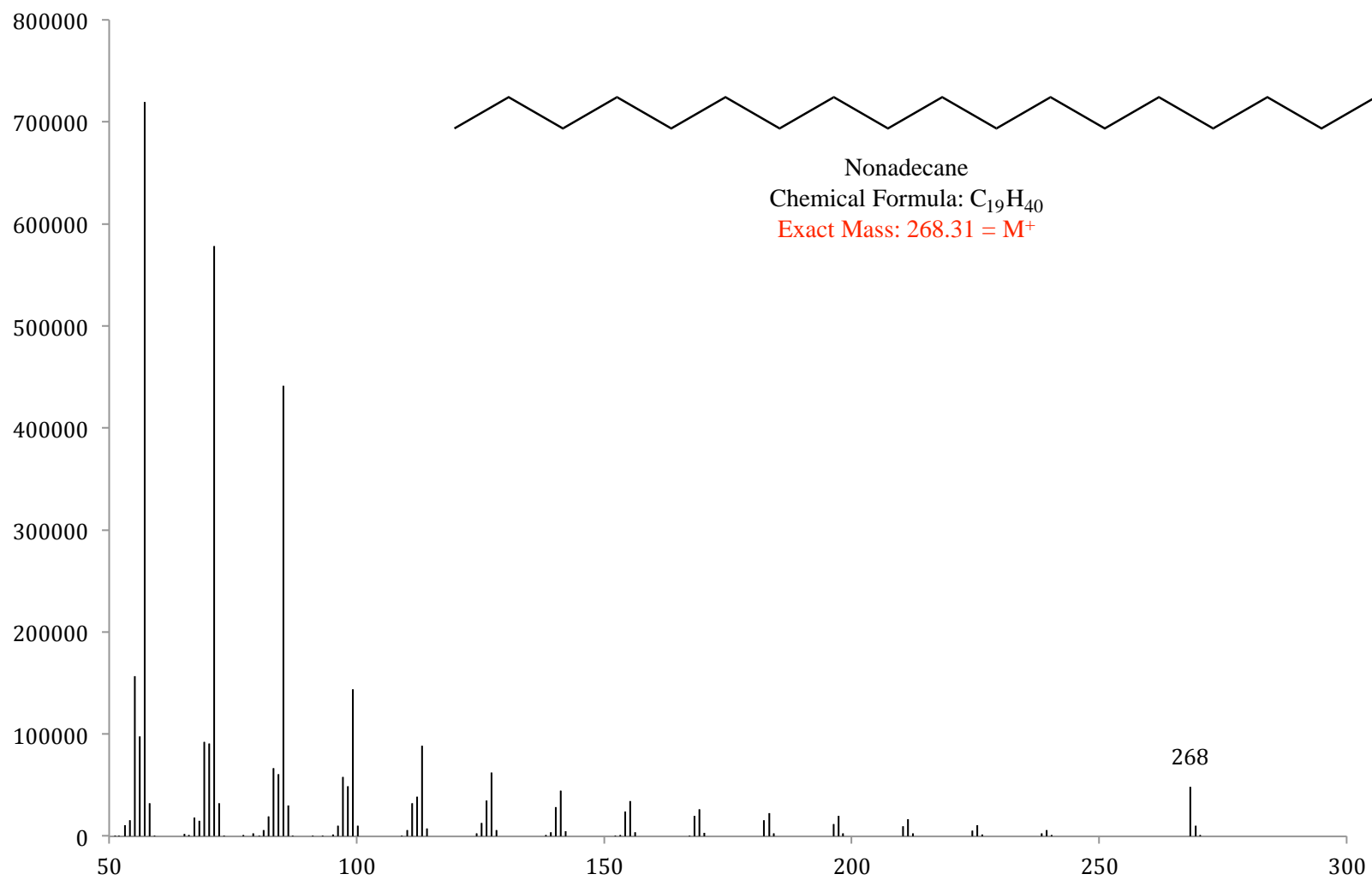


Figure B13. Mass spectrum of C19, or n-nonadecane, a purchased standard. The structure, chemical formula and expected M^+ are inset.

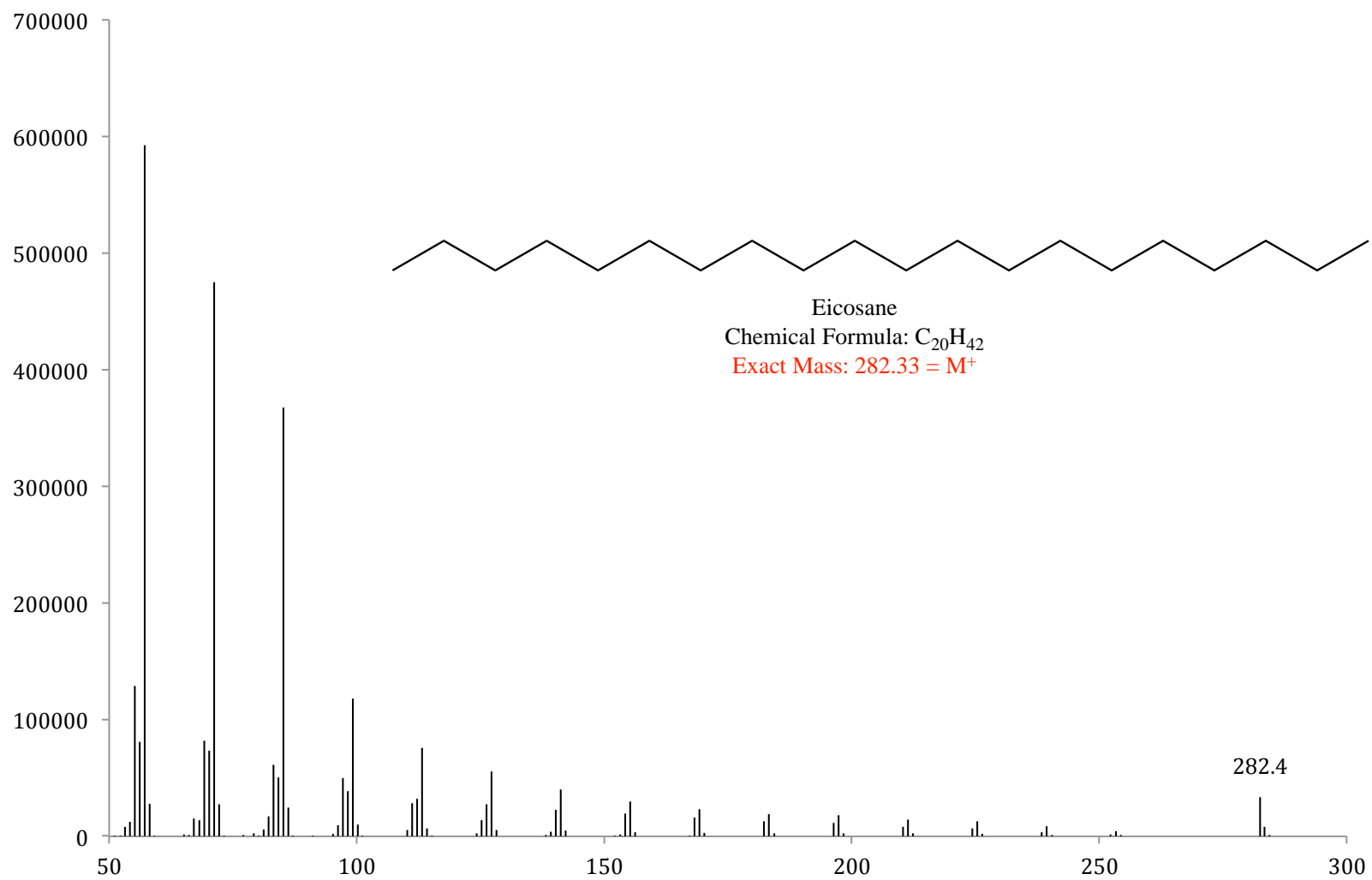


Figure B14. Mass spectrum of C₂₀, or n-eicosane, a purchased standard. The structure, chemical formula and expected M⁺ are inset.

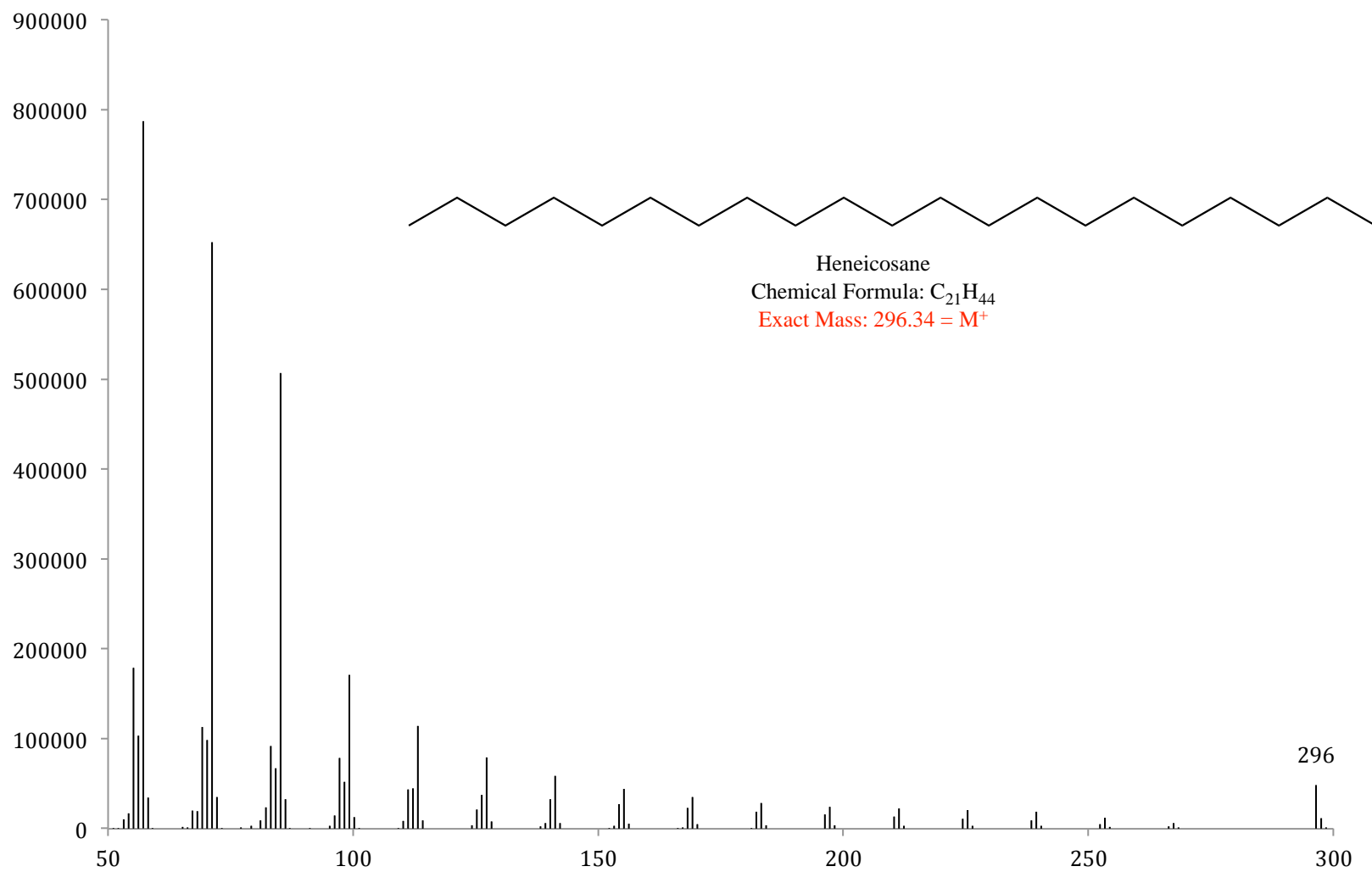


Figure B15. Mass spectrum of C₂₁, or heneicosane, a purchased standard. The structure, chemical formula and expected M⁺ are inset.

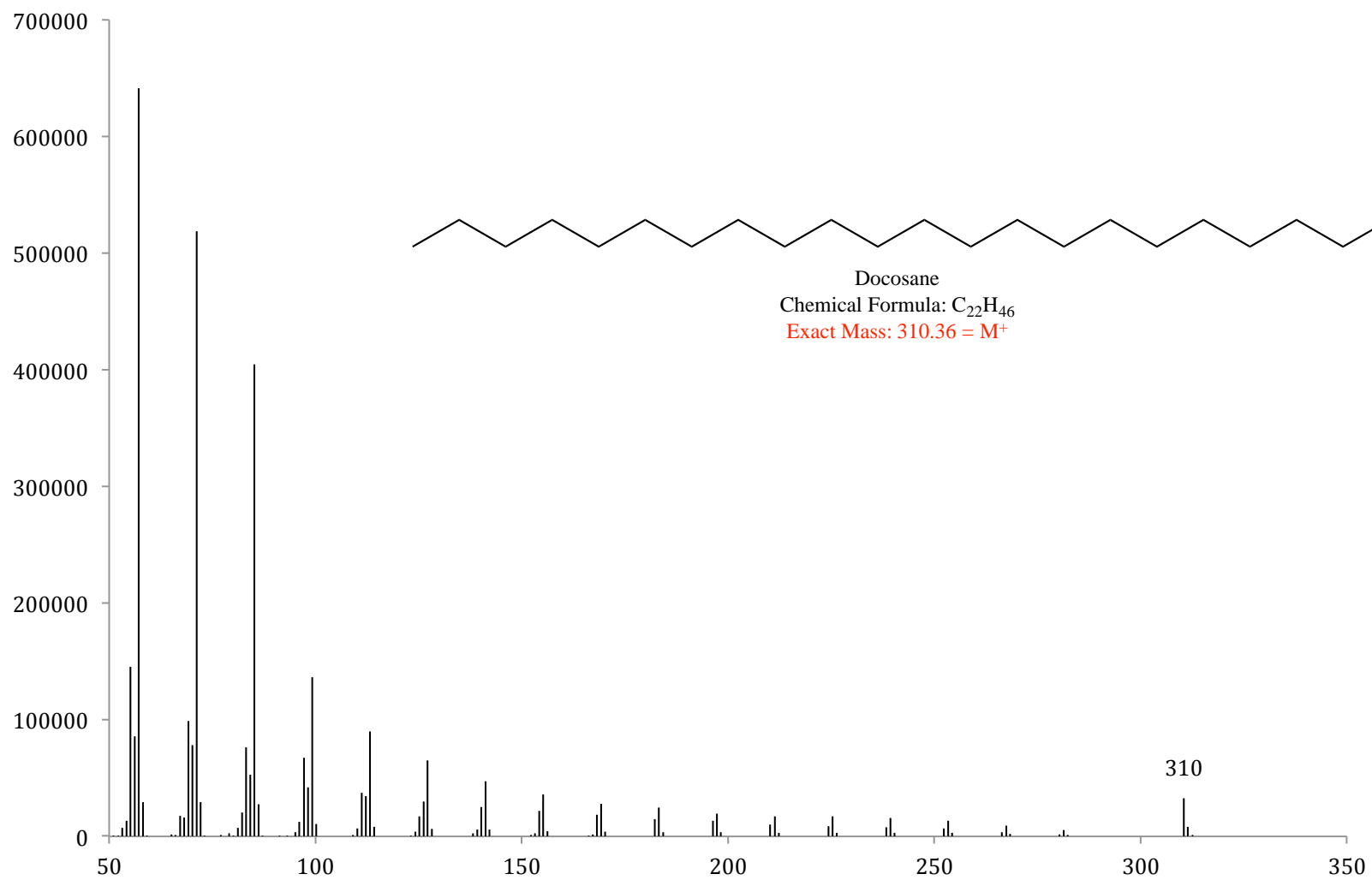


Figure B16. Mass spectrum of C₂₂, or n-docosane, a purchased standard. The structure, chemical formula and expected M⁺ are inset.

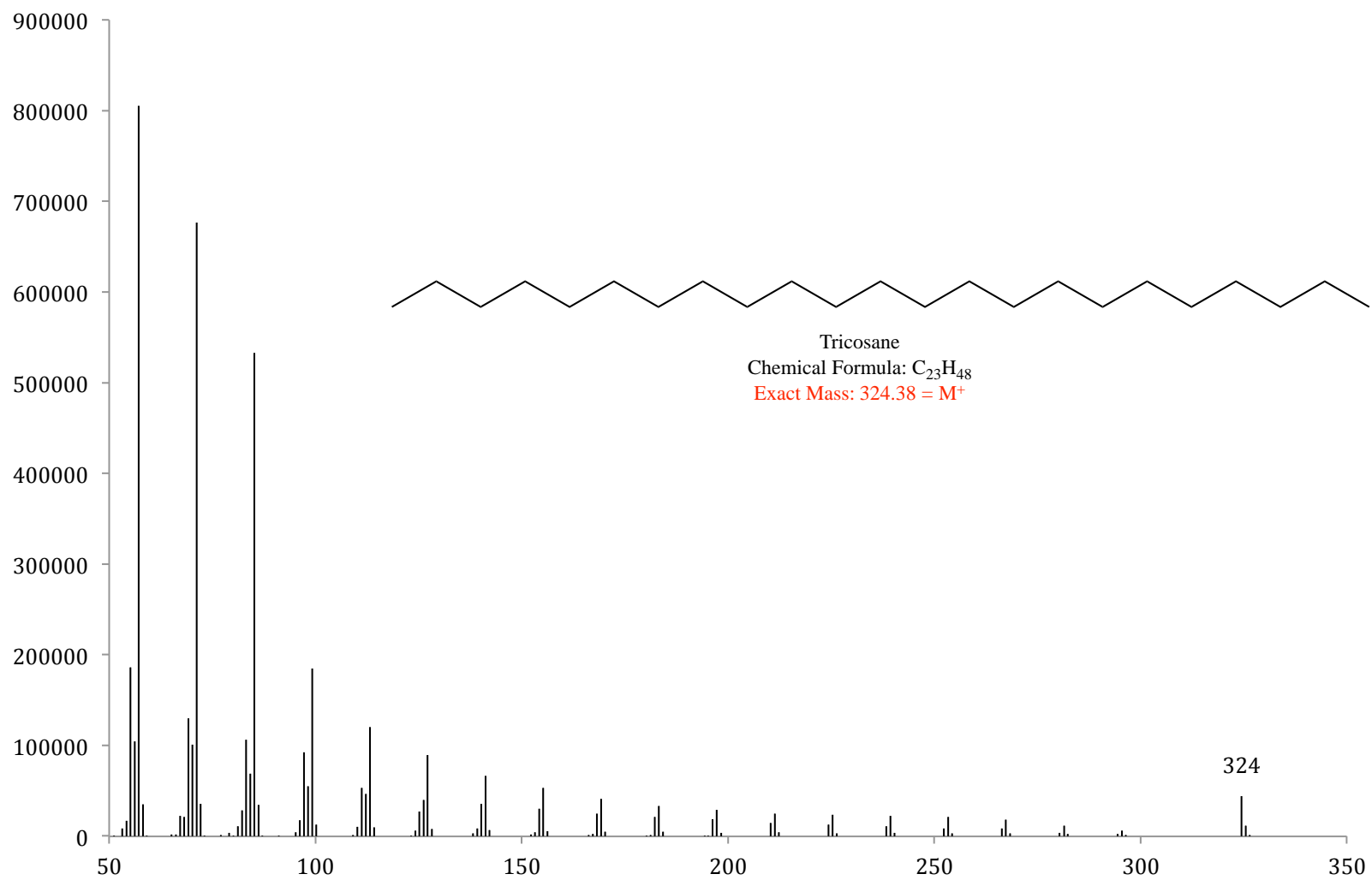


Figure B17. Mass spectrum of C23, or n-tricosane, a purchased standard. The structure, chemical formula and expected M^+ are inset.

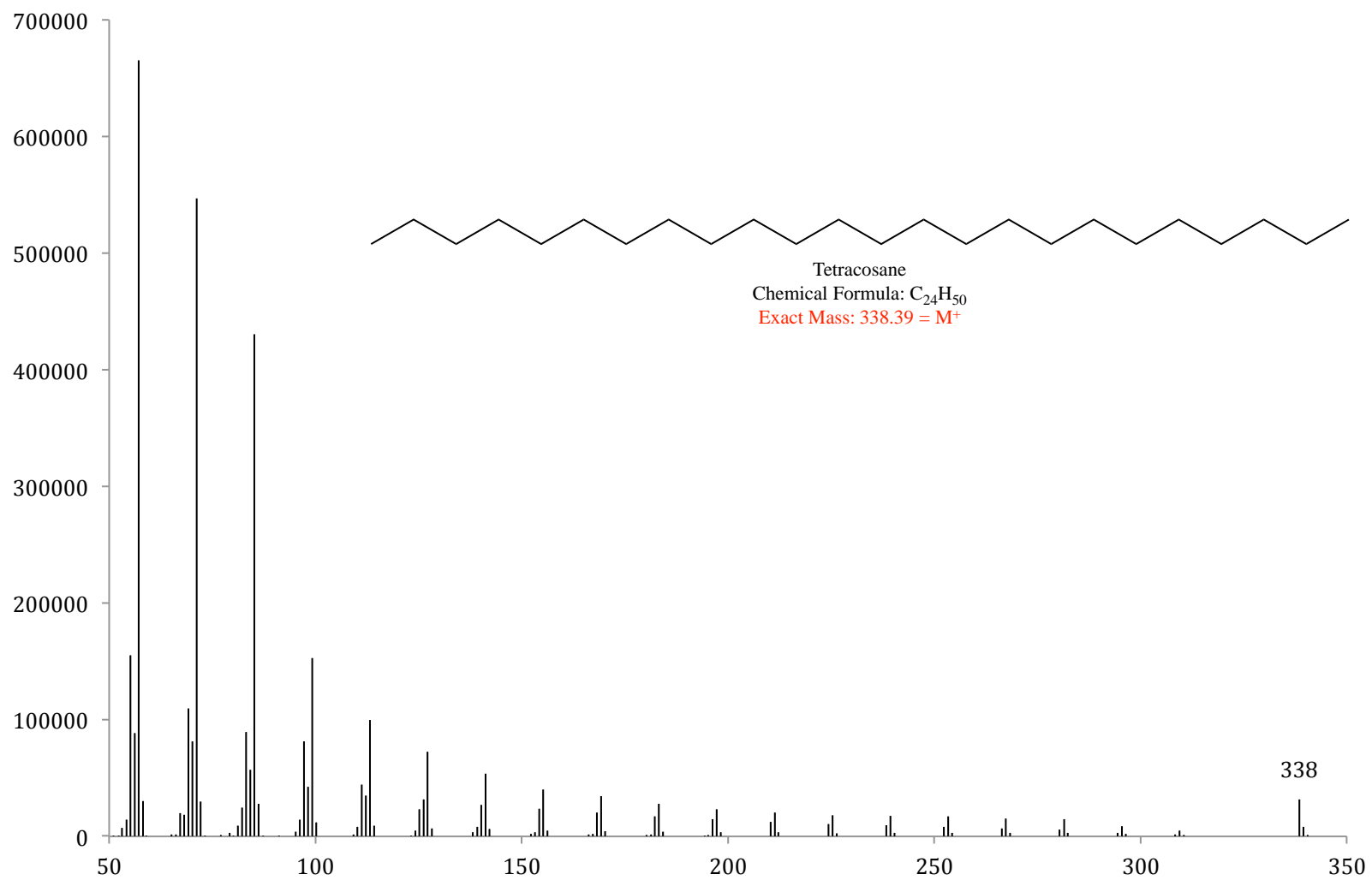


Figure B18. Mass spectrum of C₂₄, or tetracosane, a purchased standard. The structure, chemical formula and expected M⁺ are inset.

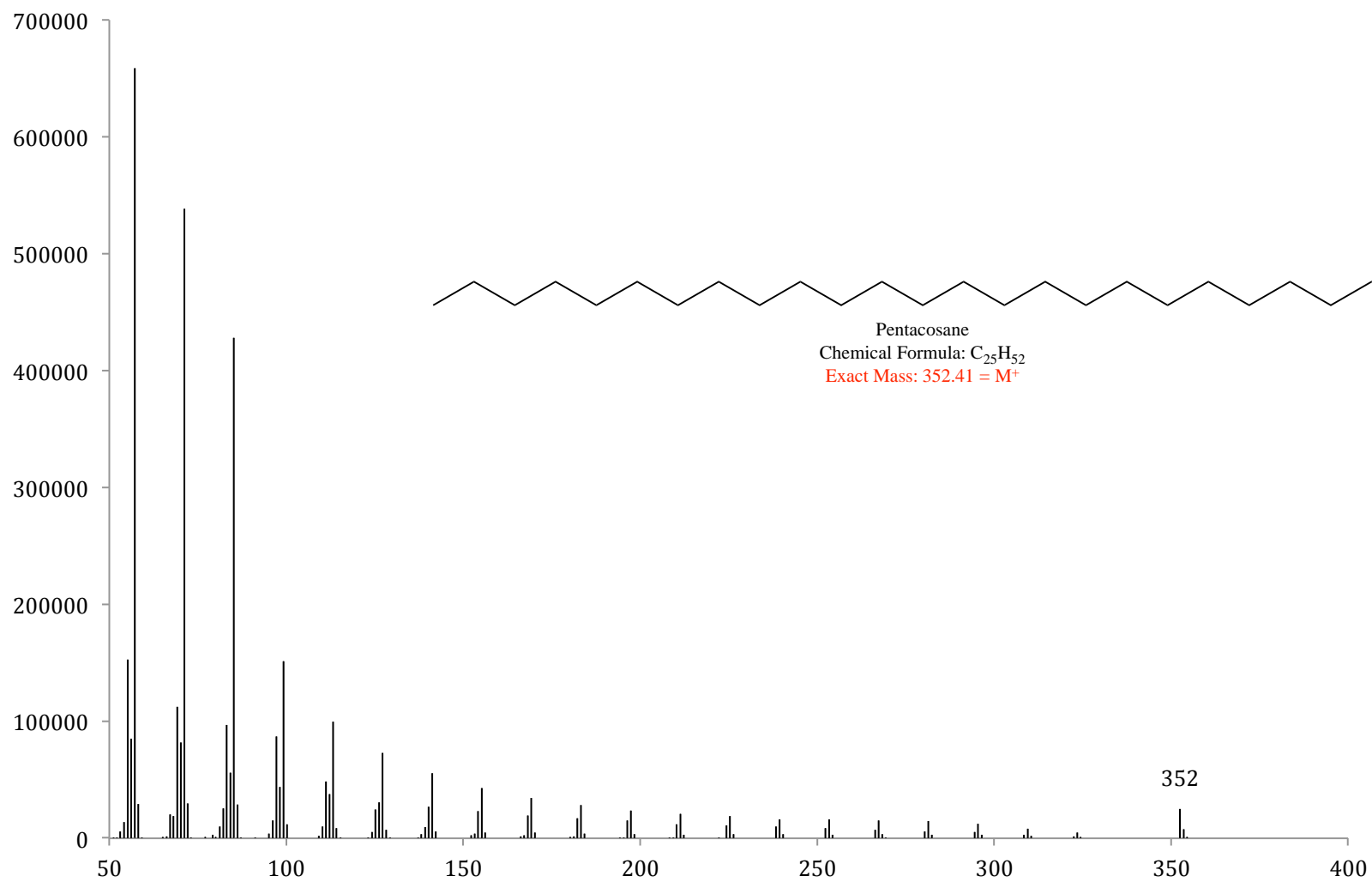


Figure B19. Mass spectrum of C₂₅, or pentacosene, a purchased standard. The structure, chemical formula and expected M⁺ are inset.

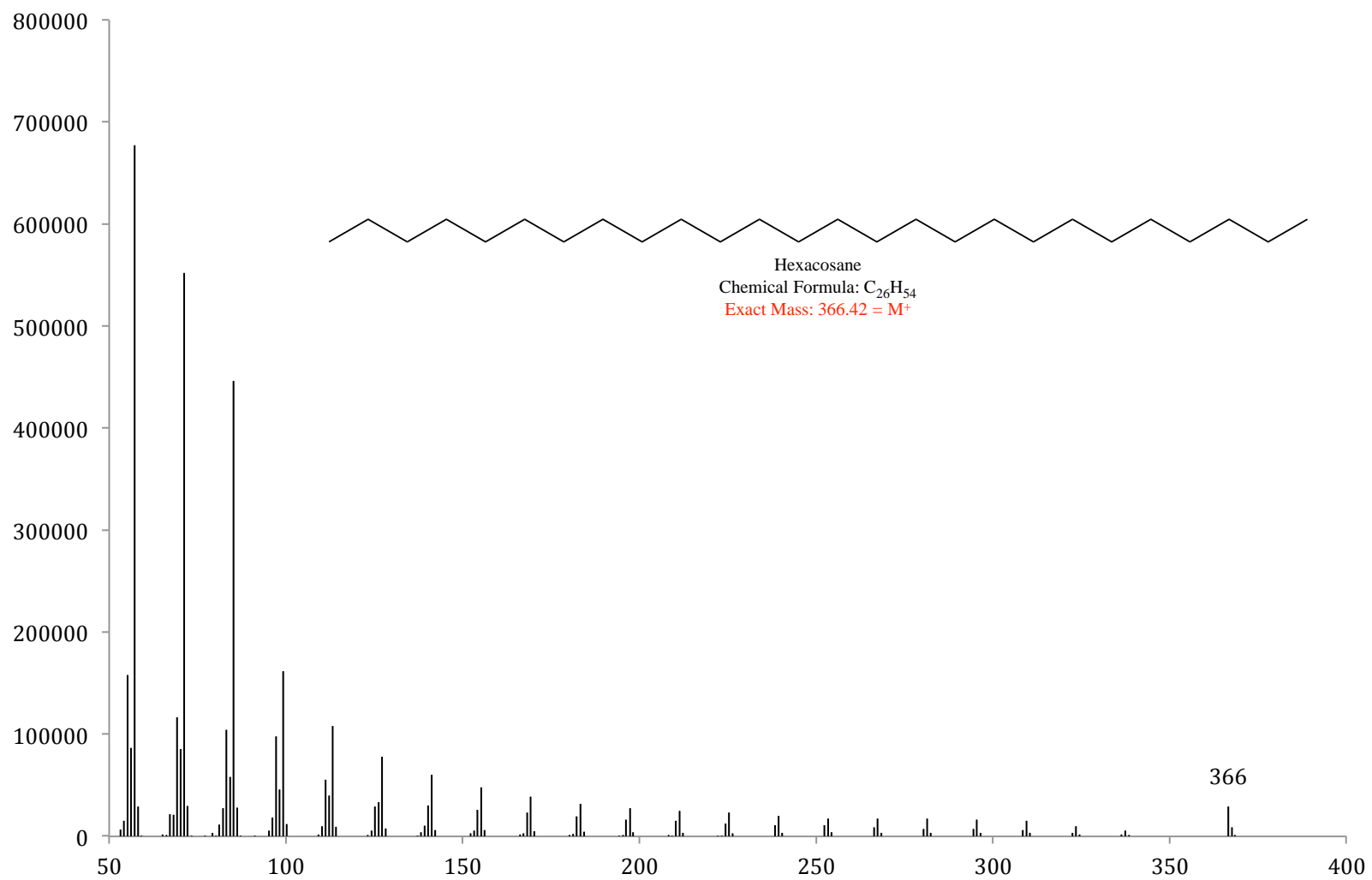


Figure B20. Mass spectrum of C₂₆, or hexacosane, a purchased standard. The structure, chemical formula and expected M⁺ are inset.

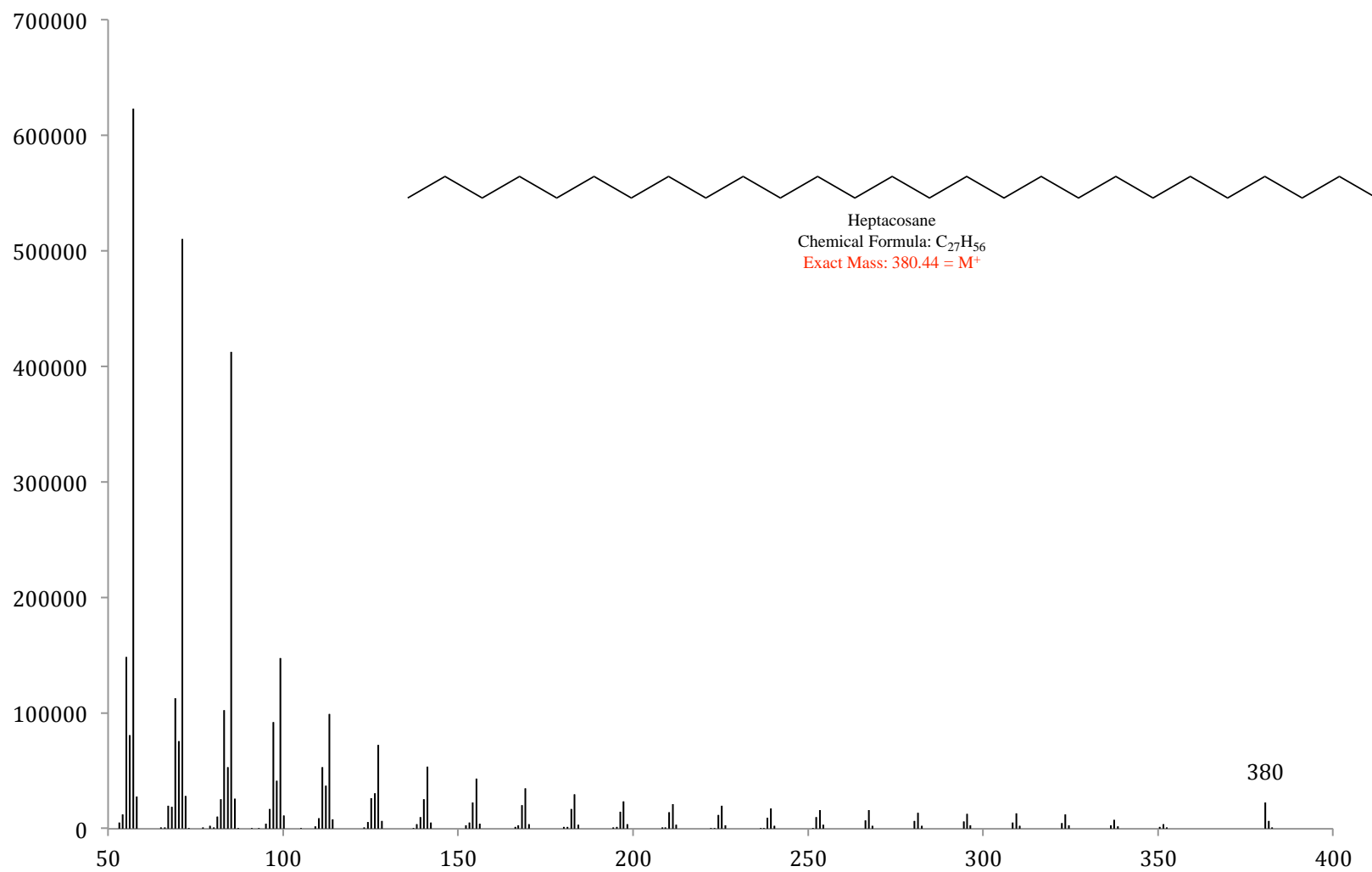


Figure B21. Mass spectrum of C₂₇, or heptacosene, a purchased standard. The structure, chemical formula and expected M⁺ are inset.

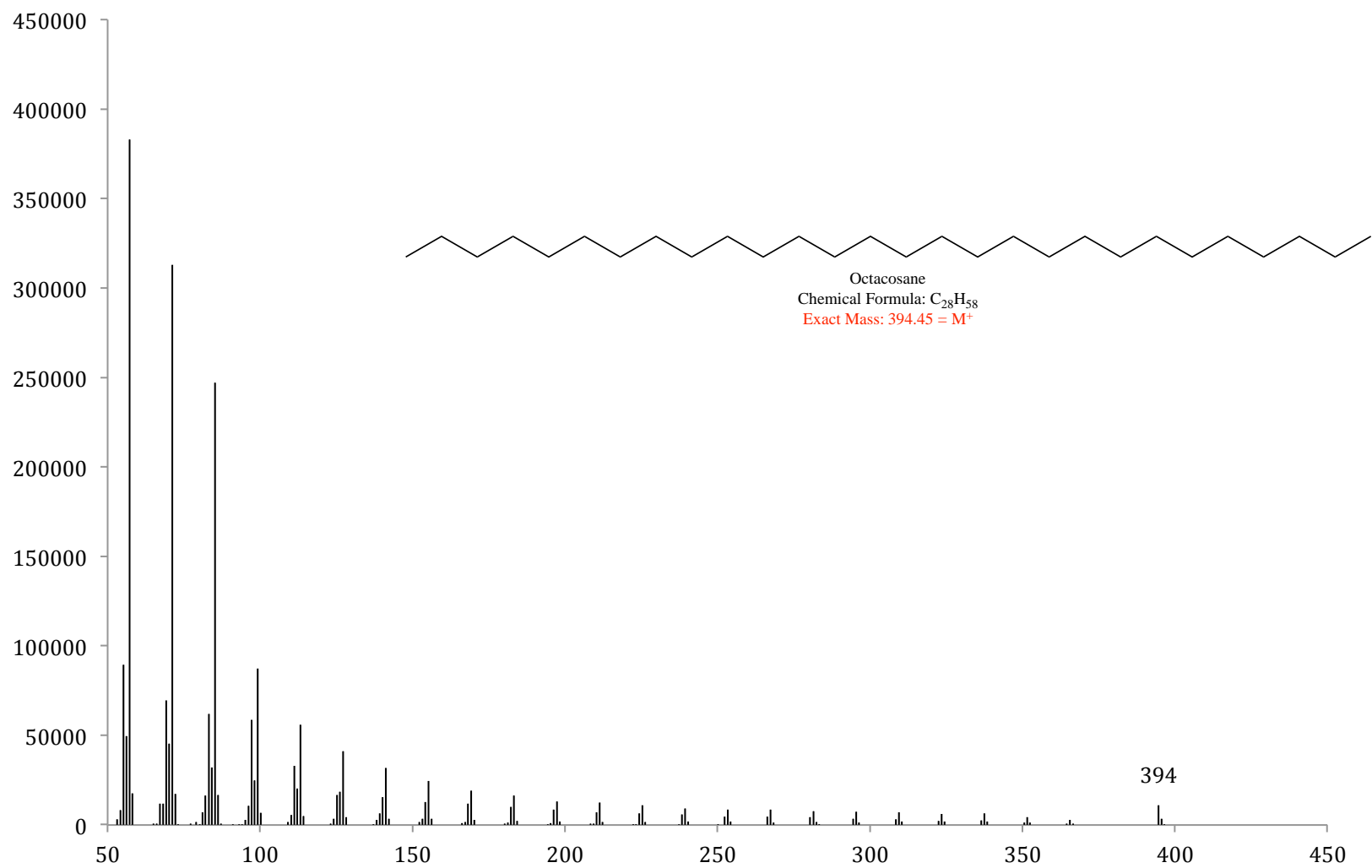


Figure B22. Mass spectrum of C_{28} , or octacosane, a purchased standard. The structure, chemical formula and expected M^+ are inset.

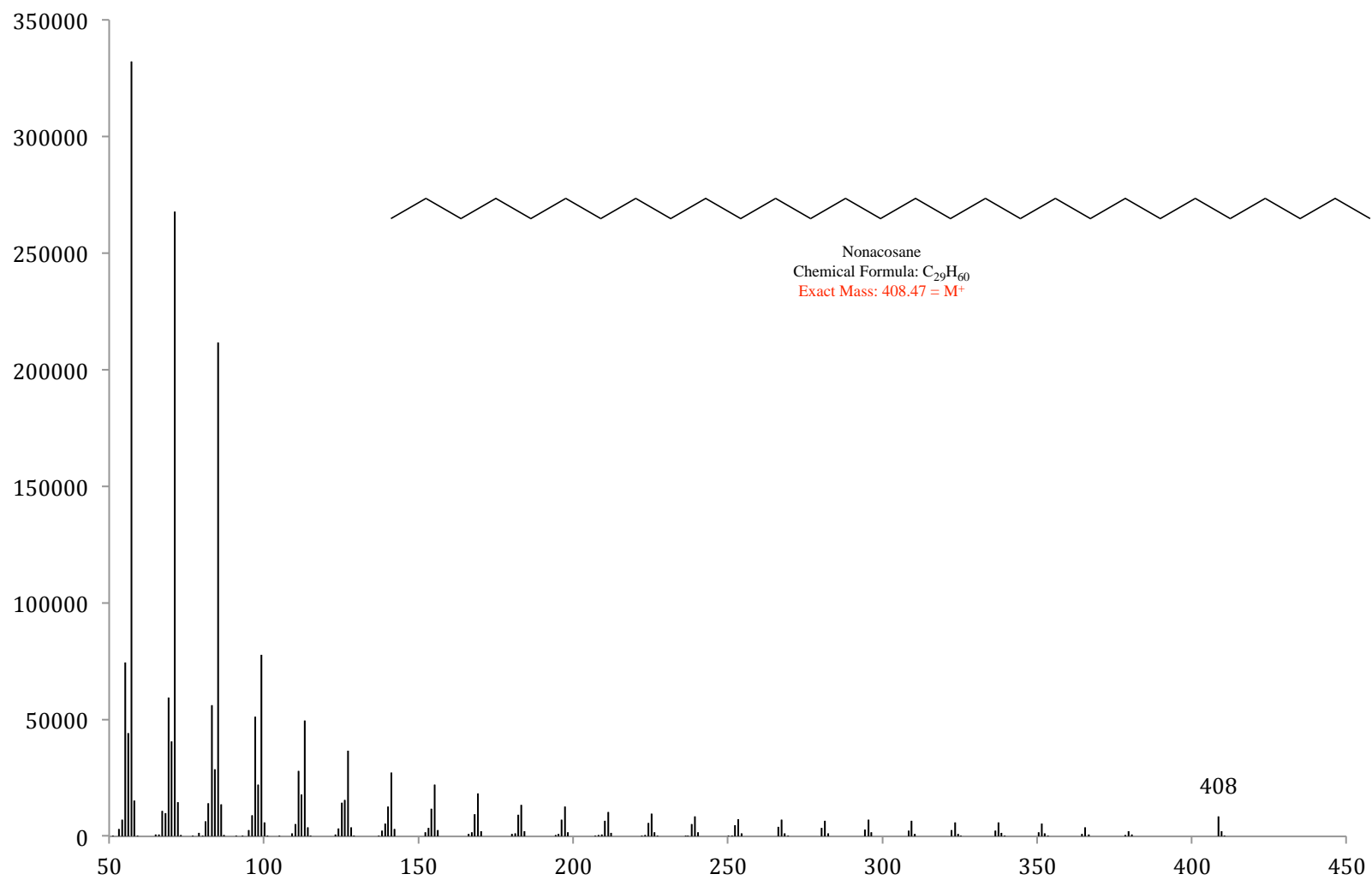


Figure B23. Mass spectrum of C₂₉, or nonacosane, a purchased standard. The structure, chemical formula and expected M^+ are inset.

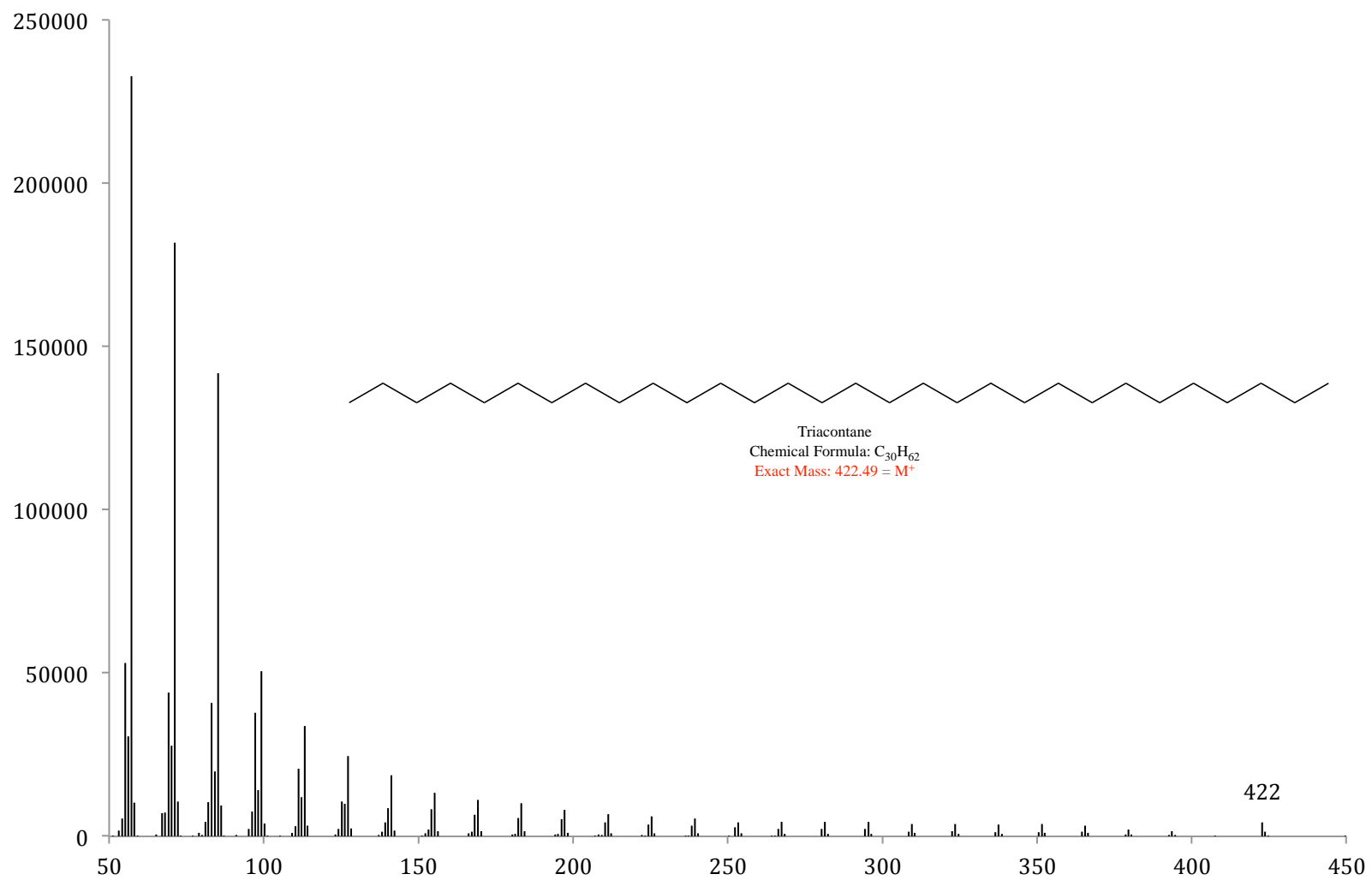


Figure B24. Mass spectrum of C₃₀, or triacontane, a purchased standard. The structure, chemical formula and expected M⁺ are inset.

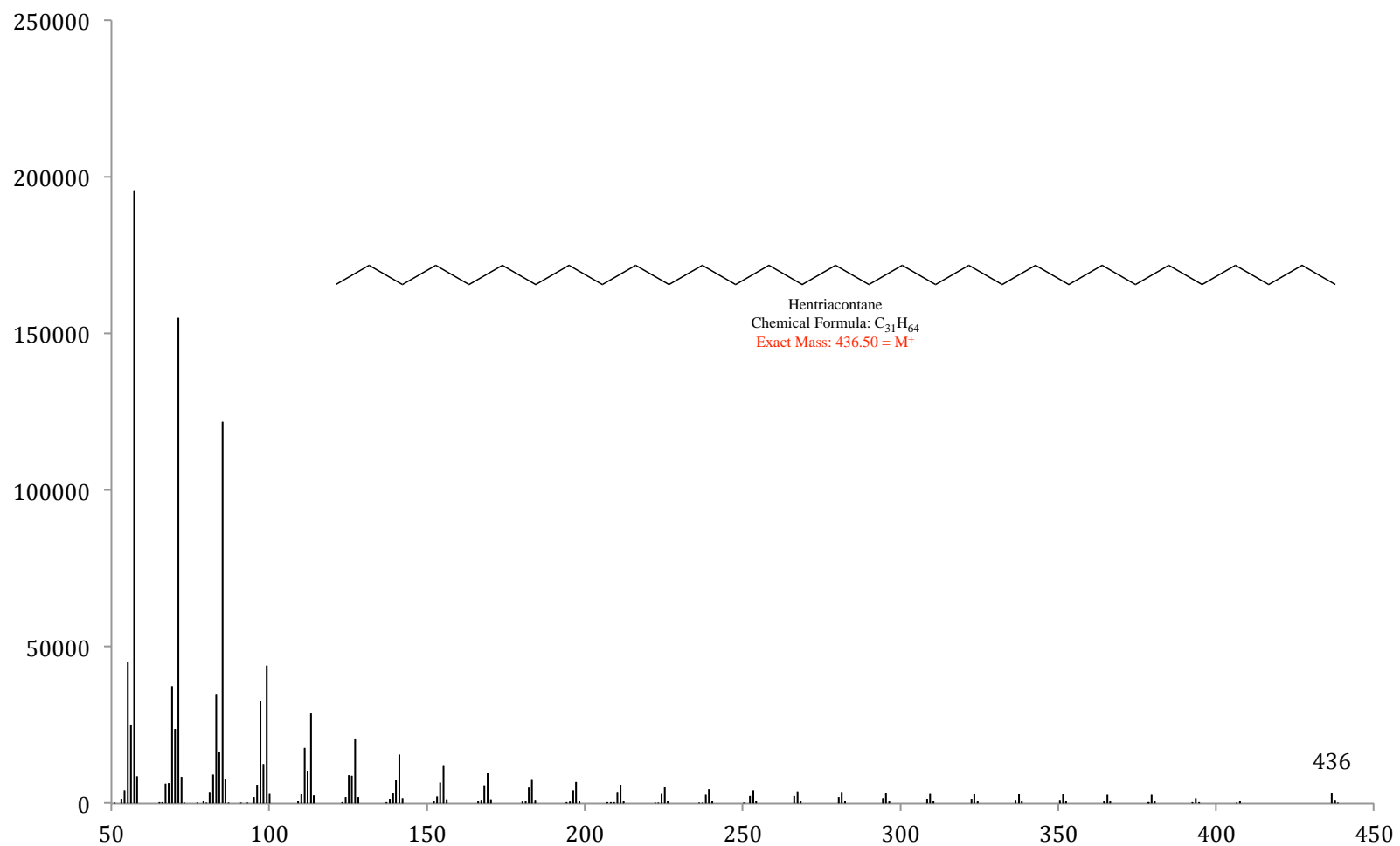


Figure B25. Mass spectrum of C31, or untriacontane, a purchased standard. The structure, chemical formula and expected M⁺ are inset.

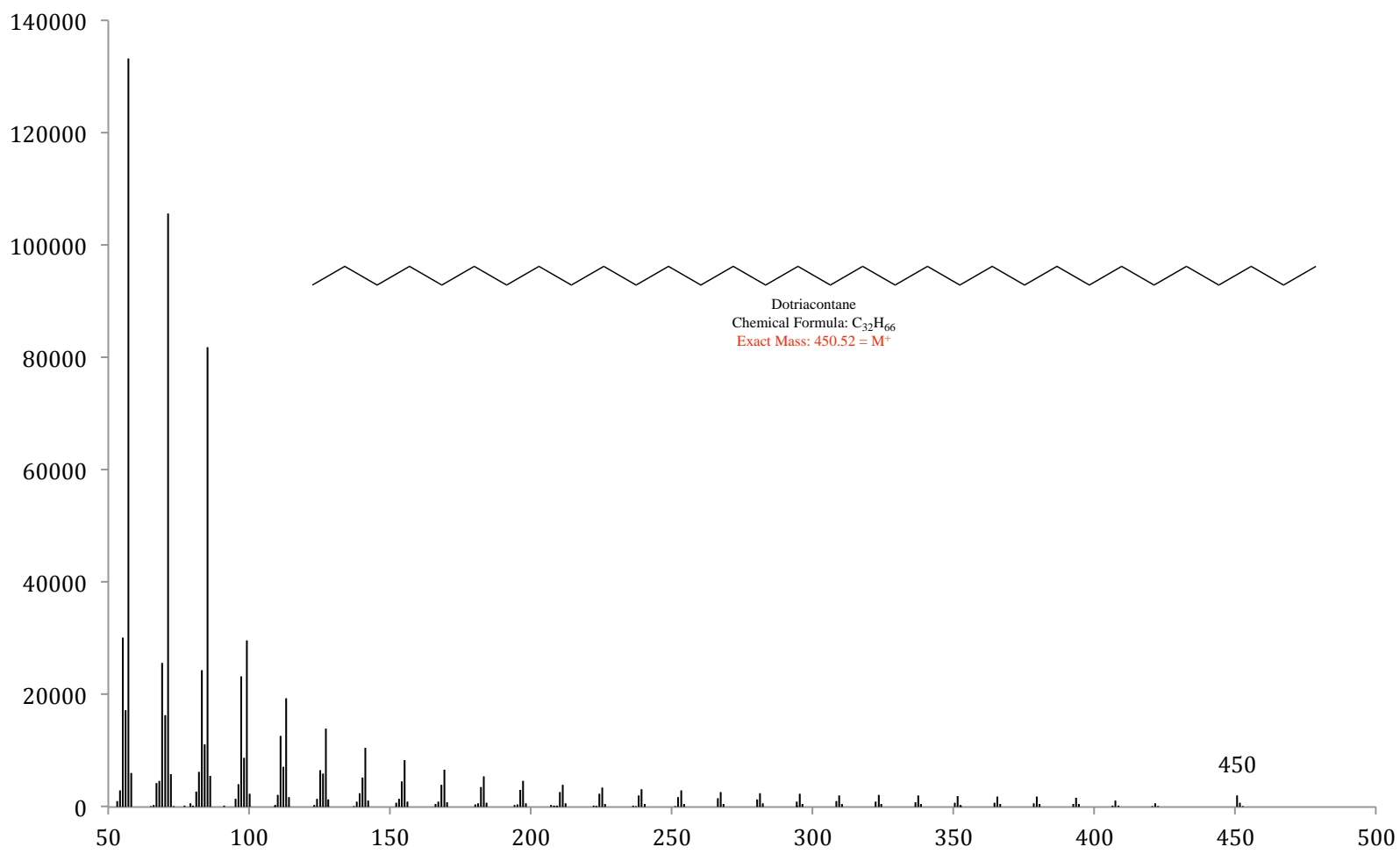


Figure B26. Mass spectrum of C32, or dotriacontane, a purchased standard. The structure, chemical formula and expected M^+ are inset.

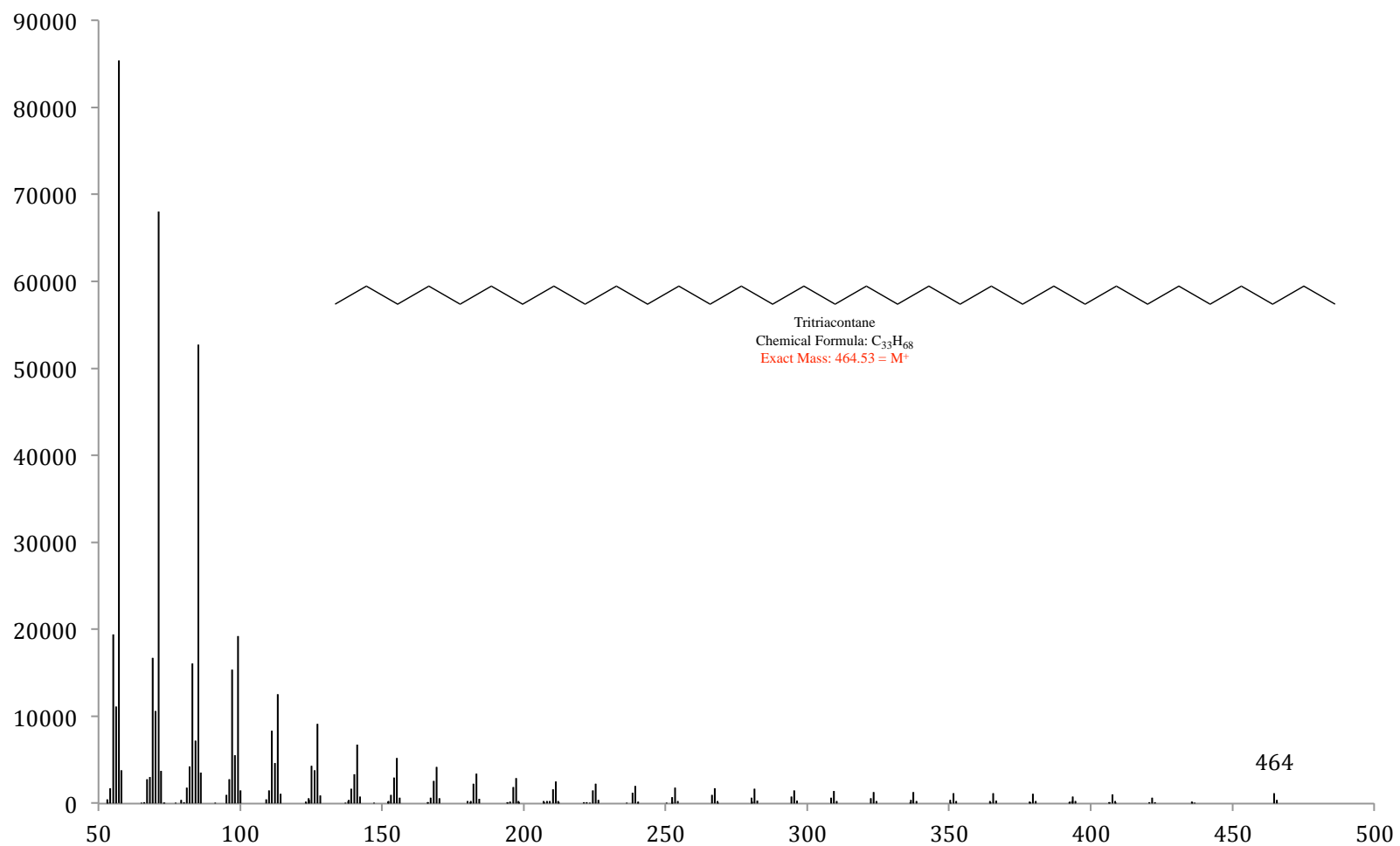


Figure B27. Mass spectrum of C₃₃, or tritriacontane, a purchased standard. The structure, chemical formula and expected M⁺ are inset.

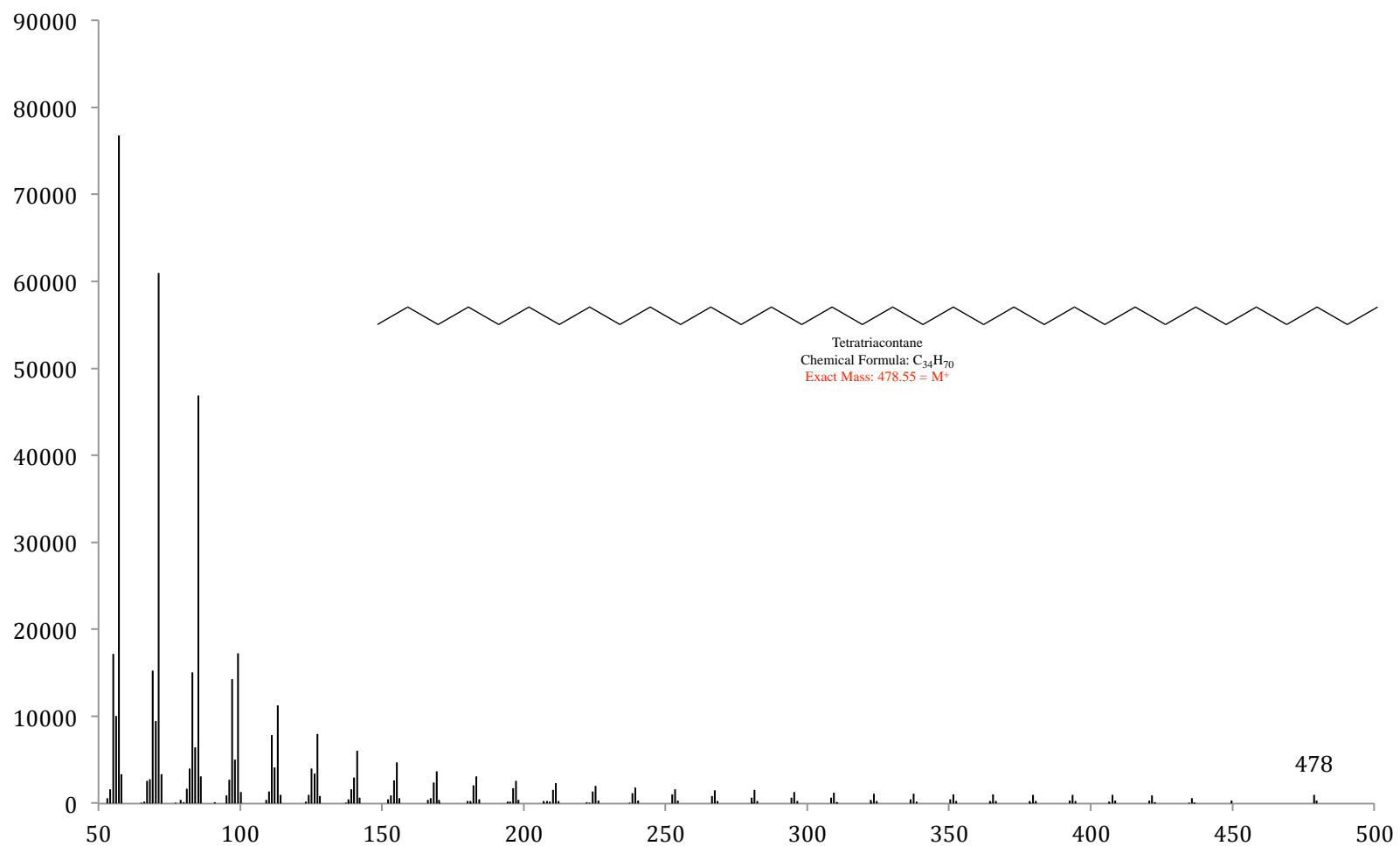


Figure B28. Mass spectrum of C₃₄, or tetratriacontane, a purchased standard. The structure, chemical formula and expected M⁺ are inset.

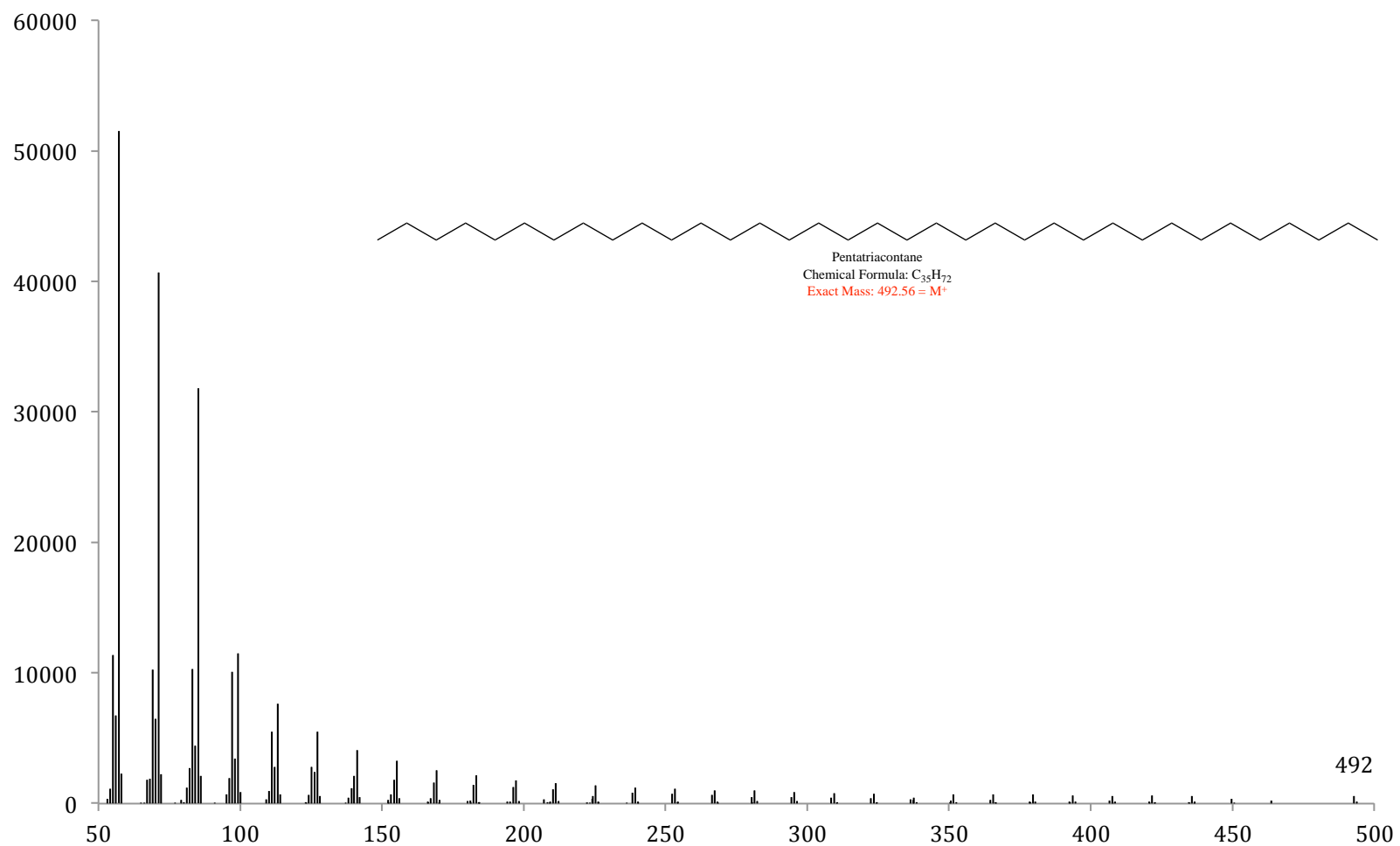


Figure B29. Mass spectrum of C35, or pentatriacontane, a purchased standard. The structure, chemical formula and expected M^+ are inset.

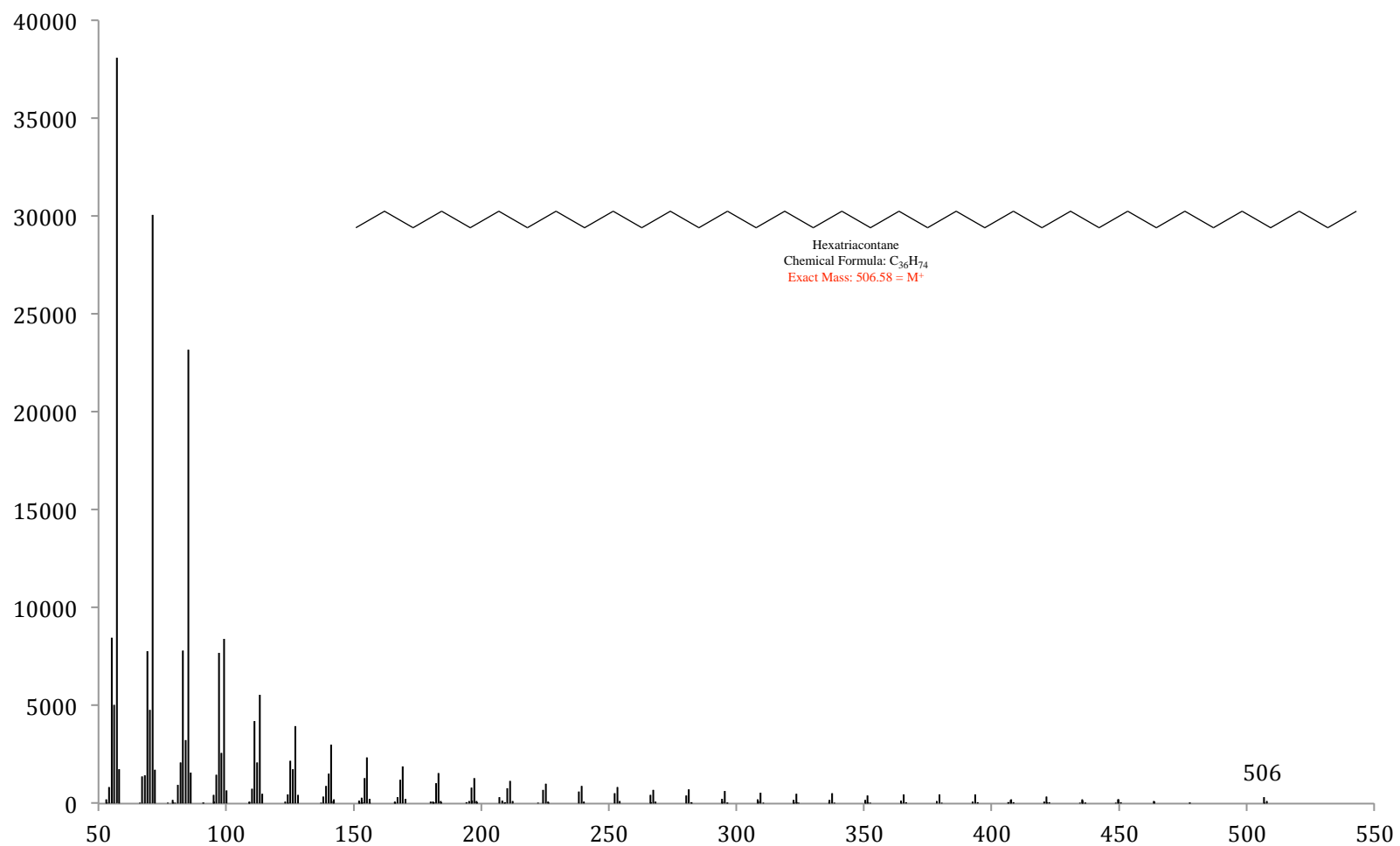


Figure B30. Mass spectrum of C₃₆, or hexatriacontane, a purchased standard. The structure, chemical formula and expected M^+ are inset.

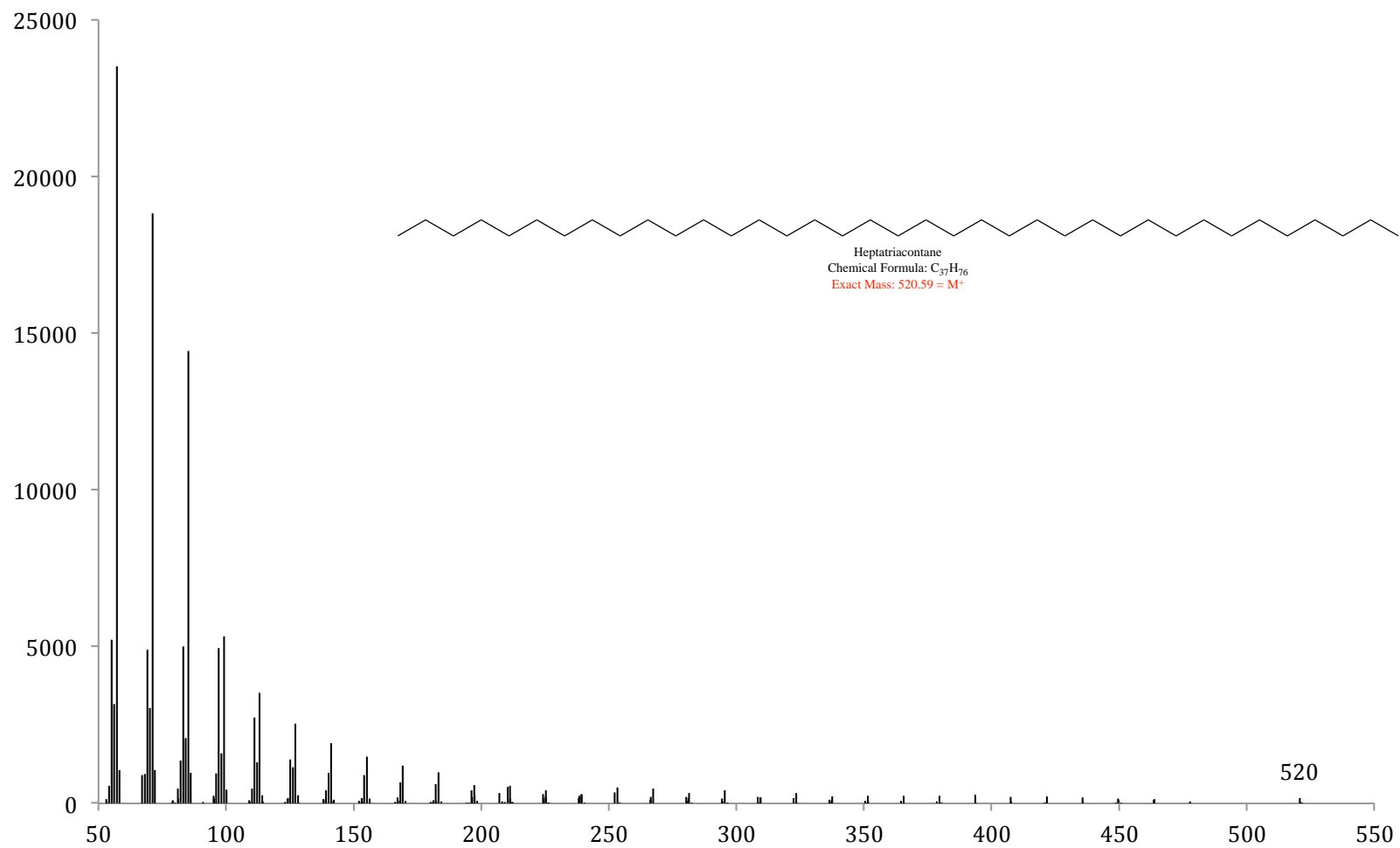


Figure B31. Mass spectrum of C37, or heptatriacontane, a purchased standard. The structure, chemical formula and expected M⁺ are inset.

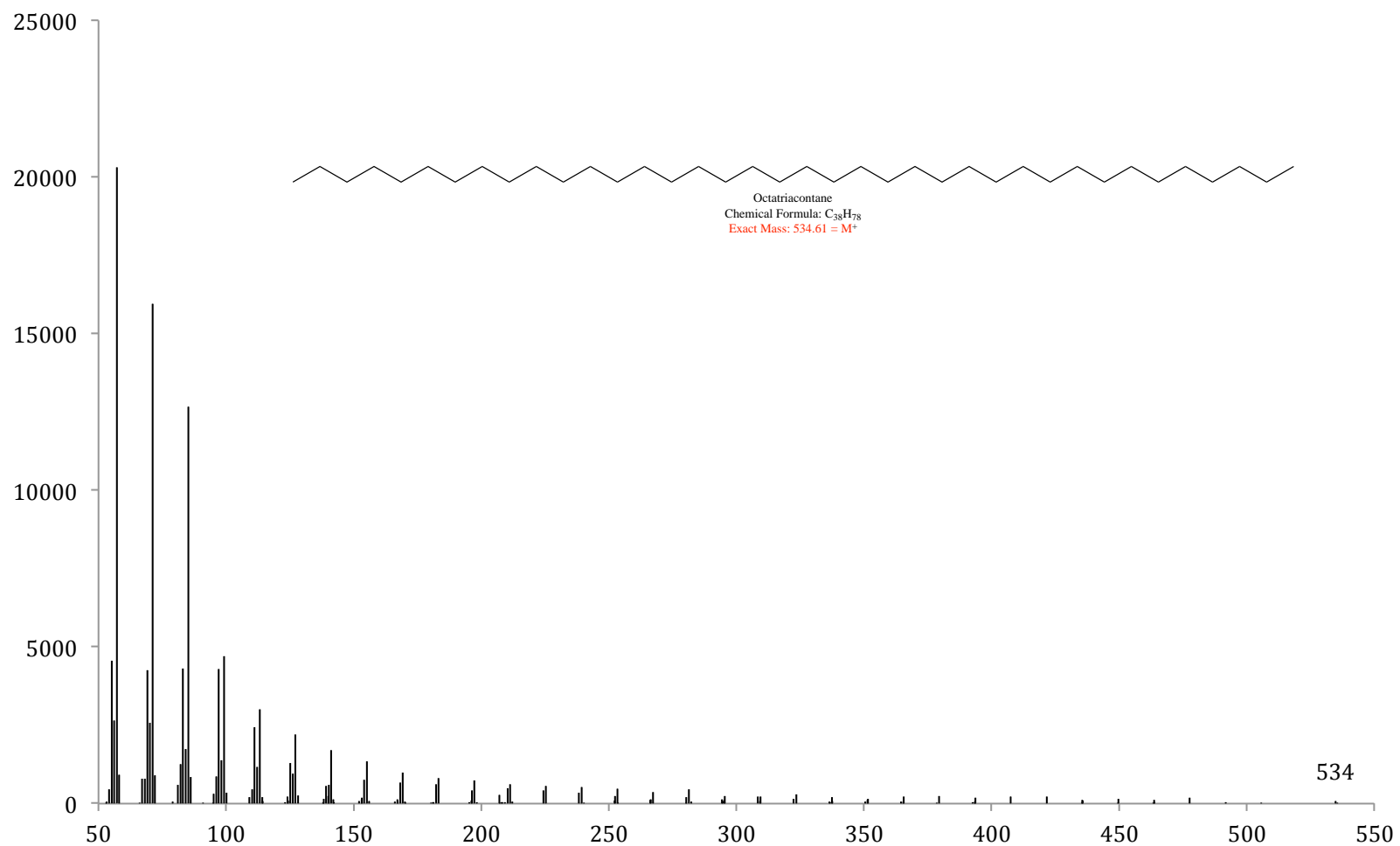


Figure B32. Mass spectrum of C38, or octatriacontane, a purchased standard. The structure, chemical formula and expected M^+ are inset.

Appendix C – 2-Methyl Branched Alkane Mass Spectra

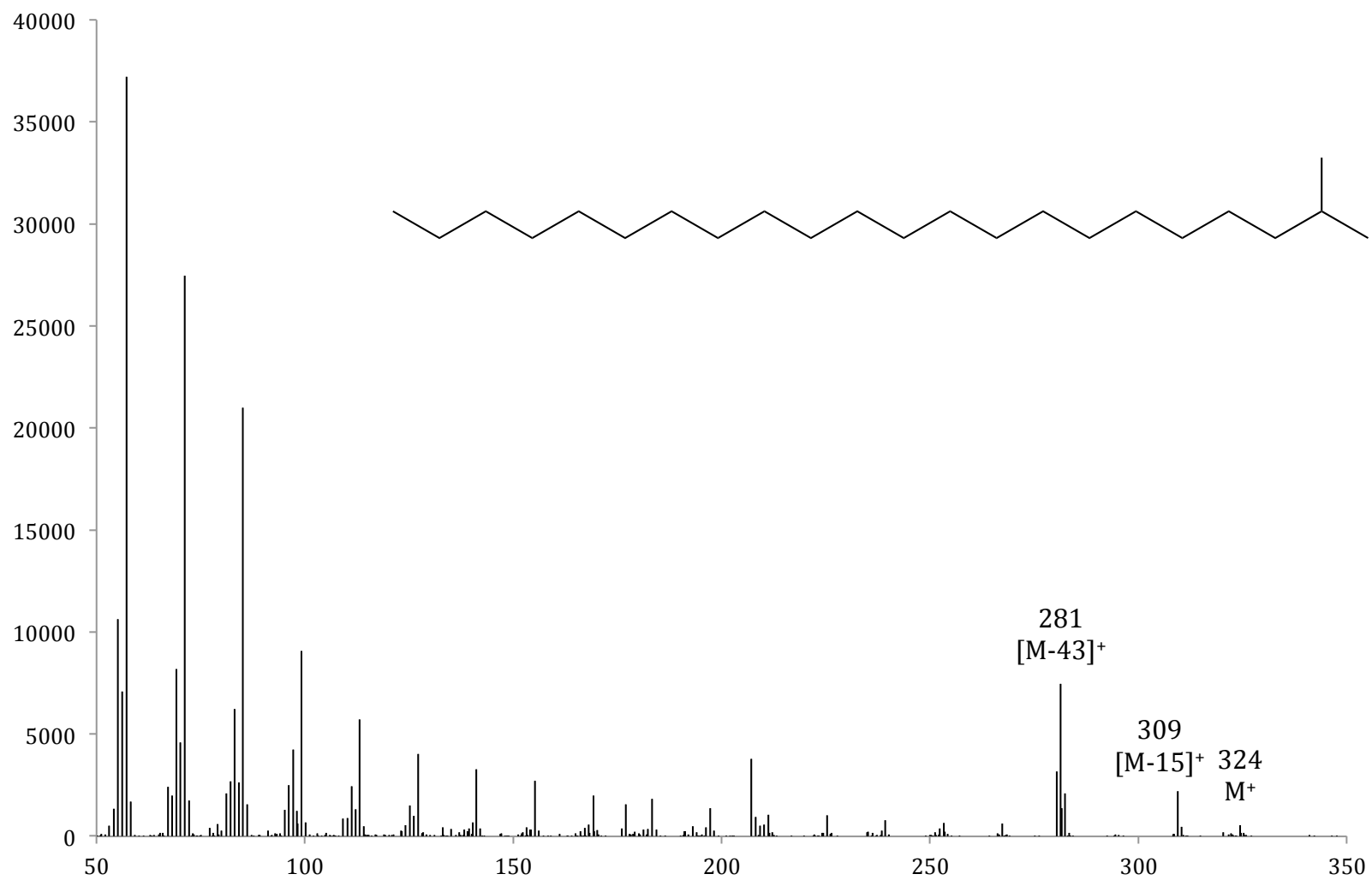


Figure C1. Mass spectrum of 2-methyltricosane, a purchased standard. Peaks at [M-15]⁺ and [M-43]⁺ indicate a branch at the second carbon. The chemical structure of this CHC is inset.

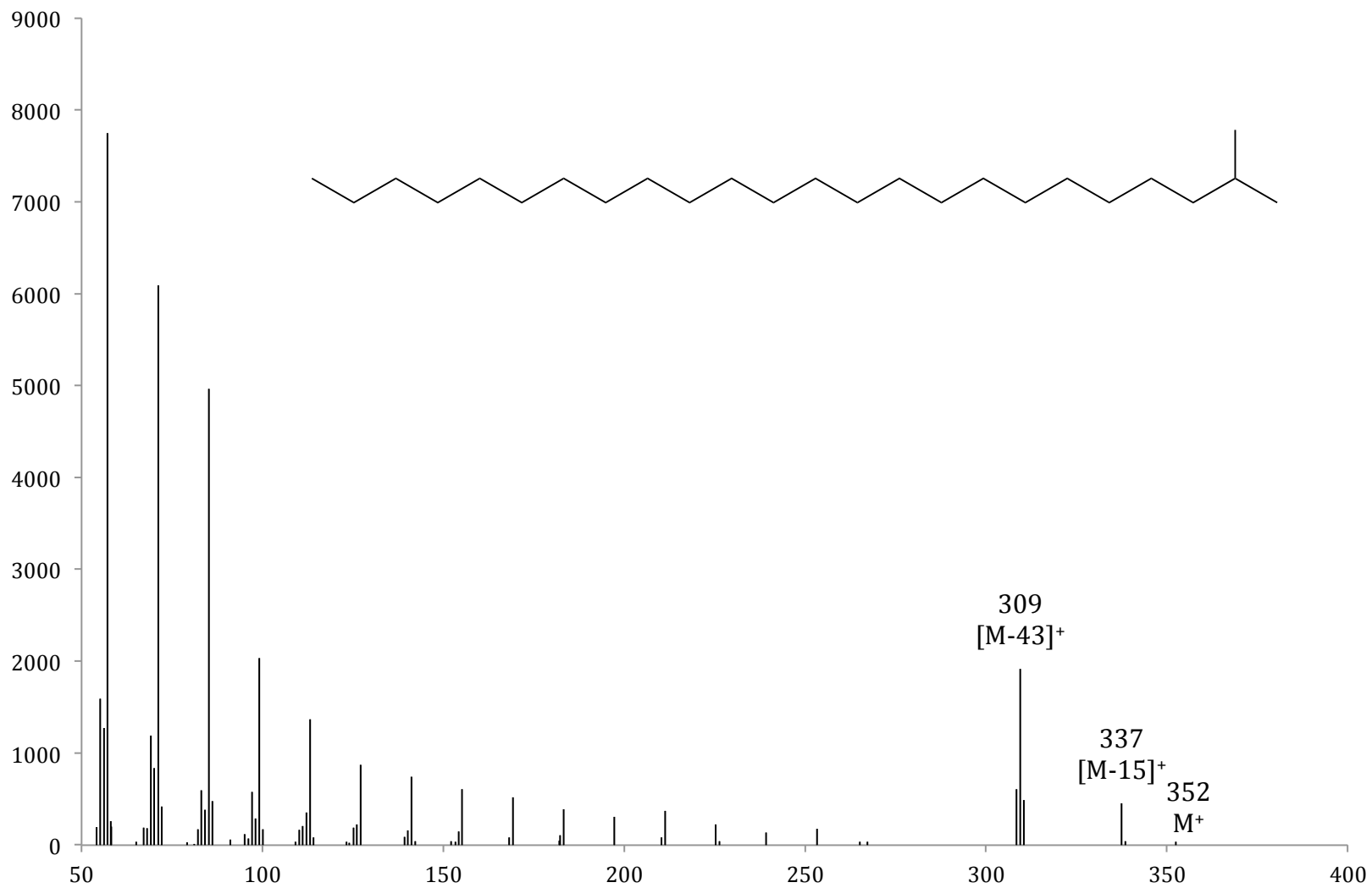


Figure C2. Mass spectrum of a CHC identified as 2-methyltetracosane. Peaks at [M-15]⁺ and [M-43]⁺ indicate a branch at the second carbon. The chemical structure of this CHC is inset.

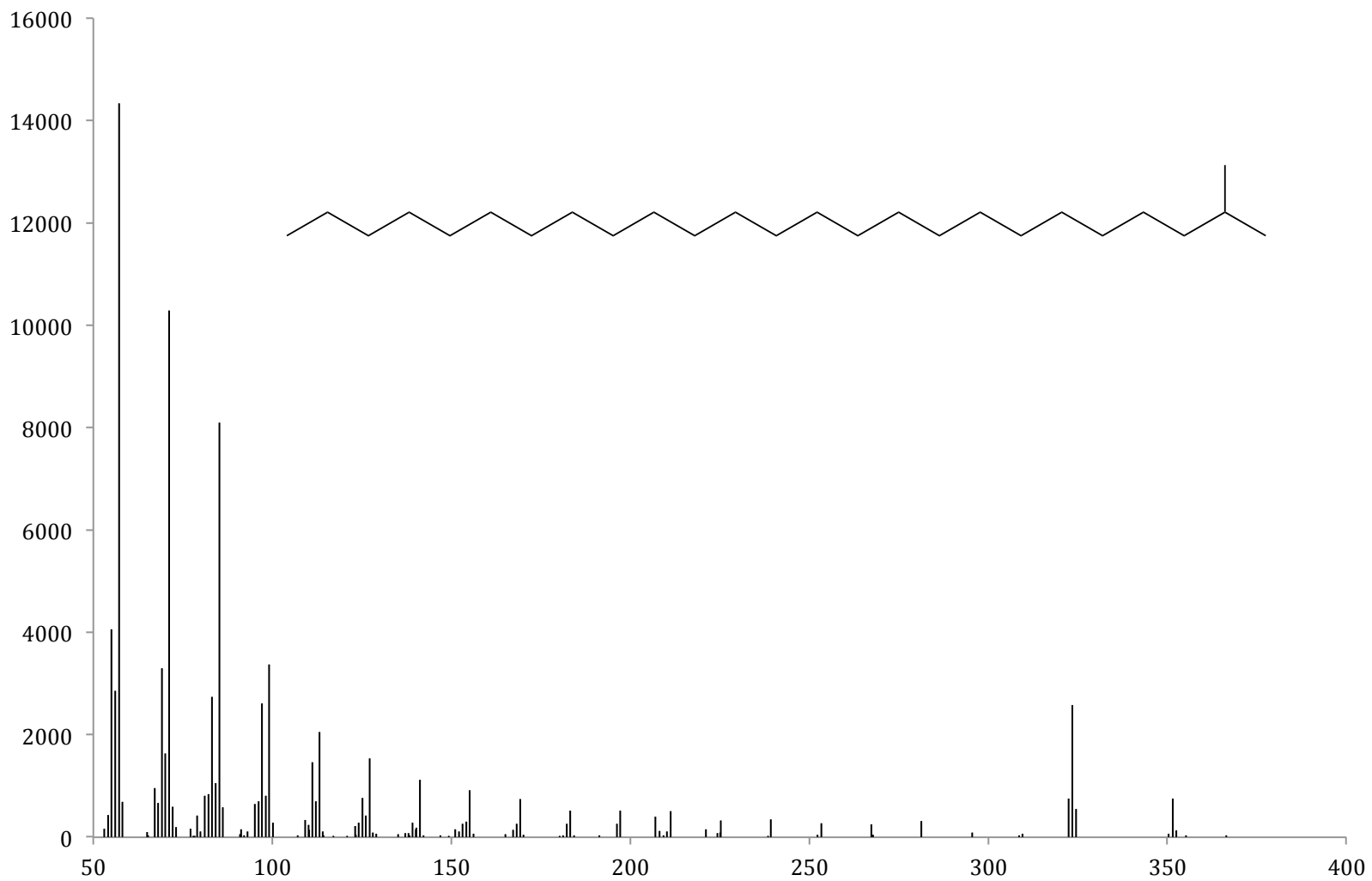


Figure C3. Mass spectrum of a CHC identified as 2-methylpentacosane. Peaks at [M-15]⁺ and [M-43]⁺ indicate a branch at the second carbon. The chemical structure of this CHC is inset.

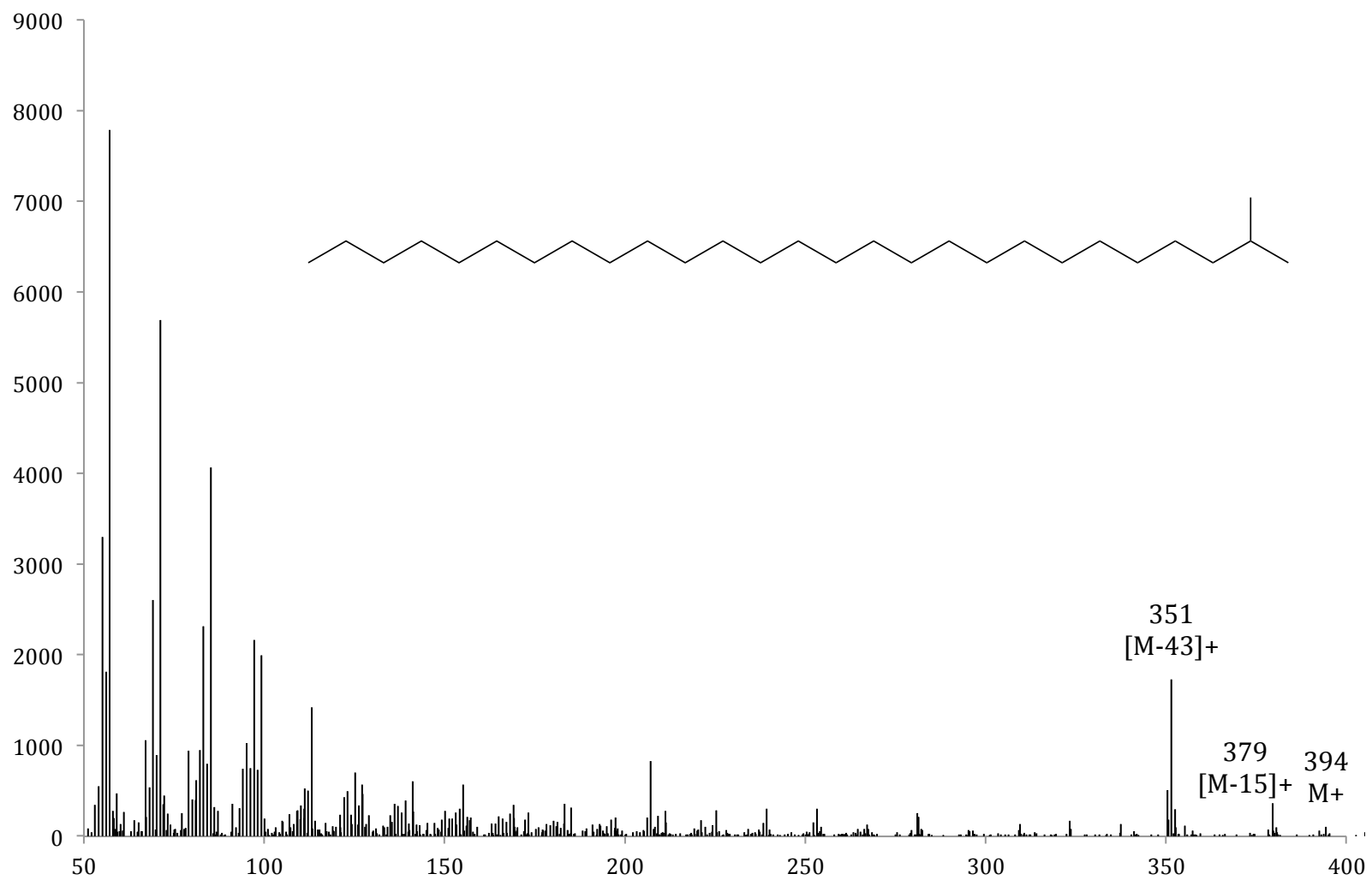


Figure C4. Mass spectrum of a CHC identified as 2-methylheptacosane. Peaks at [M-15]⁺ and [M-43]⁺ indicate a branch at the second carbon. The chemical structure of this CHC is inset.

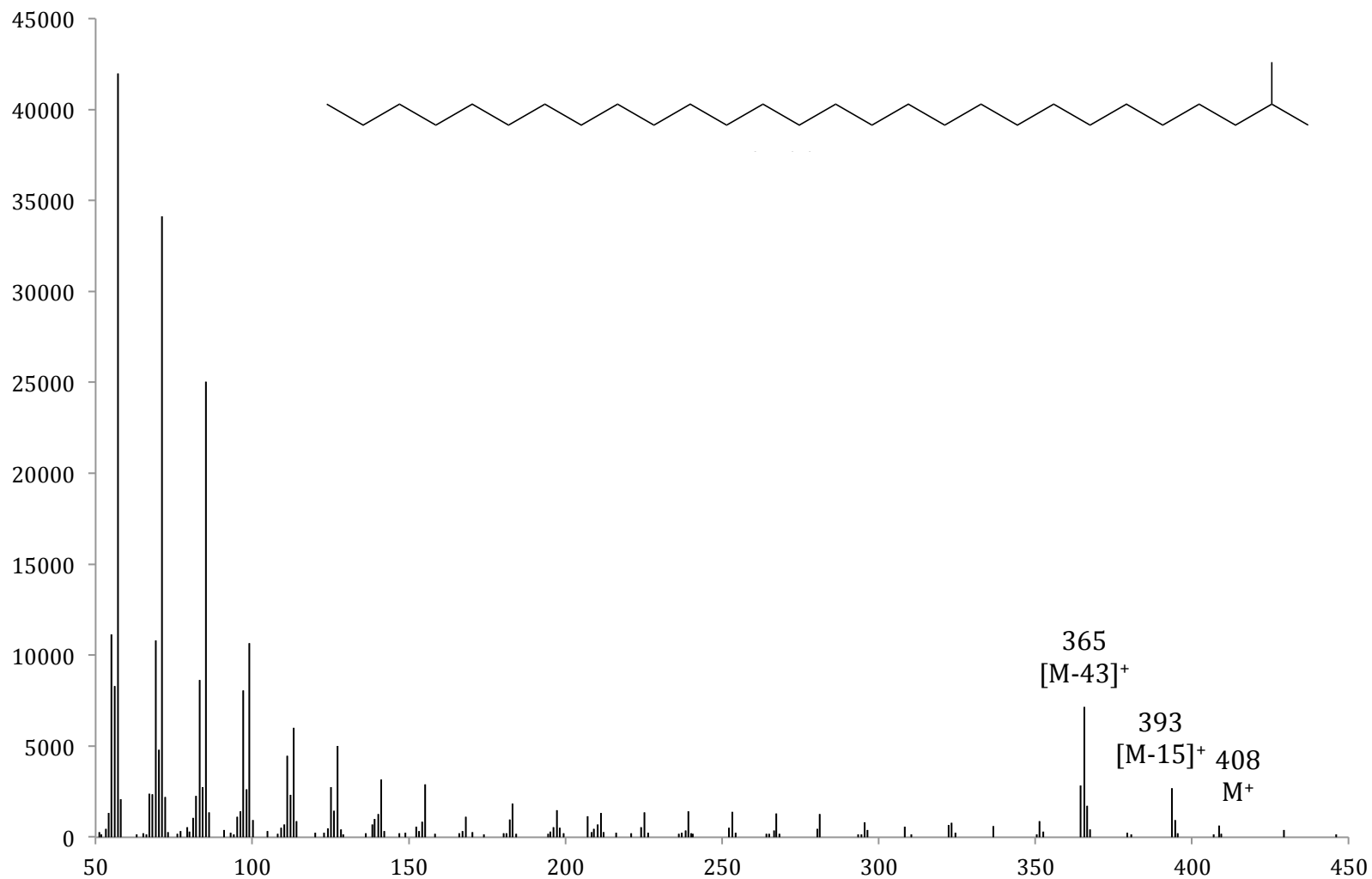


Figure C5. Mass spectrum of a CHC identified as 2-methyloctacosane. Peaks at [M-15]⁺ and [M-43]⁺ indicate a branch at the second carbon. The chemical structure of this CHC is inset.

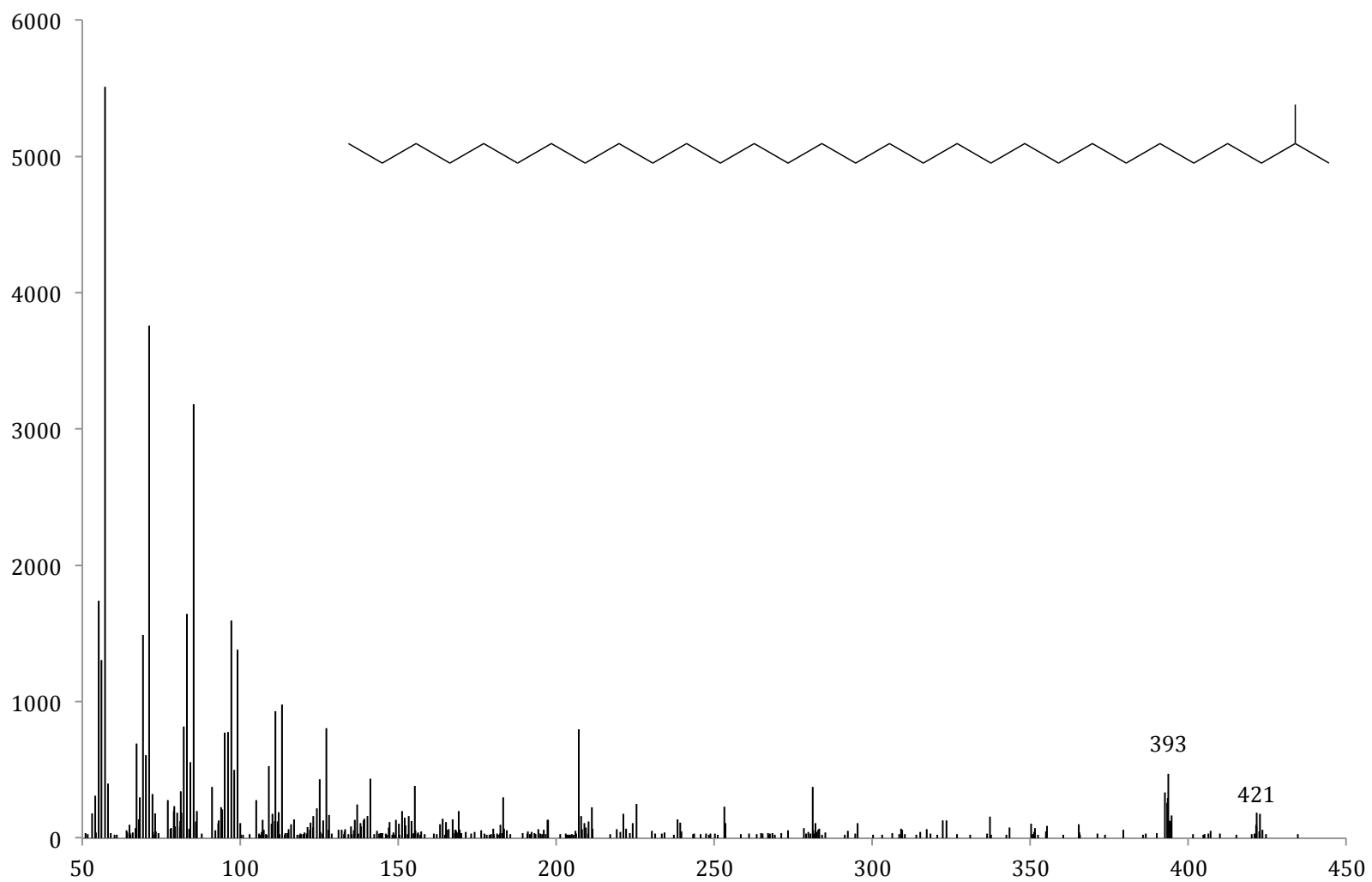


Figure C6. Mass spectrum of a CHC identified as 2-methyltriacontane. Peaks at $[M-15]^+$ and $[M-43]^+$ indicate a branch at the second carbon. The chemical structure of this CHC is inset.

Appendix D – Pre- and Post-Bromination Mass Spectra of 2-Methyl Branched Alkanes

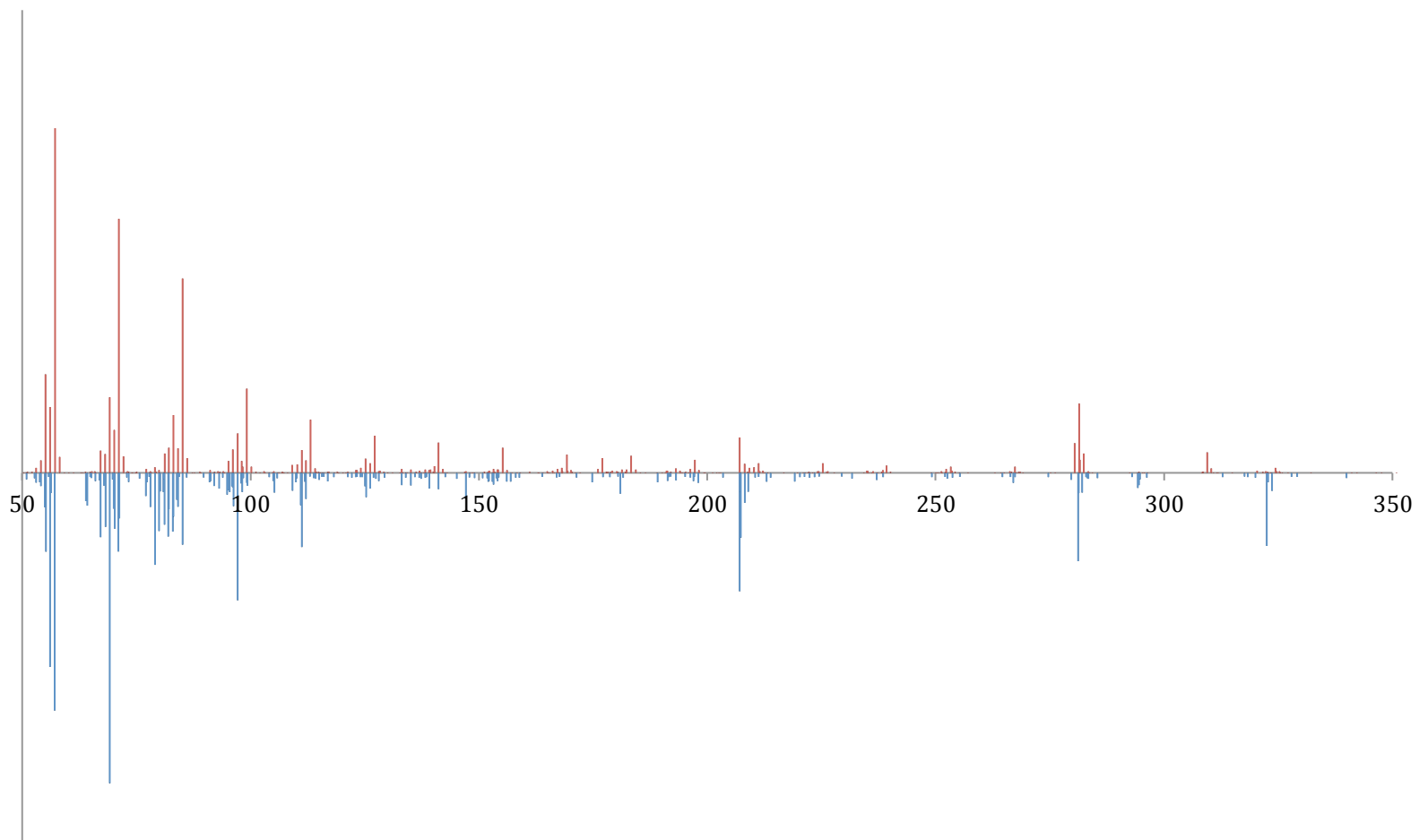


Figure D1. Pre-bromination (red) and post-bromination (blue) mass spectra of 2-methyldocosane. The loss of two m/z indicates an elimination reaction occurred.

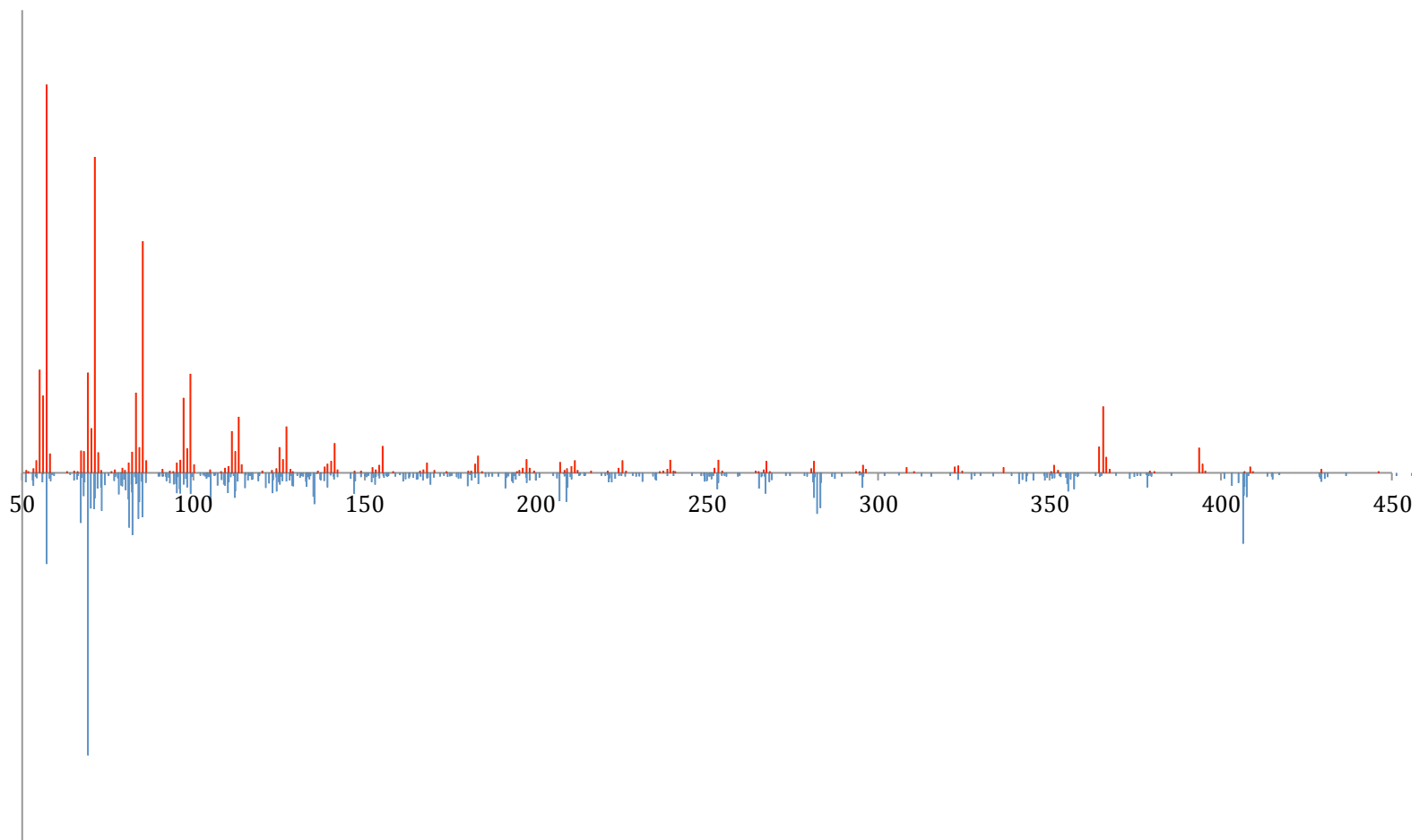


Figure D1. Pre-bromination (color) and post-bromination (color) mass spectra of 2-methyloctacosane. The loss of two m/z indicates an elimination reaction occurred.

Appendix E – Mass Spectra of Natural, Underivatized Monoenes and Dienes

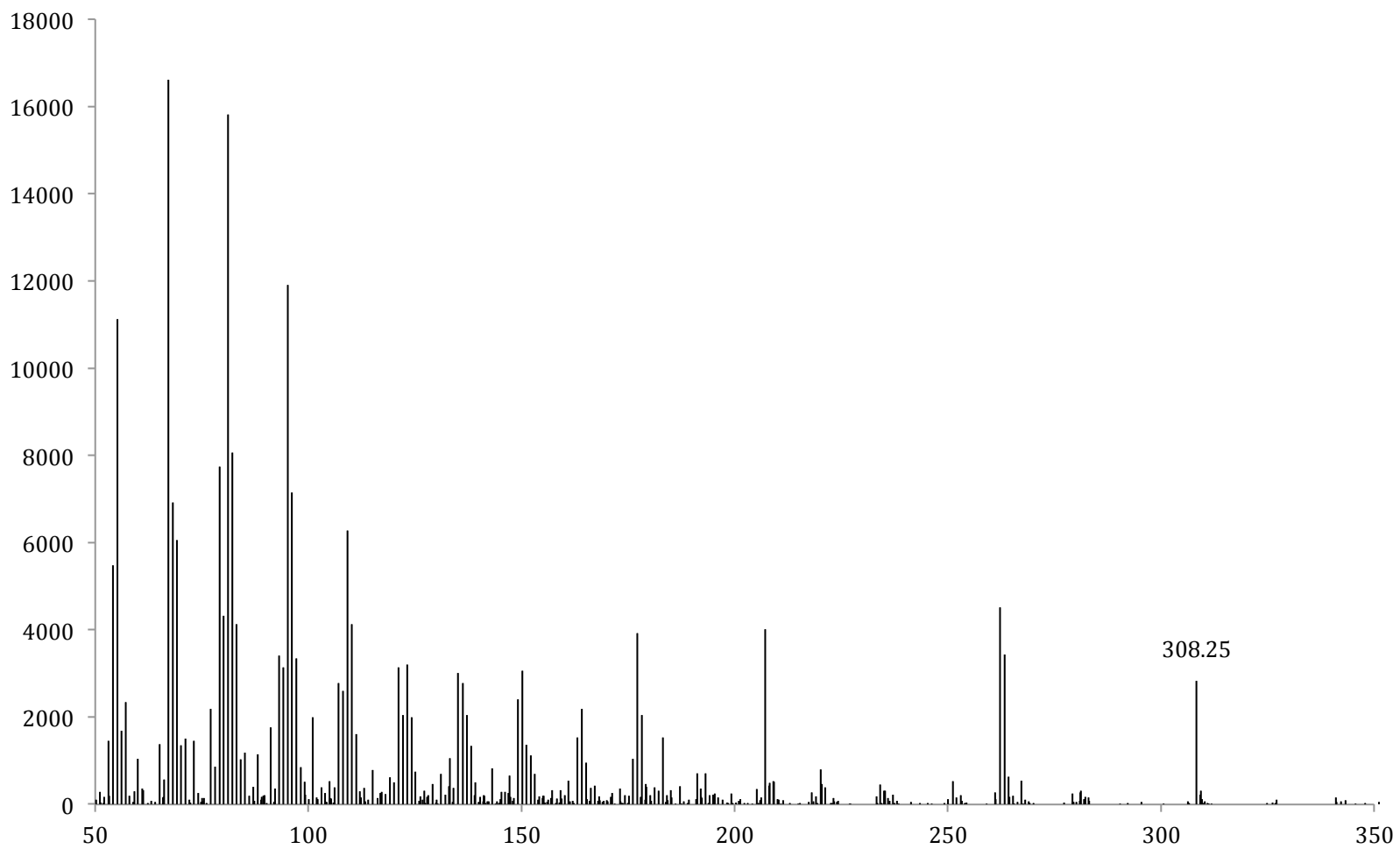


Figure E1. Mass spectrum of a proposed monoene, C₂₂:1, or docosene. DMDS-derivatization must be performed to determine the location of the unsaturation.

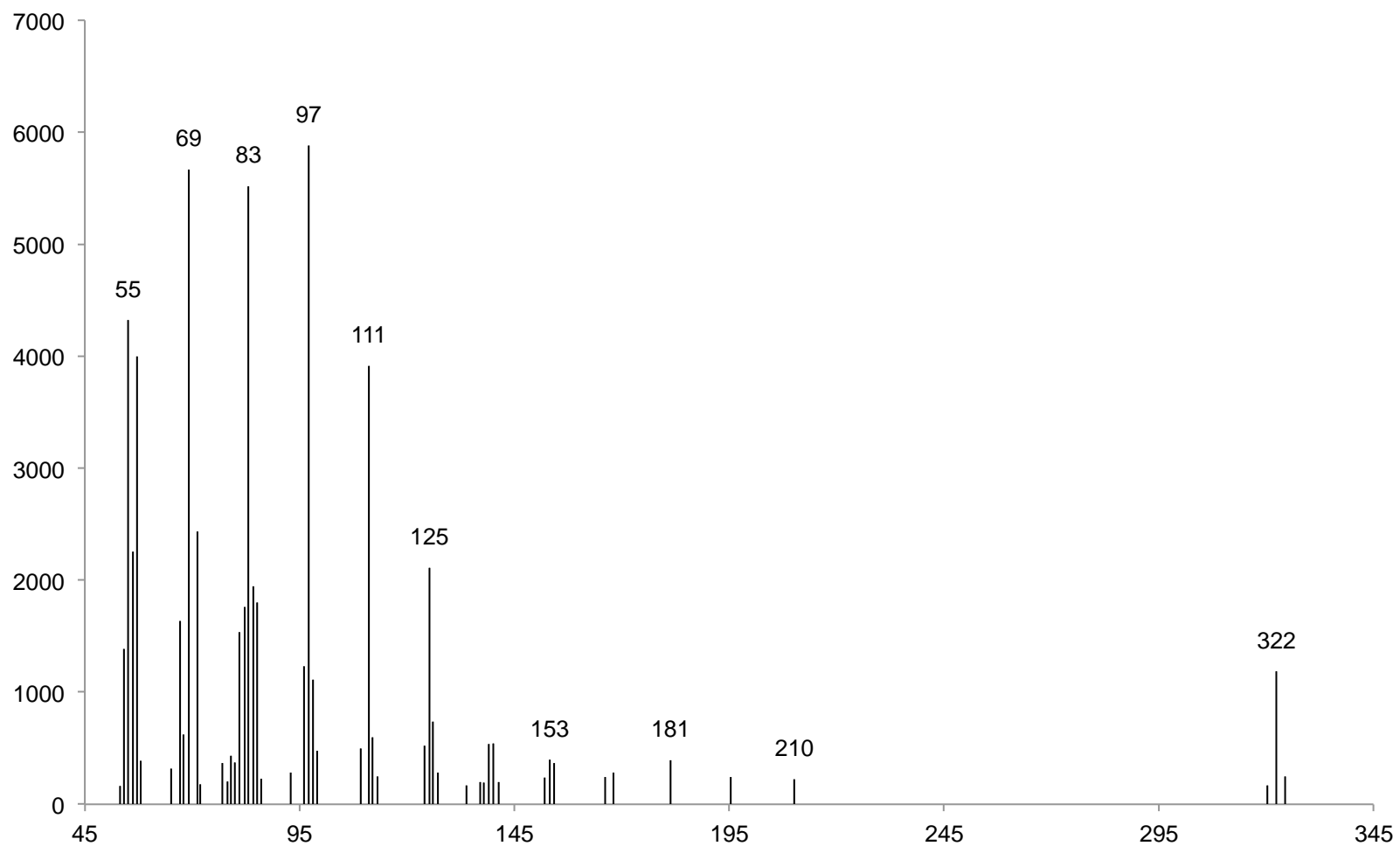


Figure E2. Mass spectrum of an underivatized (Z)11-tricosene.

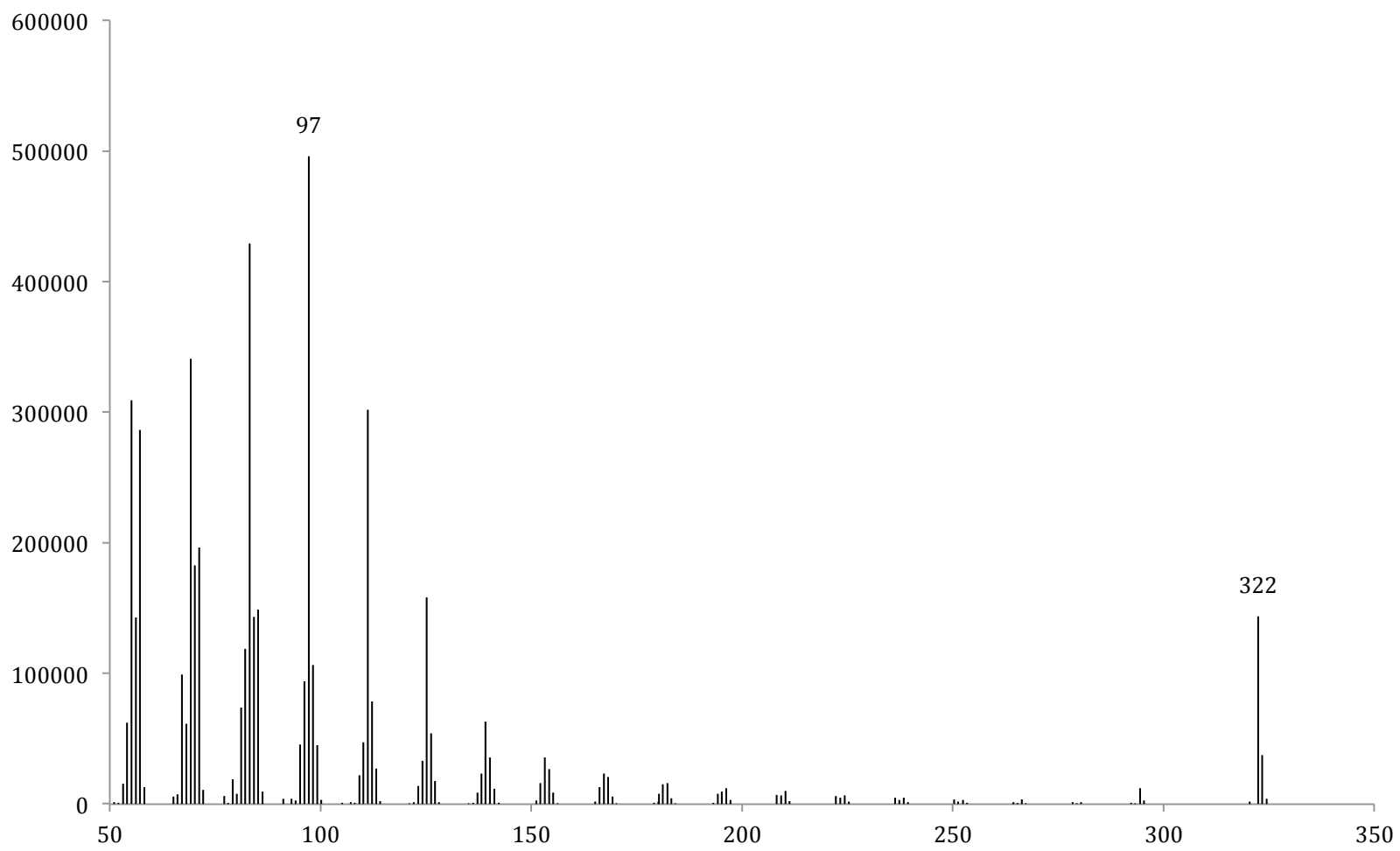


Figure E3. Mass spectrum of 7-tricosene, another CHC identified in *D. athabasca*.

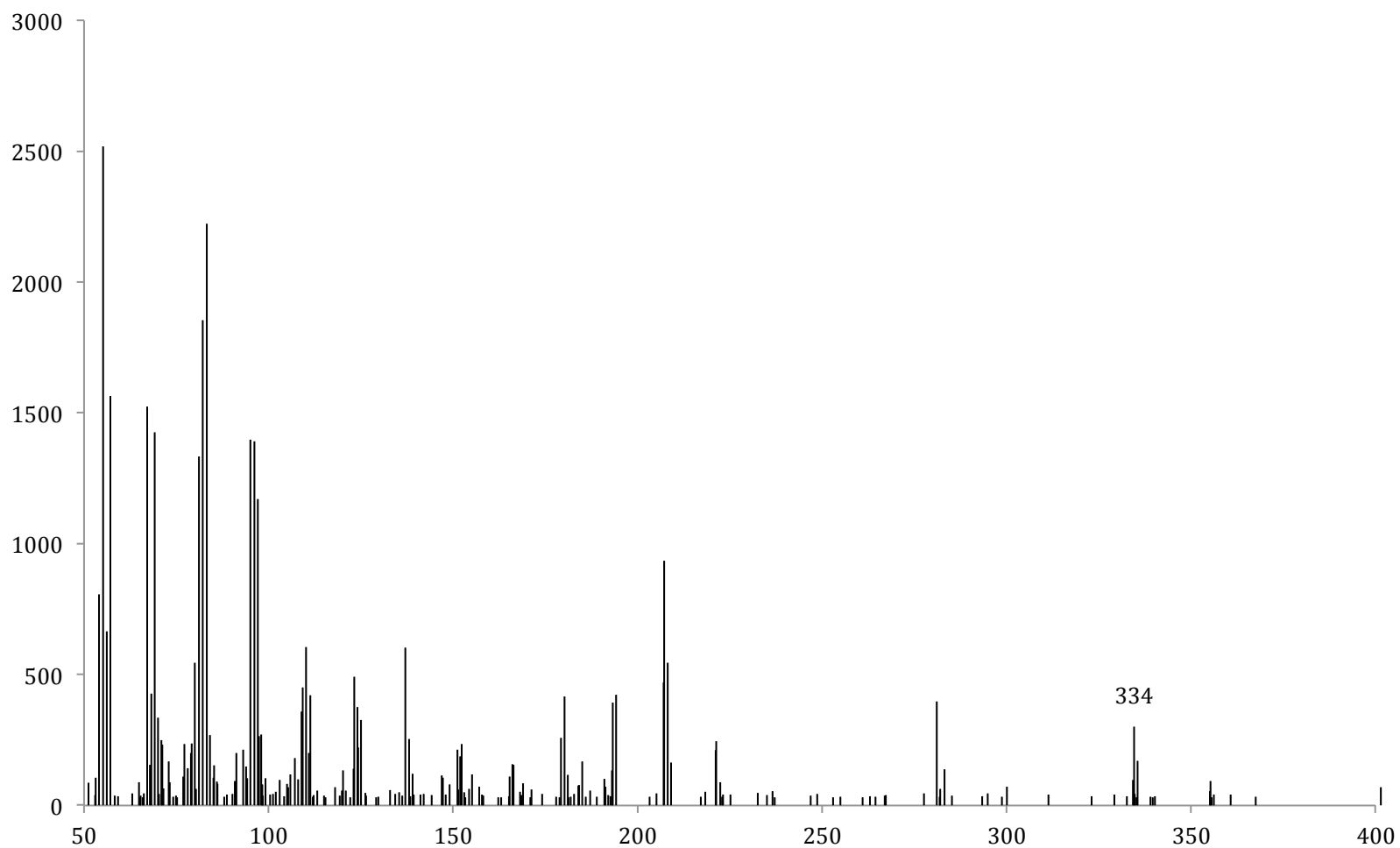


Figure E4. Mass spectrum of a tetracosadiene, C₂₄:₂ with unknown positions of unsaturation. DMDS derivatization must be performed to accurately determine the location of the unsaturations.

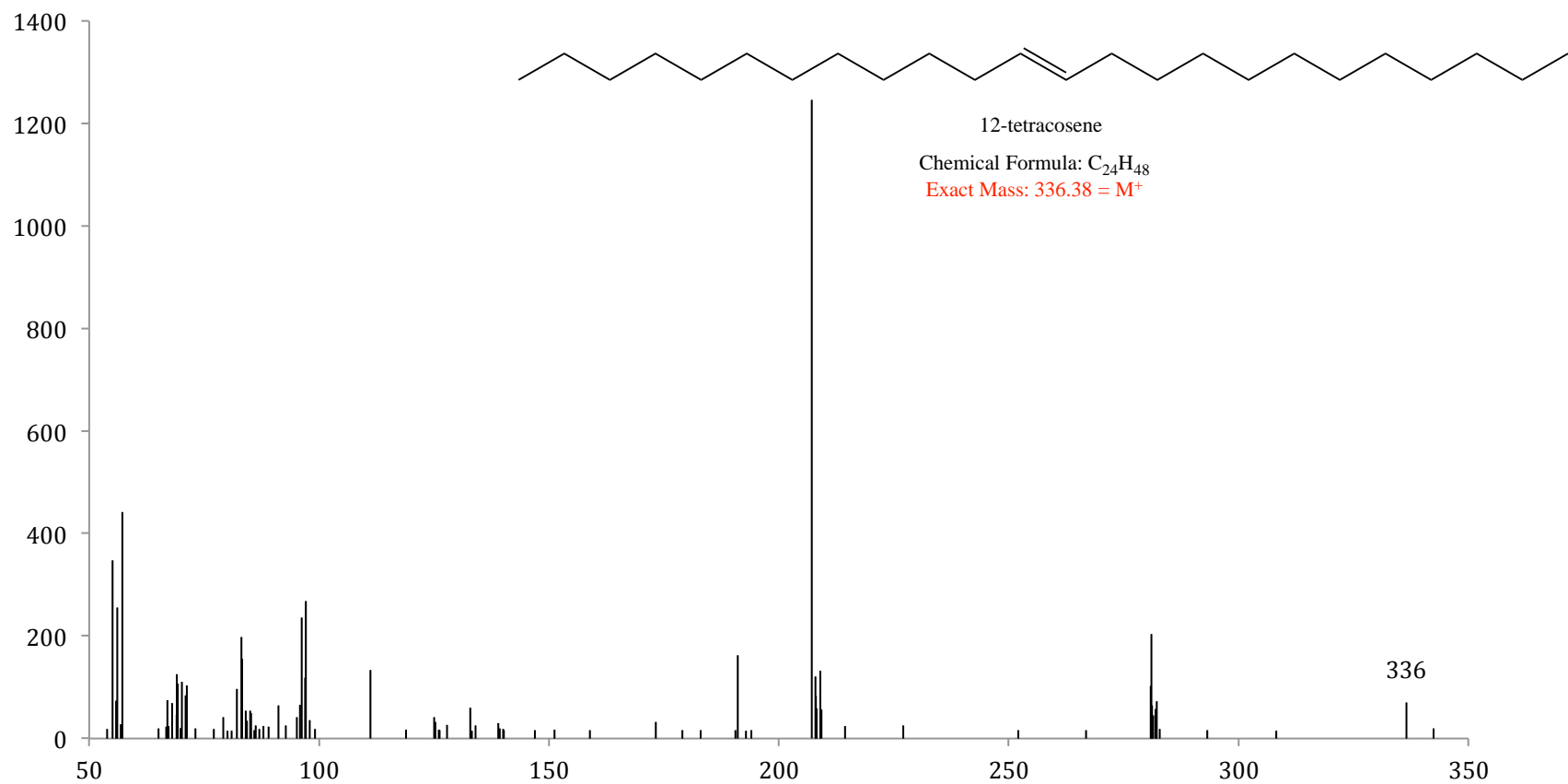


Figure E5. Mass spectrum of underivatized 12-tetracosene.

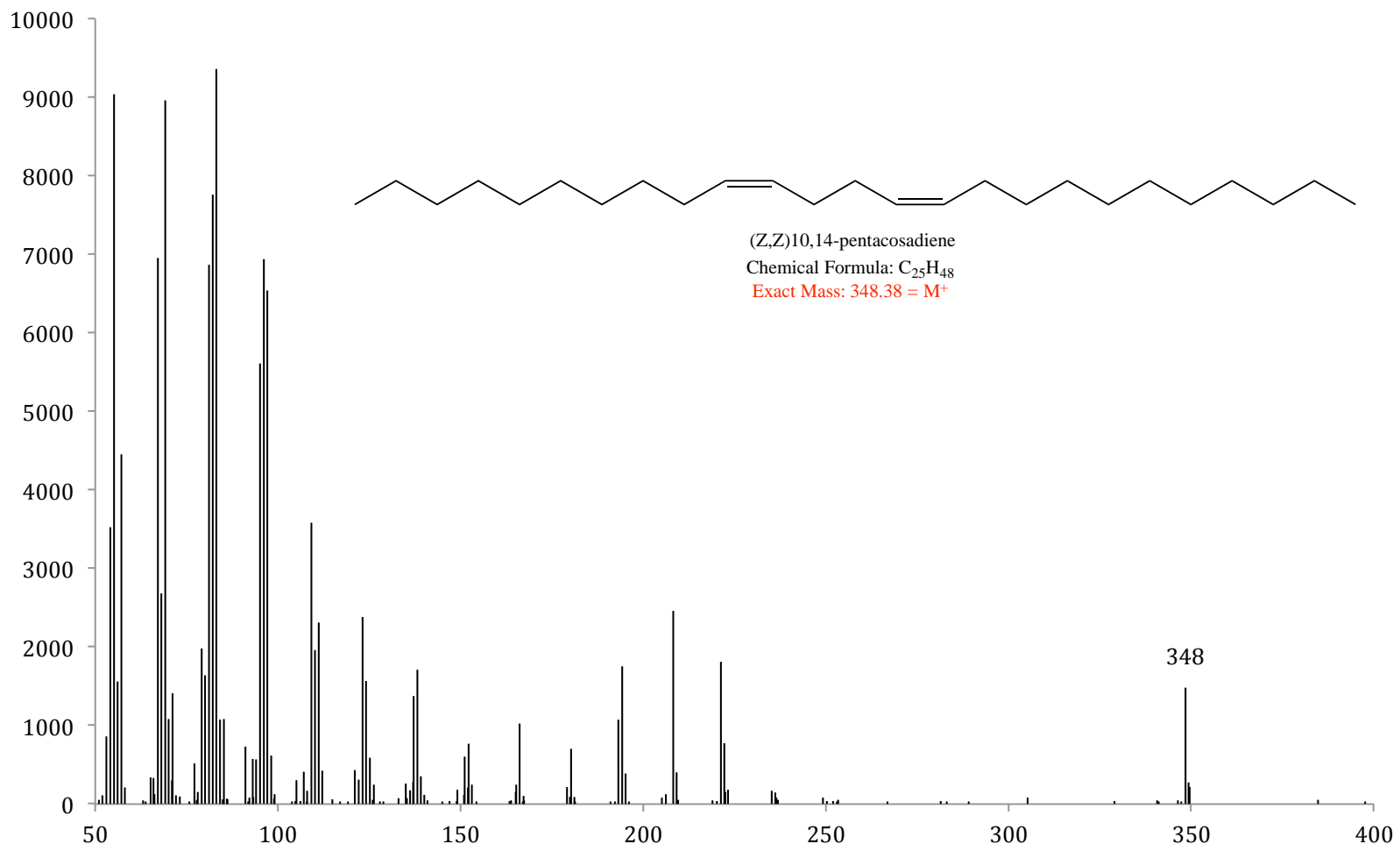


Figure E6. Mass spectrum of underivatized 10,14-pentacosadiene.

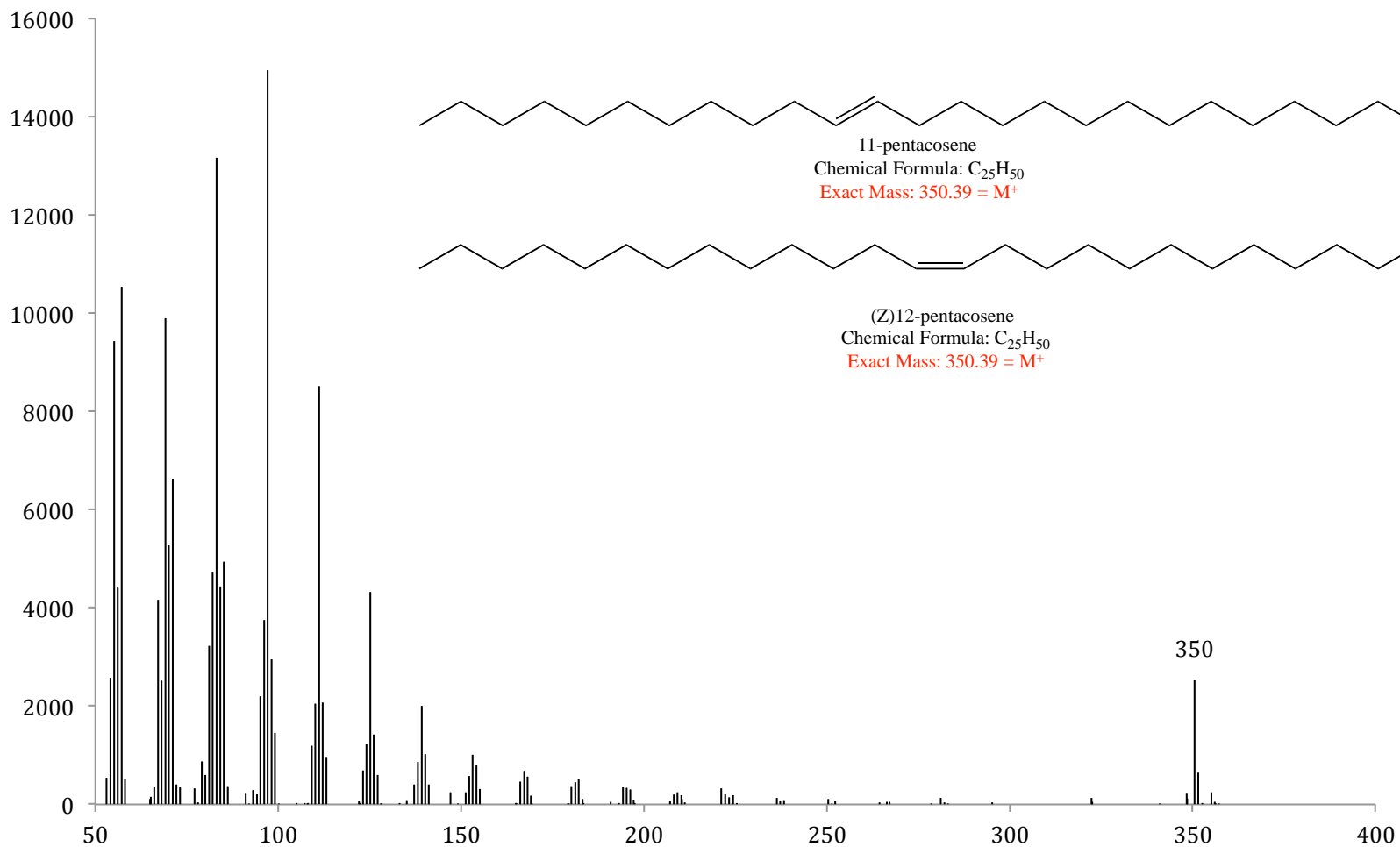


Figure E7. Mass spectrum of the underivatized (Z)11-pentacosene/ (Z)12-pentacosene mixture.

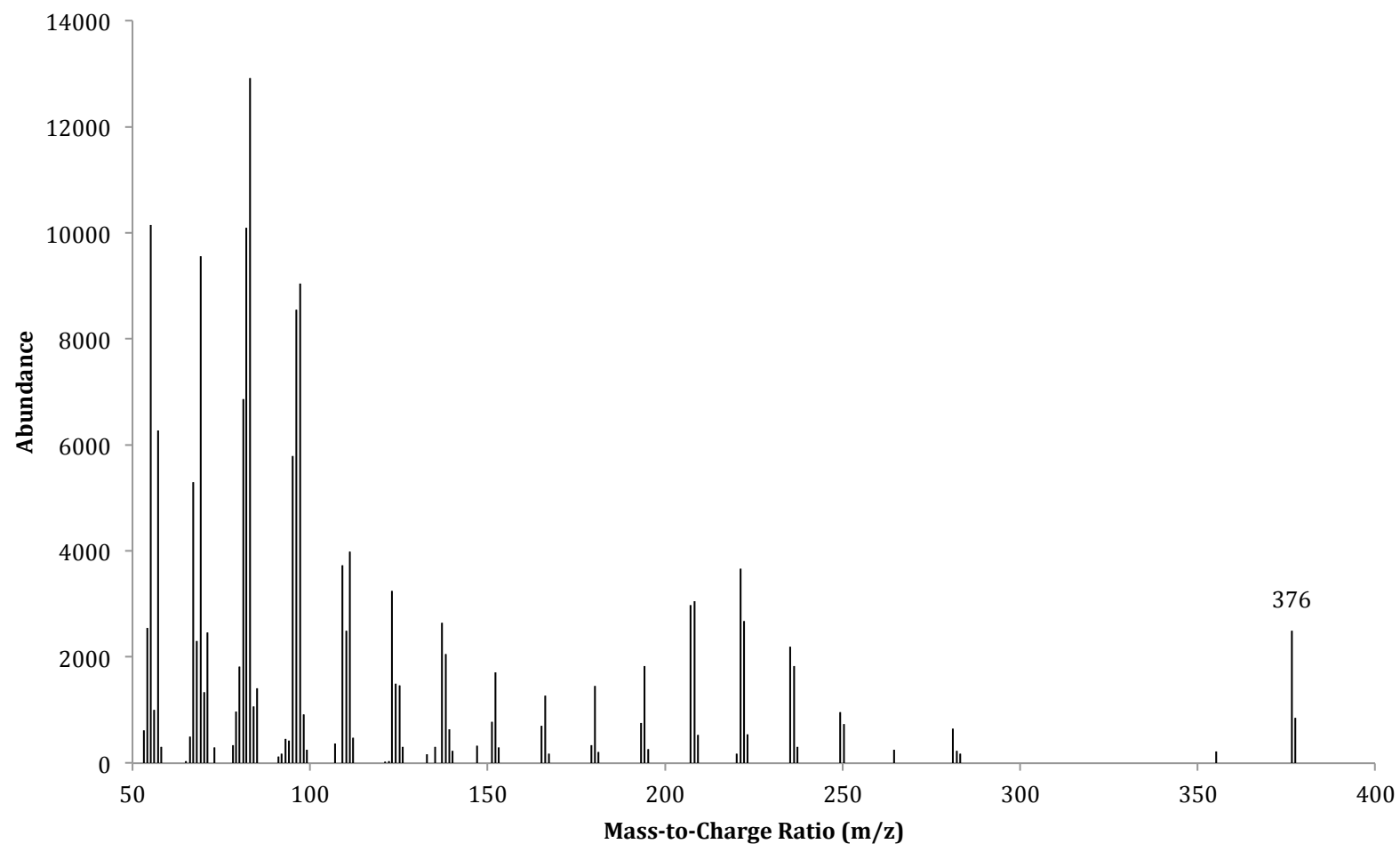


Figure E8. Mass spectrum of a proposed heptacosadiene (C₂₇:₂). DMDS derivatization must be performed to locate the positions of the double bonds in this CHC.

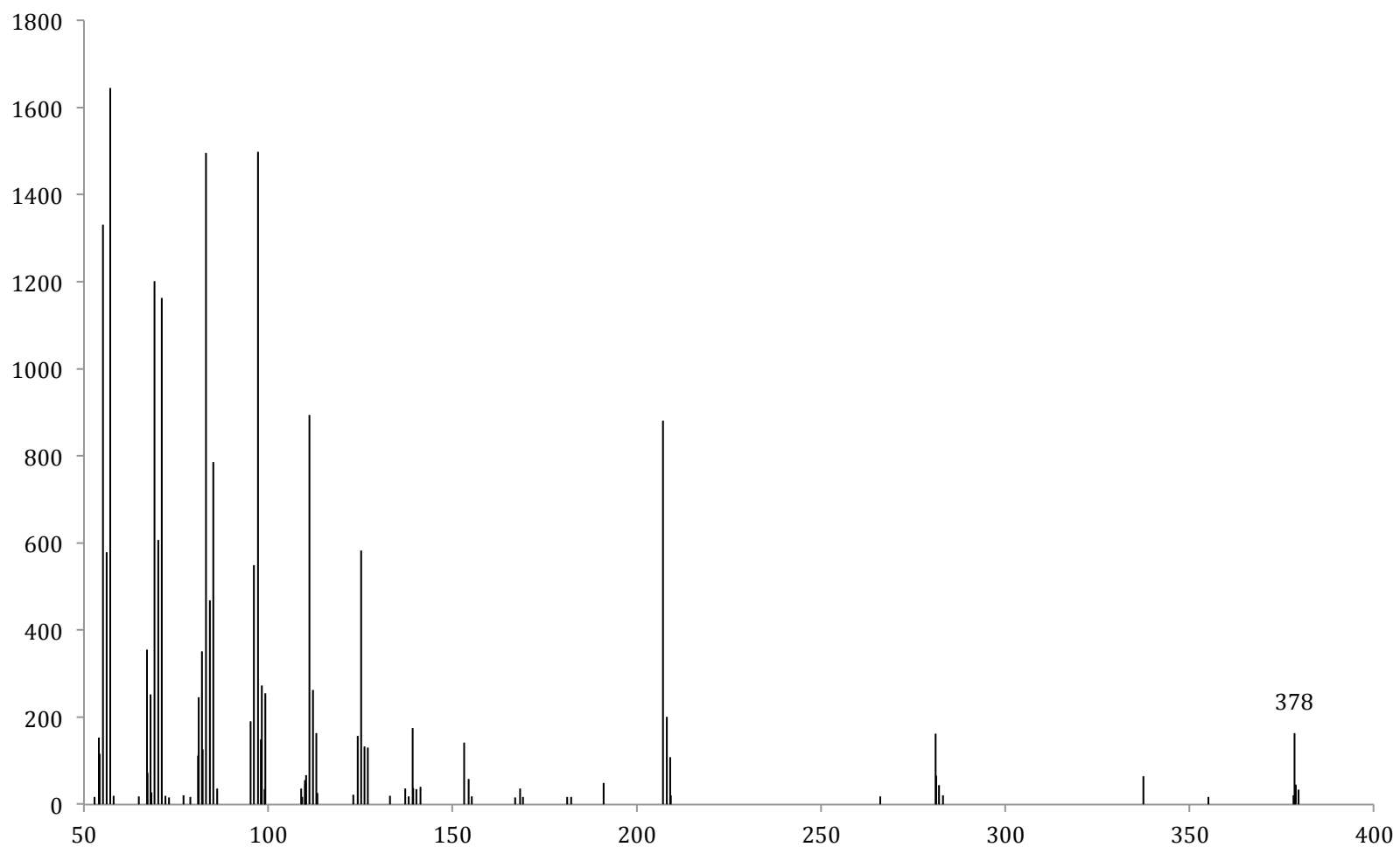


Figure E9. Mass spectrum of a proposed heptacosene (C₂₇:1). DMDS derivatization must be performed to locate the positions of the unsaturation in this CHC.

Appendix F – Carboxylic Acids and Methyl Esters

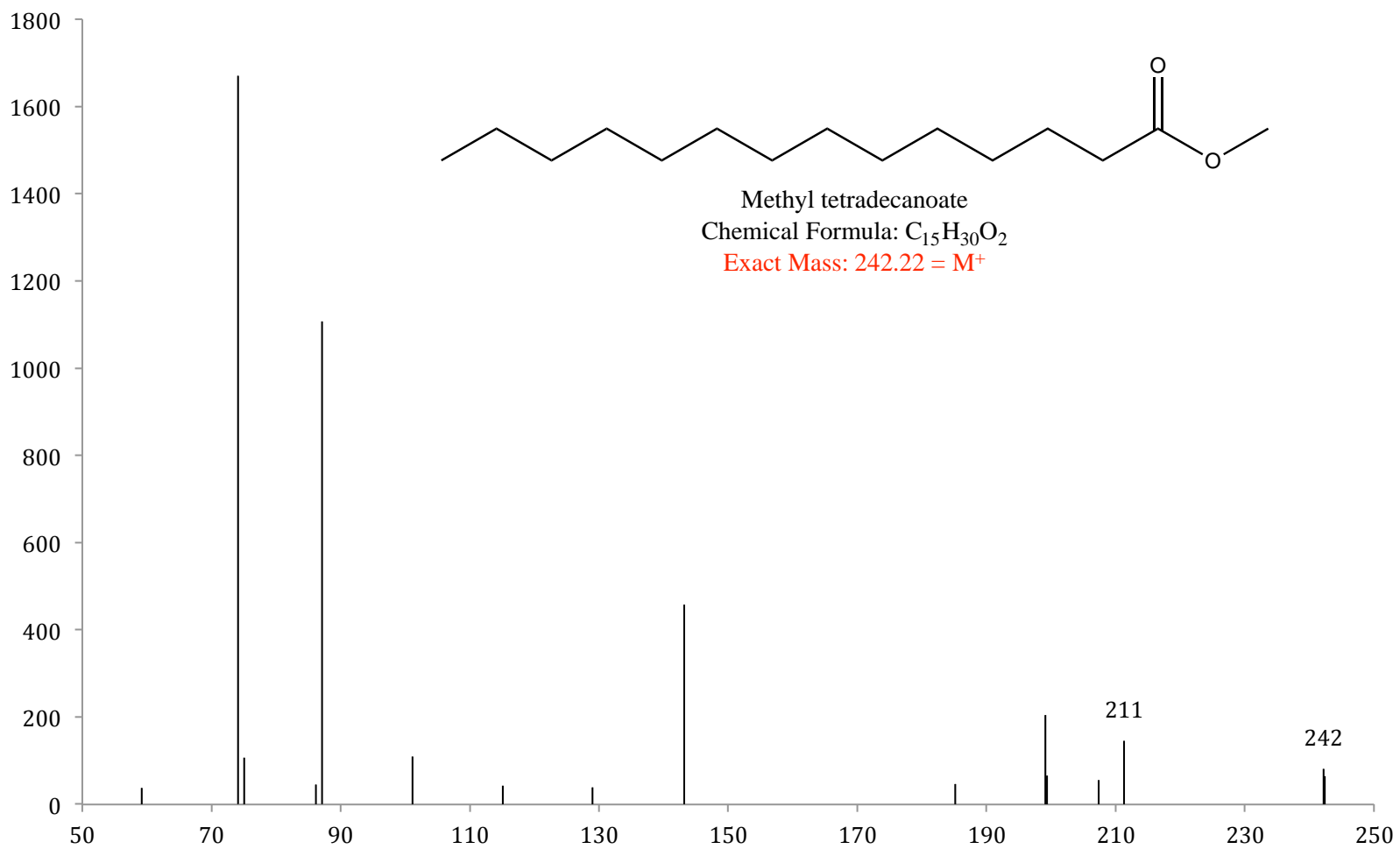


Figure F1. Mass spectrum of methyl tetradecanoate.

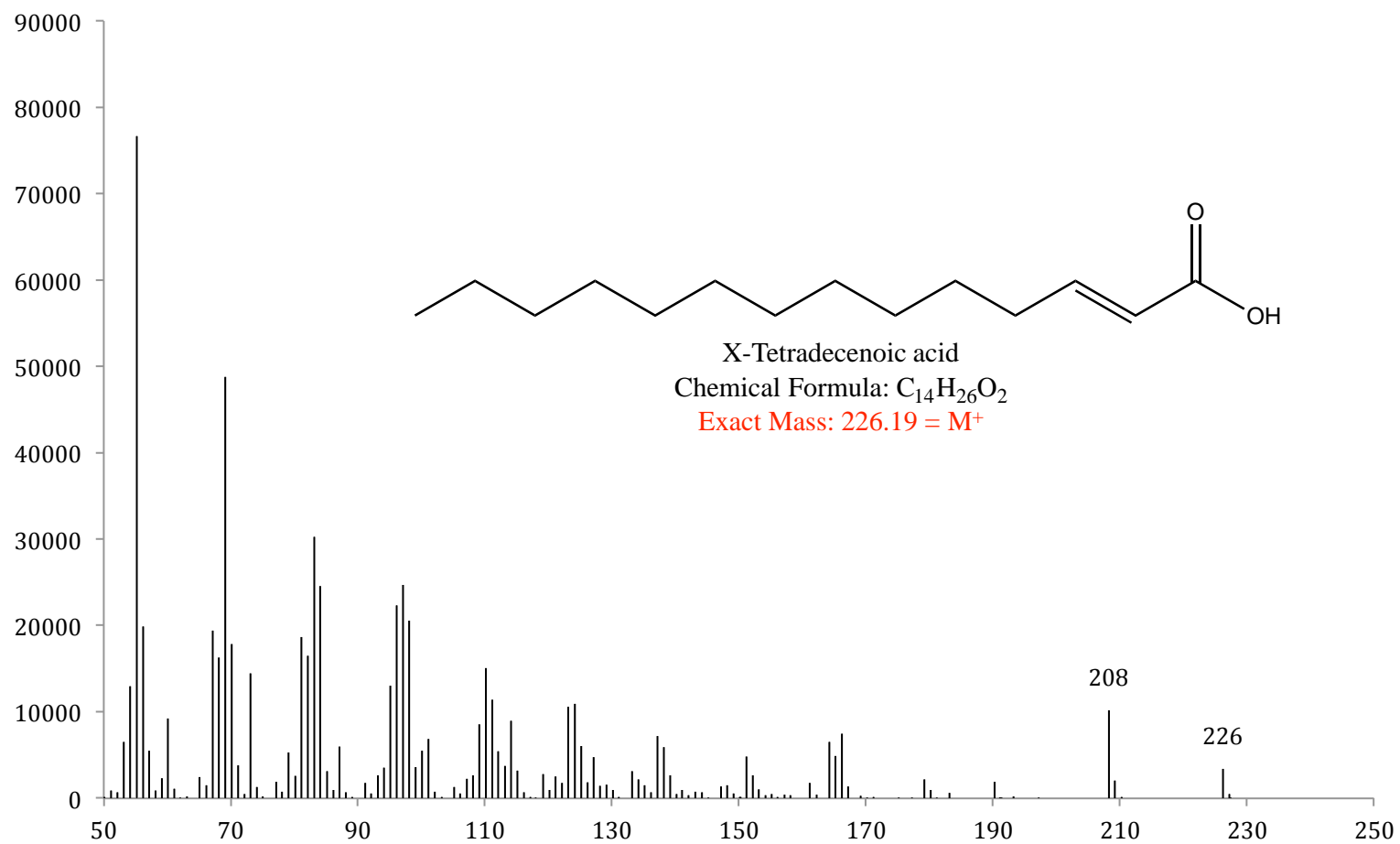


Figure F2. Mass spectrum of a tetradecenoic acid.

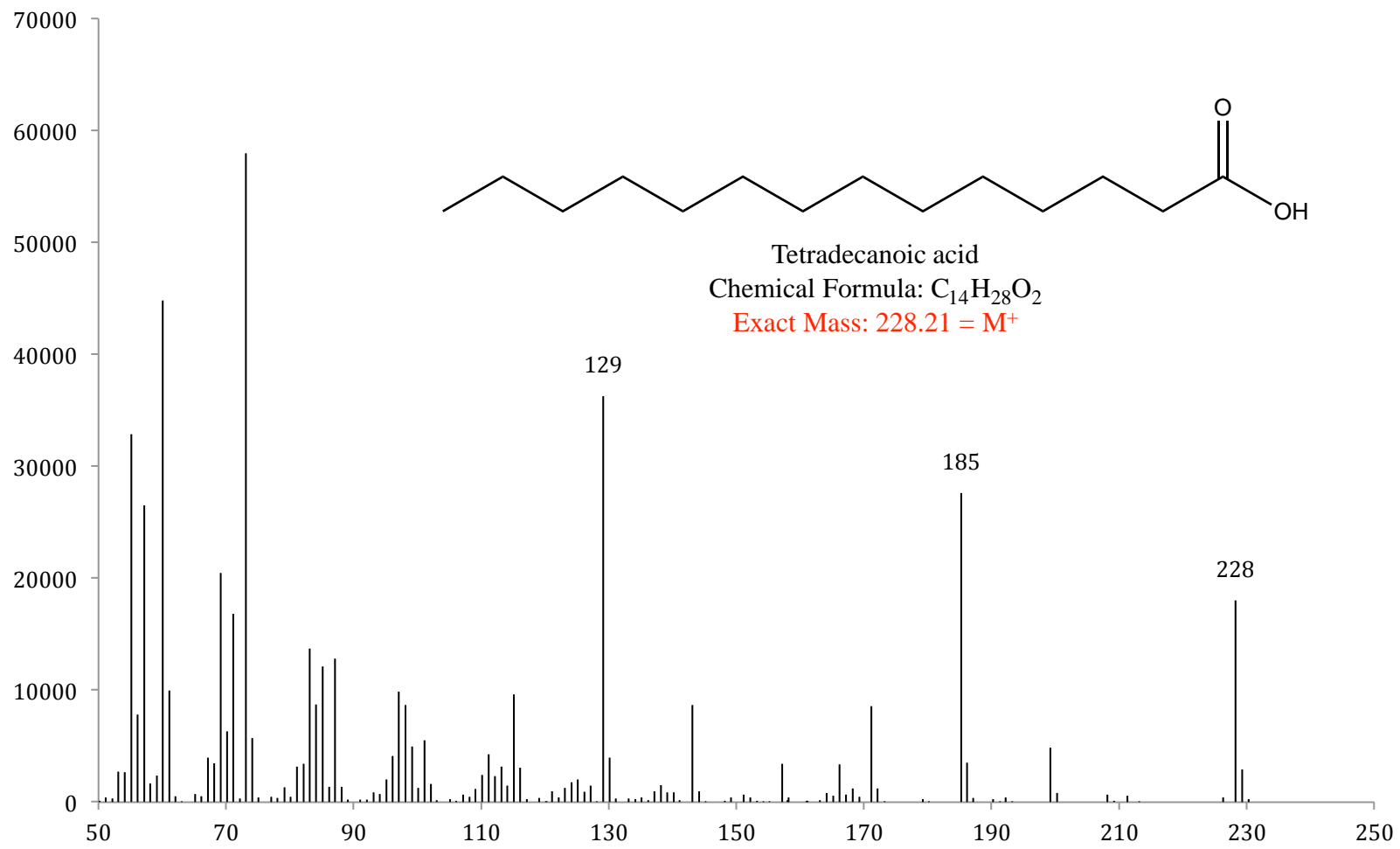


Figure F3. Mass spectrum of tetradecanoic acid.

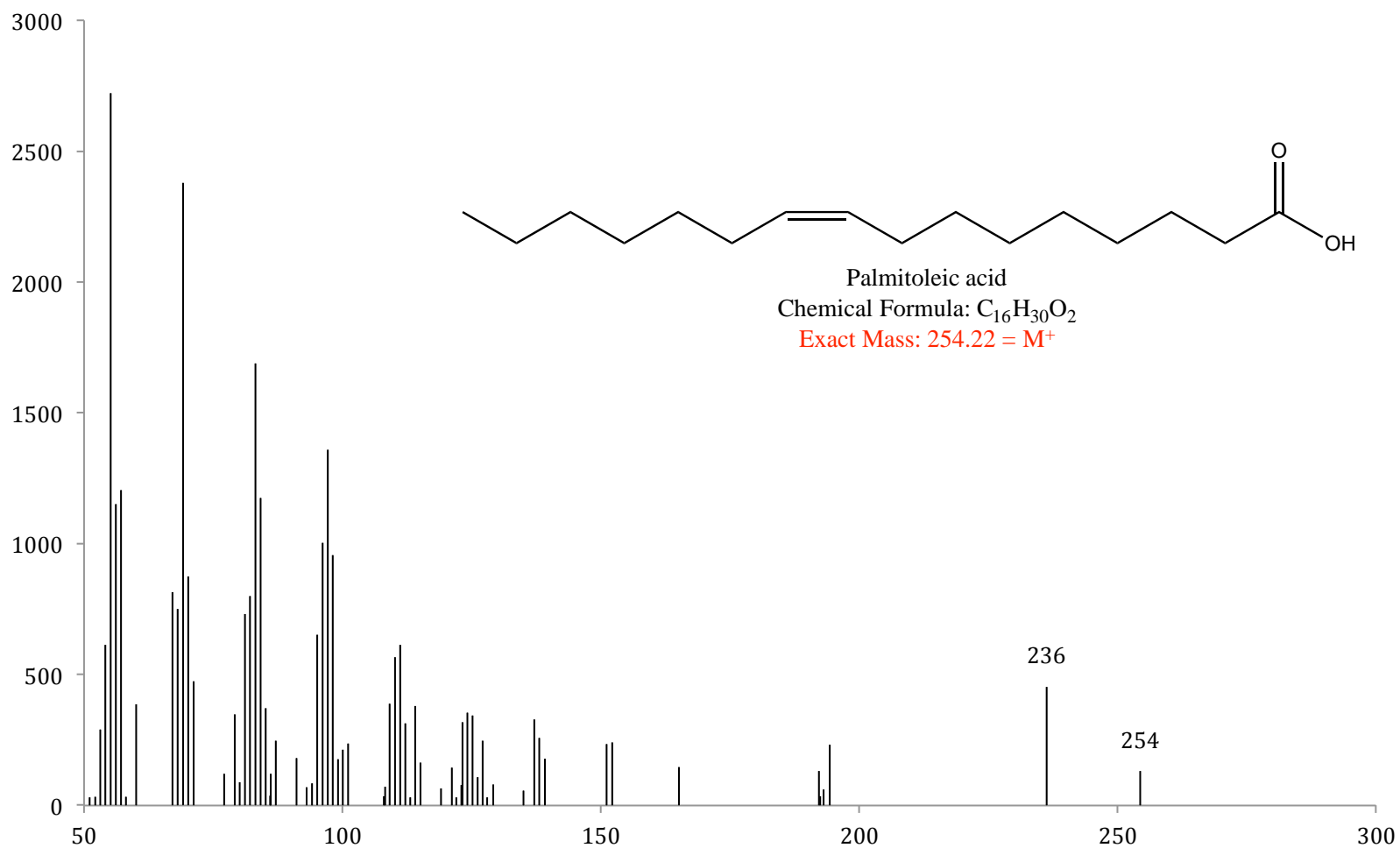


Figure F4. Mass spectrum of a proposed hexadecenoic acid. DMDS derivatization must be performed to locate the position of unsaturation.

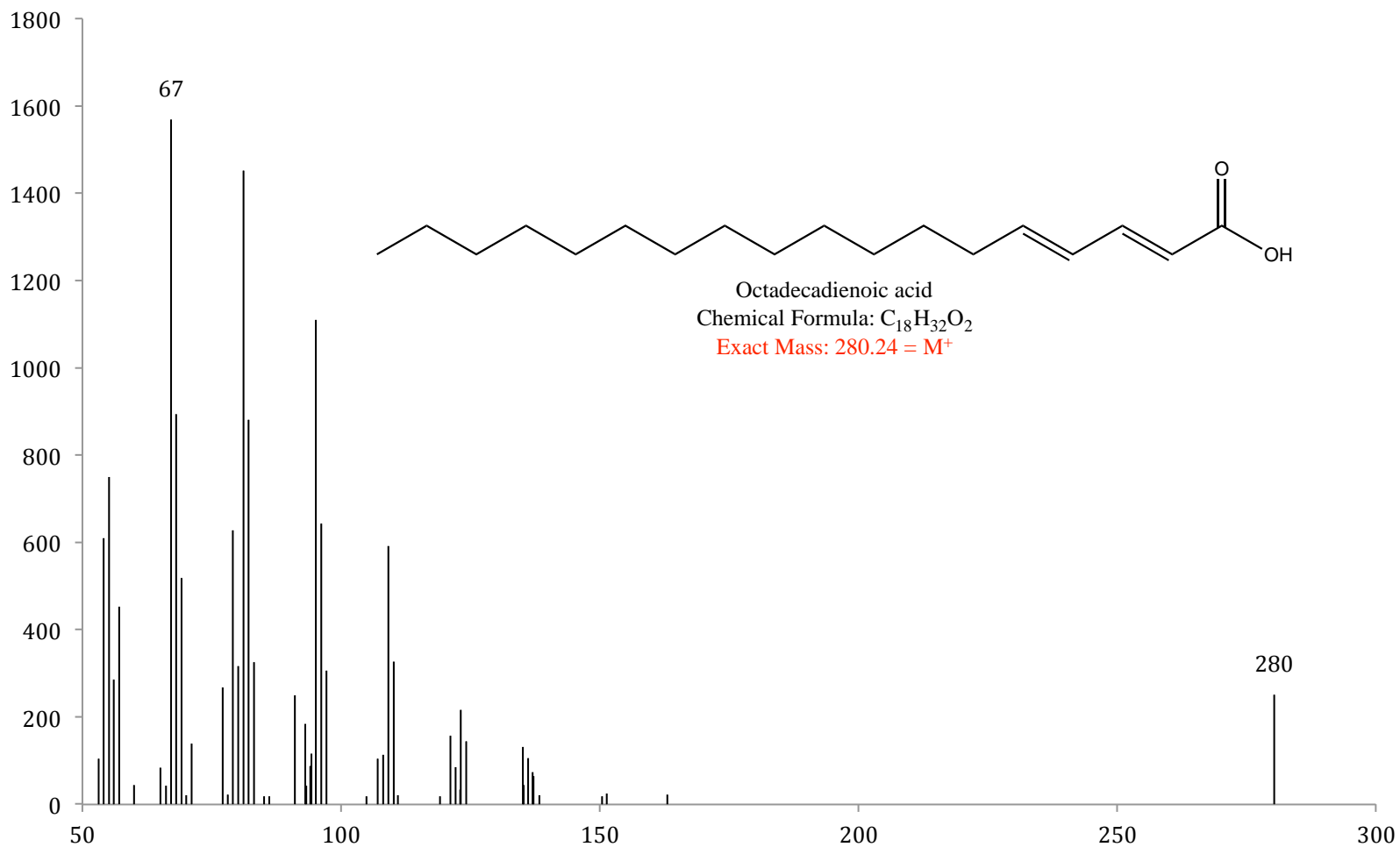


Figure F5. Mass spectrum of an octadecadienoic acid. The location of the two unsaturations in this CHC must be further investigated using DMDS derivatization.

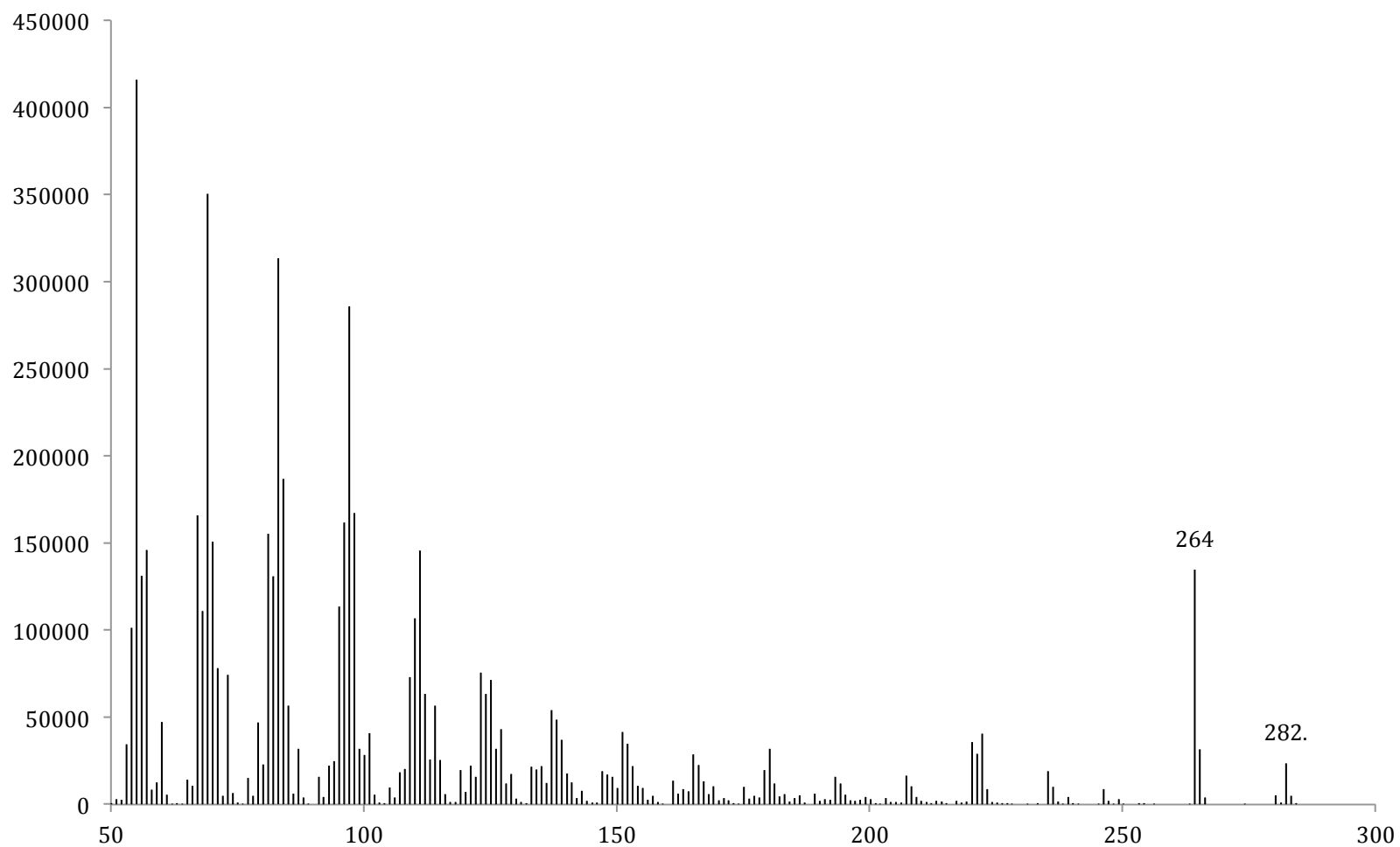


Figure F6. Mass spectrum of synthetic oleic acid used to identify the CHC at 19.32 m in all races of *D. athabasca*.

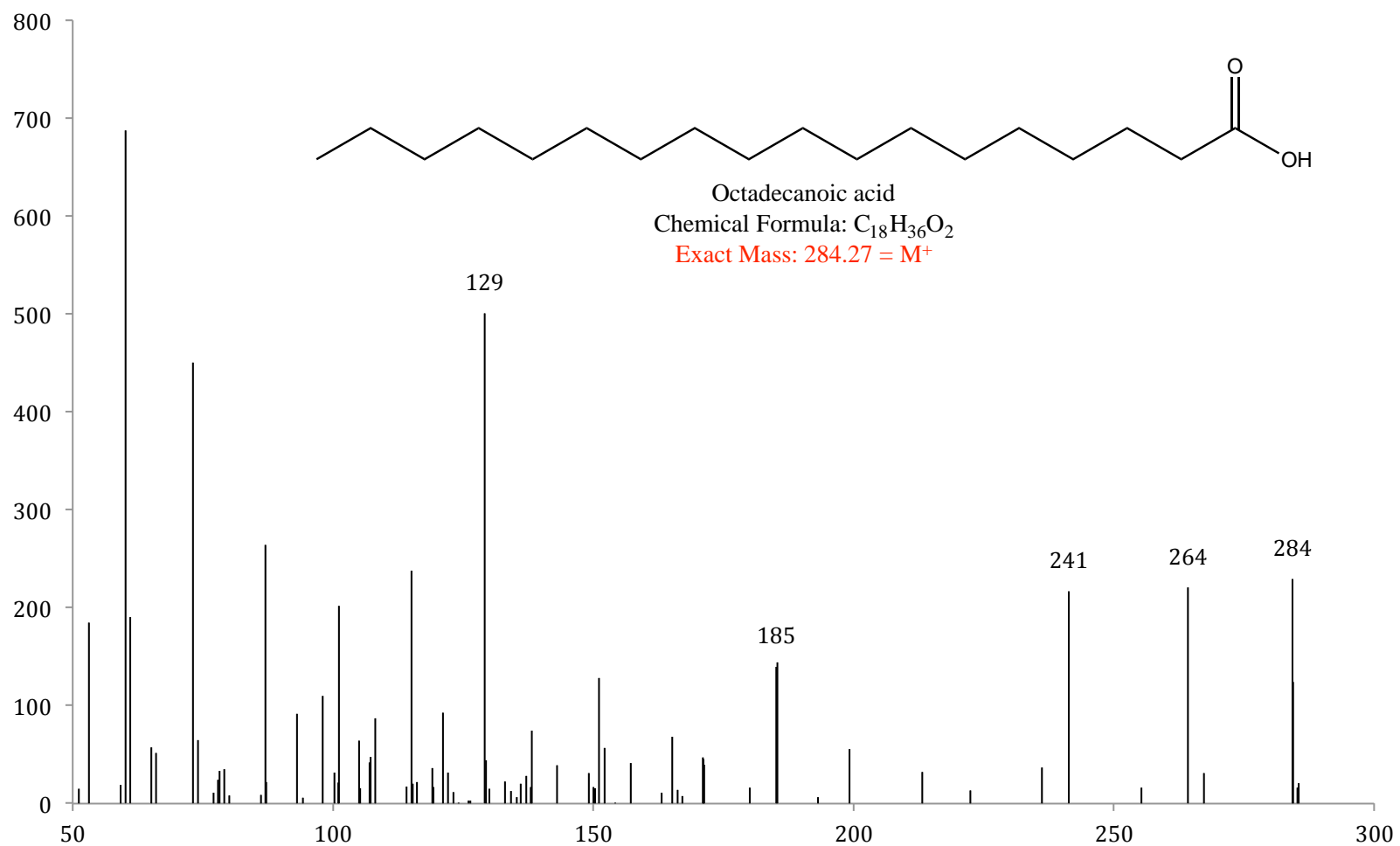


Figure F7. Mass spectrum of octadecanoic acid.

Appendix G – External Standard Curves of Synthetic CHCs

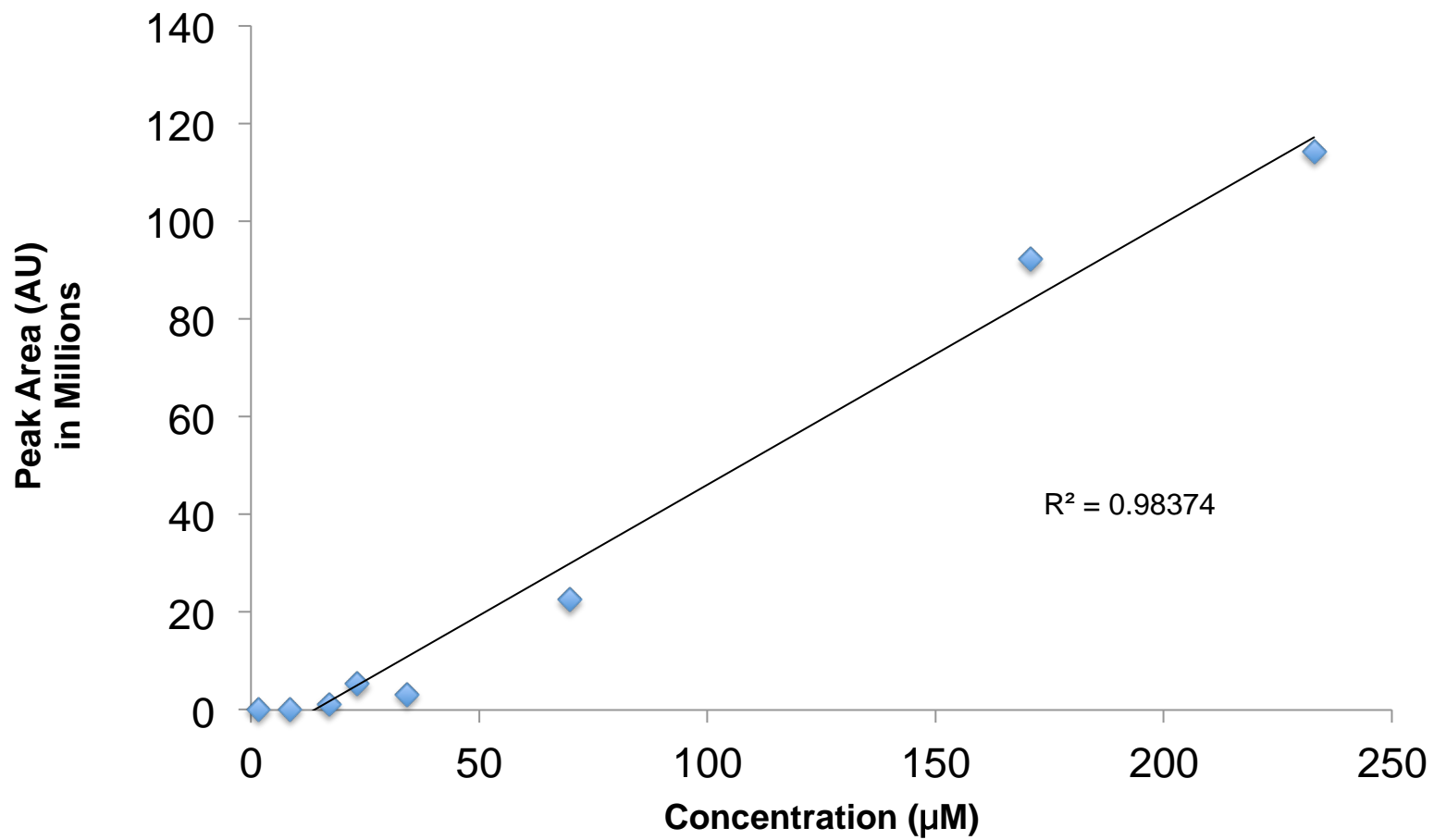


Figure G1. External standard curves for (Z)7-tricosene.

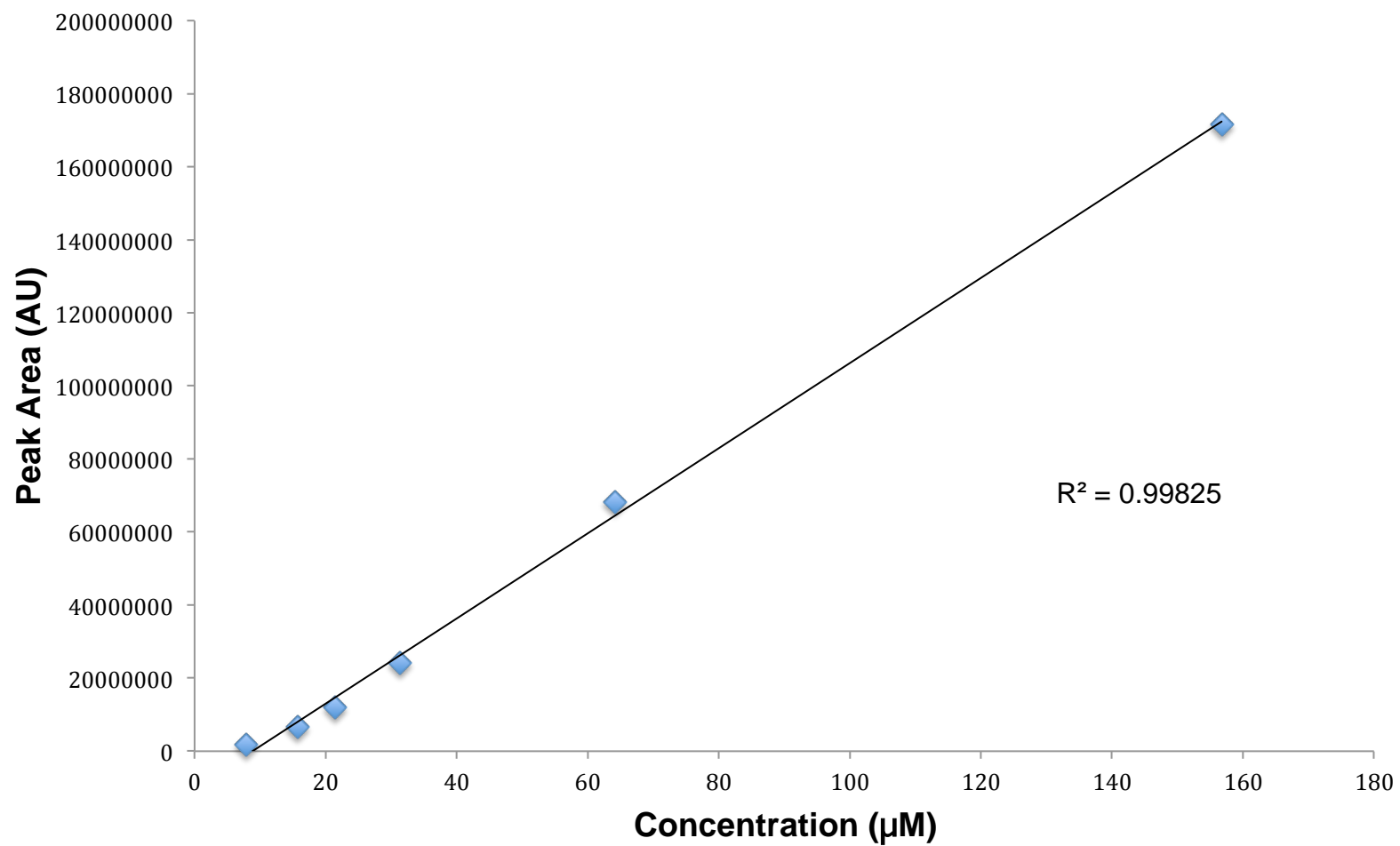


Figure G2. External standard curve for (Z)7-pentacosene.

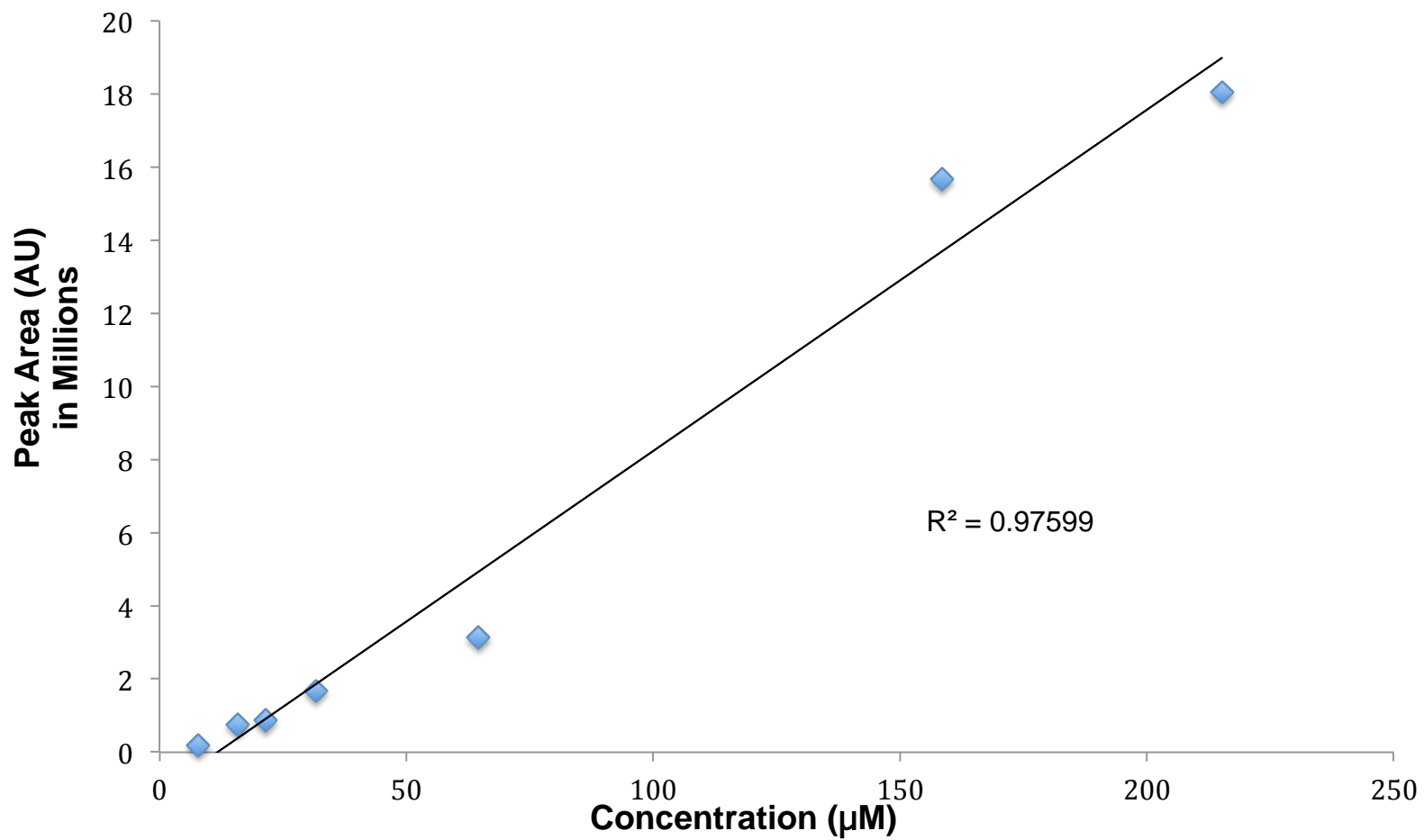


Figure G3. External standard curve for (Z,Z)7,11-pentacosadiene.

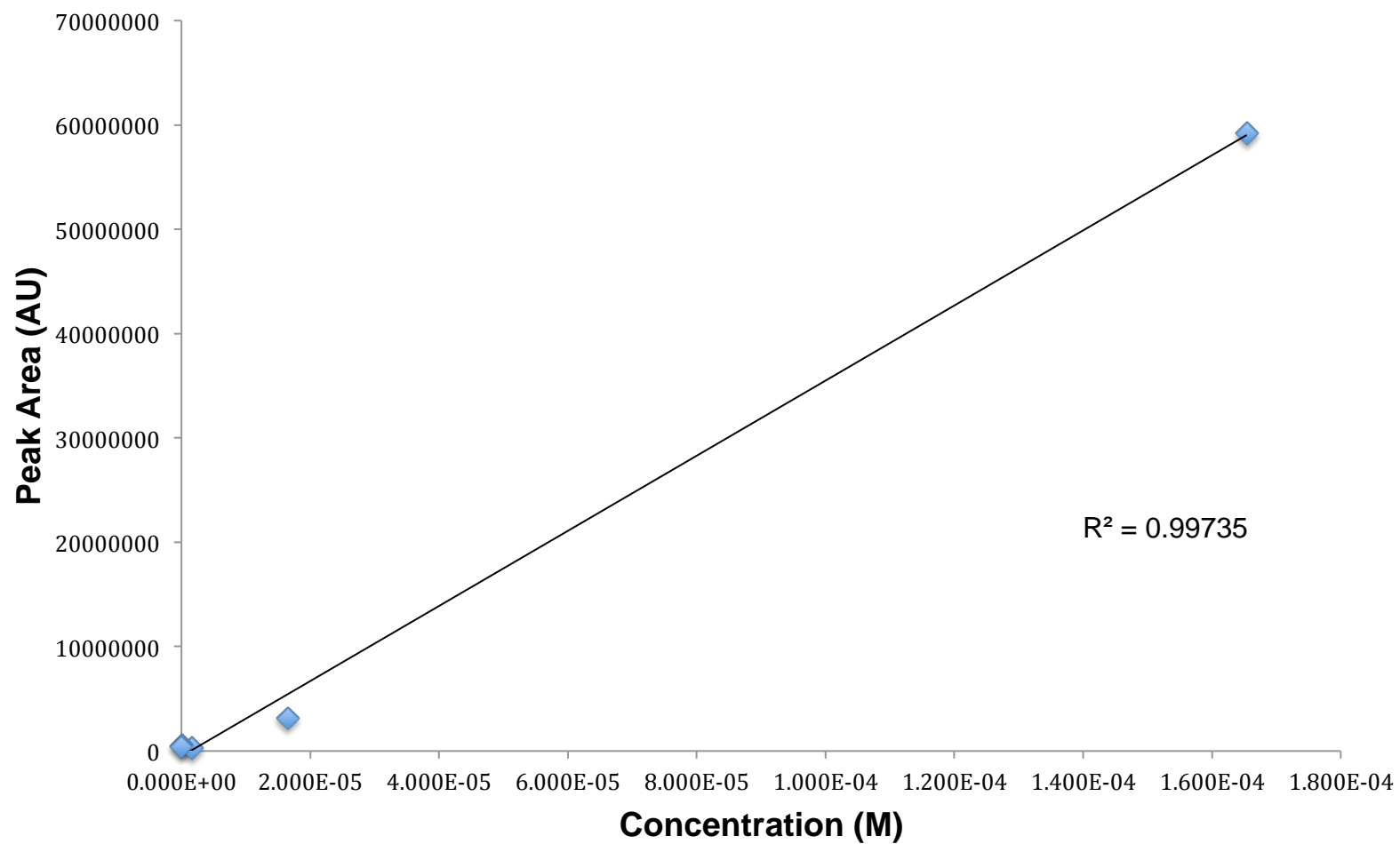


Figure G4. External standard curve for (Z)9-tricosene.

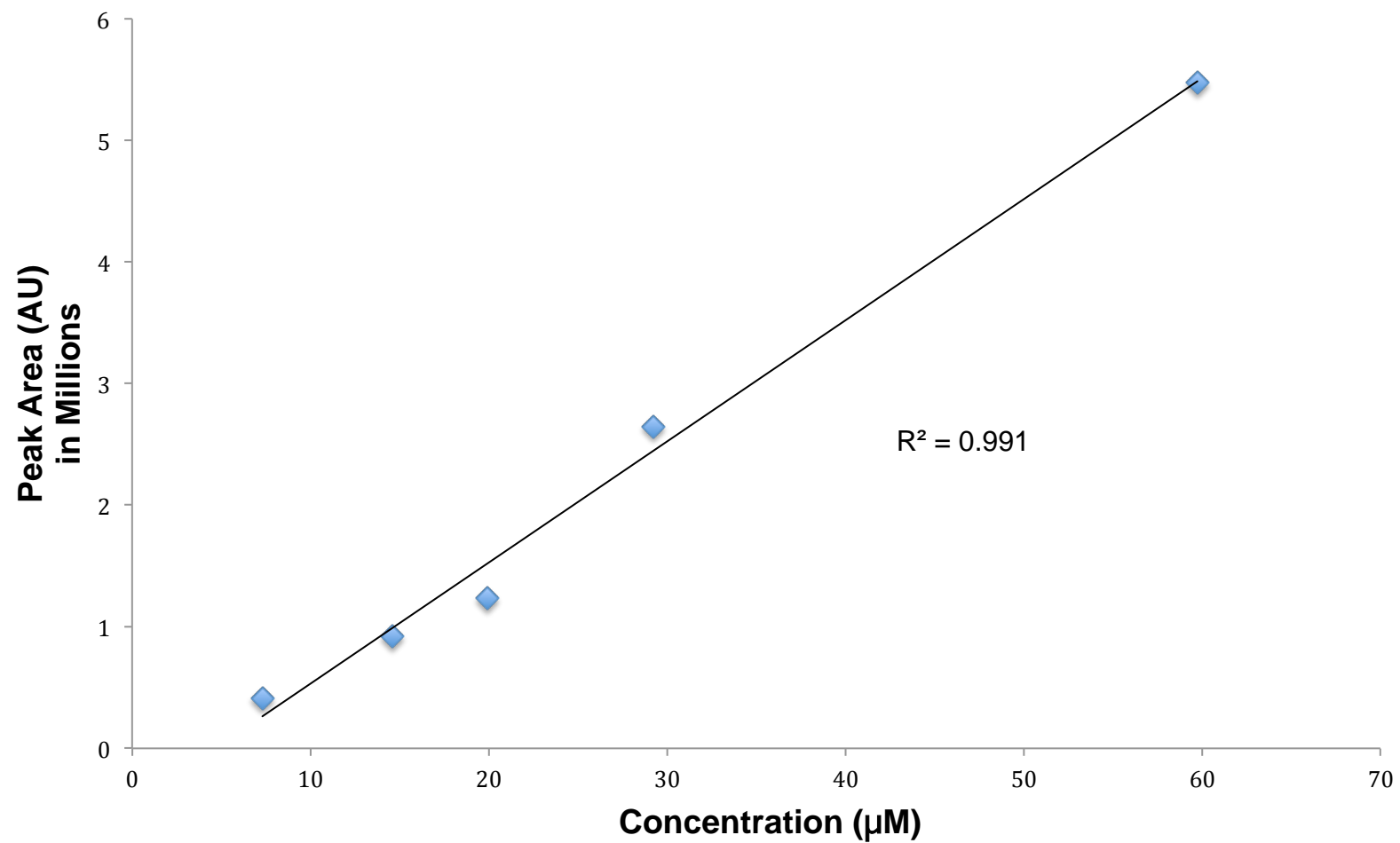


Figure G5. External standard curve for (Z,Z)7,11-heptacosadiene.